



Fisheries and Oceans
Canada

Pêches et Océans
Canada

Ecosystems and
Oceans Science

Sciences des écosystèmes
et des océans

Canadian Science Advisory Secretariat (CSAS)

Research Document 2016/056

Quebec Region

Physical Oceanographic Conditions in the Gulf of St. Lawrence in 2015

P.S. Galbraith¹, J. Chassé², C. Caverhill³, P. Nicot⁴, D. Gilbert¹,
B. Pettigrew¹, D. Lefaivre¹, D. Brickman³, L. Devine¹, C. Lafleur¹

¹ Fisheries and Oceans Canada, Québec Region,
Maurice Lamontagne Institute,
P.O. Box 1000, Mont-Joli, Québec, G5H 3Z4

² Fisheries and Oceans Canada, Gulf Region,
P.O. Box 5030, Moncton, New Brunswick, E1C 9B6

³ Fisheries and Oceans Canada, Maritimes Region,
Bedford Institute of Oceanography
P.O. Box 1006, Dartmouth, Nova Scotia, B2Y 4A2

⁴ Institut des sciences de la mer de Rimouski
Université du Québec à Rimouski
310 allée des Ursulines, Rimouski, Québec, G5L 3A1

Foreword

This series documents the scientific basis for the evaluation of aquatic resources and ecosystems in Canada. As such, it addresses the issues of the day in the time frames required and the documents it contains are not intended as definitive statements on the subjects addressed but rather as progress reports on ongoing investigations.

Research documents are produced in the official language in which they are provided to the Secretariat.

Published by:

Fisheries and Oceans Canada
Canadian Science Advisory Secretariat
200 Kent Street
Ottawa ON K1A 0E6

[http://www.dfo-mpo.gc.ca/csas-sccs/
csas-sccs@dfo-mpo.gc.ca](http://www.dfo-mpo.gc.ca/csas-sccs/csas-sccs@dfo-mpo.gc.ca)



© Her Majesty the Queen in Right of Canada, 2016
ISSN 1919-5044

Correct citation for this publication:

Galbraith, P.S., Chassé, J., Caverhill, C., Nicot, P., Gilbert, D., Pettigrew, B., Lefavre, D., Brickman, D., Devine, L., and Lafleur, C. 2016. Physical Oceanographic Conditions in the Gulf of St. Lawrence in 2015. DFO Can. Sci. Advis. Sec. Res. Doc. 2016/056. v + 90 p.

TABLE OF CONTENTS

ABSTRACT.....	IV
RÉSUMÉ	V
INTRODUCTION	1
AIR TEMPERATURE	2
PRECIPITATION AND FRESHWATER RUNOFF.....	2
SURFACE LAYER	3
SST SEASONAL CYCLE CLIMATOLOGY.....	4
SST IN 2015	4
SEA ICE.....	6
WINTER WATER MASSES	8
COLD INTERMEDIATE LAYER.....	9
PREDICTION FROM THE MARCH SURVEY	9
AUGUST CIL BASED ON THE MULTI-SPECIES SURVEY	9
NOVEMBER CIL CONDITIONS IN THE ST. LAWRENCE ESTUARY	10
GILBERT AND PETTIGREW (1997) CIL INDEX.....	10
MAGDALEN SHALLOWS JUNE SURVEY	11
BOTTOM WATER TEMPERATURES ON THE MAGDALEN SHALLOWS	11
DEEP WATERS (>150 M).....	12
BOTTOM WATER TEMPERATURES IN AUGUST AND SEPTEMBER	12
TEMPERATURE AND SALINITY MONTHLY MEANS	13
DISSOLVED OXYGEN AND HYPOXIA IN THE ST. LAWRENCE ESTUARY.....	13
SEASONAL AND REGIONAL AVERAGE TEMPERATURE STRUCTURE	14
CURRENTS AND TRANSPORTS	15
HIGH FREQUENCY SAMPLING AZMP STATIONS.....	16
OUTLOOK FOR 2015.....	16
SUMMARY	17
KEY FINDINGS.....	17
ACKNOWLEDGEMENTS	18
REFERENCES	19

ABSTRACT

An overview of physical oceanographic conditions in the Gulf of St. Lawrence (GSL) in 2015 is presented as part of the Atlantic Zone Monitoring Program (AZMP). AZMP data as well as data from regional monitoring programs are analysed and presented in relation to long-term means. The annual average freshwater runoff of the St. Lawrence River measured at Québec City was below normal and its combination with rivers flowing into the Estuary (RIVSUM II) was about normal in 2015 (-1.0 SD and +0.1 SD respectively). The spring freshet was below-normal at -1.1 SD and -0.5 SD, but its timing was normal. The cold winter of 2015 created a thick surface mixed layer over the GSL with near-freezing temperatures, but a sea ice cover that was only slightly above-normal. The August cold intermediate layer (CIL) showed warmer minimum temperature (+0.8 SD) and thinner volume colder than 1°C (-1.5 SD) than normal in spite of the cold winter conditions. Including the colder temperatures from the June survey led to a near-normal CIL minimum temperature index (+0.3 SD). Sea-surface temperatures averaged over the Gulf were generally below normal until July and above normal from August to September 2015, leading to a near-normal May-November average (+0.3°C, +0.5 SD). Record highs were nevertheless reached in September averaged over the Gulf (+1.8°C, +2.3 SD) and in the following regions: Estuary (+1.9°C, +2.3 SD), Northwest Gulf (+1.9°C, +1.9 SD), Anticosti Channel (+2.1°C, +2.1 SD) and Magdalen Shallows (+1.4°C, +2.0 SD). The timing of summer warming onset was near-normal while fall cooling was later than normal (+1.7 weeks, +1.4 SD). Deep water temperatures have been increasing overall in the Gulf, with inward advection from Cabot Strait where temperature had reached a record high (since 1915) in 2012 at 200 m. Temperature averaged over the Gulf at depths from 150 to 300 m all show record highs in 2015 and attained values above 6°C at 250 and 300 m for the first time since 1915. The bottom area covered by waters warmer than 6°C increased in 2015 in Anticosti Channel, Esquiman Channel and Central Gulf, reaching a record high value in Anticosti Channel and Esquiman Channel while reducing its bottom habitat area in the temperature range of 5–6°C.

Conditions océanographiques physiques dans le golfe du Saint-Laurent en 2015

RÉSUMÉ

Le présent document donne un aperçu des conditions d'océanographie physique qui ont prévalu dans le golfe du Saint-Laurent en 2015 et est un produit du Programme de monitoring de la zone Atlantique (PMZA). Les données du PMZA ainsi que de programmes de monitoring régionaux sont analysées et présentées en relation avec des moyennes à long terme. Les débits du fleuve Saint-Laurent et de l'indice RIVSUM II étaient respectivement sous et près de la normale en 2015 (- 1,0 É.T. et + 0,1 É.T. respectivement). La crue printanière était sous la normale (- 1,1 É.T. et - 0,5 É.T.) mais sa phénologie était normale. L'hiver froid de 2015 a causé la formation d'une volumineuse couche de surface avec des températures près du point de congélation, par contre le couvert de glace de mer n'a atteint un volume saisonnier maximal que légèrement au-dessus de la normale. La couche intermédiaire froide (CIF) du mois d'août était chaude (+ 0,8 É.T.) et mince (- 1,5 É.T. pour le volume des eaux sous 1 °C) en dépit de l'hiver froid. L'inclusion des données plus froides de juin mène à l'évaluation d'une CIF près de la normale (+ 0,3 É.T.). Les températures de l'eau à la surface de étaient généralement sous la normale jusqu'en juillet, et au-dessus de la normale en août et septembre, conduisant à une moyenne de mai à novembre qui a été près de la normale (+ 0,3 °C, + 0,5 É.T.). Le mois de septembre a néanmoins connu un record de + 1,8 °C au-dessus de la climatologie (+ 2,3 É.T.). Des records ont aussi été battus dans les régions suivantes : estuaire (+ 1,9 °C, + 2,3 É.T.), nord-ouest du golfe (+ 1,9 °C, + 1,9 É.T.), chenal Anticosti (+ 2,1 °C, + 2,1 É.T.) et le Plateau madelinien (+ 1,4 °C, + 2,0 É.T.). Le réchauffement printanier est survenu à une date normale, tandis que le refroidissement d'automne a été tardif (+ 1,7 semaine, + 1,4 É.T.). Les températures des eaux profondes du golfe ont depuis quelques années été en augmentation avec le transport depuis le détroit de Cabot d'eaux qui avaient atteint une température record (depuis 1915) en 2012 à 200 m. Globalement, les températures de 150 m à 300 m de profondeur ont atteint un record de série et dépassent le seuil de 6 °C pour la première fois à 250 et 300 m depuis 1915. La superficie du fond marin recouvert par des températures plus grandes que 6 °C a augmenté dans le chenal d'Anticosti, le chenal Esquiman ainsi que dans le centre du golfe, atteignant un record de série dans le chenal d'Anticosti ainsi que dans le chenal Esquiman au détriment de l'habitat de fond dans la plage de température de 5 à 6 °C.

INTRODUCTION

This document examines the physical oceanographic conditions and related atmospheric forcing in the Gulf of St. Lawrence in 2015 (Figure 1). It complements similar reviews of the environmental conditions on the Newfoundland and Labrador Shelf and the Scotian Shelf and Gulf of Maine as part of the Atlantic Zone Monitoring Program (AZMP; see Therriault et al., 1998 for background information on the program and Colbourne et al. 2015, and Hebert et al. 2015 for examples of past reviews in other AZMP regions). The last detailed report of physical oceanographic conditions in the Gulf of St. Lawrence was produced for the year 2014 (Galbraith et al. 2015). Specifically, it discusses air temperature, freshwater runoff, sea-ice volume, surface water temperature and salinity, winter water mass conditions (e.g., the near-freezing mixed layer volume, the volume of dense water that entered the Gulf through the Strait of Belle Isle), the summertime cold intermediate layer (CIL), and the temperature, salinity, and dissolved oxygen of the deeper layers. Some of the variables are spatially averaged over distinct regions of the Gulf (Figure 2). The report uses data obtained from the Department of Fisheries and Oceans' (DFO) Atlantic Zone Monitoring Program (AZMP), other DFO surveys, and other sources. Environmental variables are usually expressed as anomalies, i.e., deviations from their long-term mean. The long-term mean or normal conditions are calculated for the standard 1981–2010 reference period when possible. Furthermore, because these series have different units ($^{\circ}\text{C}$, m^3 , m^2 , etc.), each anomaly time series is normalized by dividing by its standard deviation (SD), also calculated for the standard reference when possible. This allows a more direct comparison of the various series. Missing data are represented by grey cells in the tables, values within ± 0.5 SD of the average as white cells, and conditions corresponding to warmer than normal (higher temperatures, reduced ice volumes, reduced cold-water volumes or areas) by more than 0.5 SD as red cells, with more intense reds corresponding to increasingly warmer conditions. Similarly, blue represents colder than normal conditions. Higher than normal freshwater inflow is shown as red, but does not necessarily correspond to warmer-than-normal conditions. Higher than normal stratification values are shown in blue because they are usually caused by lower upper layer salinity.

The summertime water column in the Gulf of St. Lawrence consists of three distinct layers: the surface layer, the cold intermediate layer (CIL), and the deeper water layer (Figure 3). Surface temperatures typically reach maximum values in early to mid-August. Gradual cooling occurs thereafter, and wind forced mixing during the fall leads to a progressively deeper and cooler mixed layer, eventually encompassing the CIL. During winter, the surface layer thickens partly because of buoyancy loss (cooling and reduced runoff) and brine rejection associated with sea-ice formation, but mostly from wind-driven mixing prior to ice formation (Galbraith 2006). The surface winter layer extends to an average depth of 75 m but >150 m in places such as the Mécatina Trough (where intruding waters through the Strait of Belle Isle from the Labrador Shelf may extend from the surface to the bottom in depths >200 m) by the end of March when temperatures have decreased to near freezing (-1.8 to 0°C) (Galbraith 2006). During spring, surface warming, sea-ice melt waters, and continental runoff produce a lower-salinity and higher-temperature surface layer. Underneath this surface layer, cold waters from the previous winter are partly isolated from the atmosphere and form the summer CIL. This layer will persist until the next winter, gradually warming up and deepening during summer (Gilbert and Pettigrew 1997; Cyr et al. 2011) and more rapidly during the fall as vertical mixing intensifies.

This report considers these three layers in turn but first air temperature is examined because it is a significant driver of the surface layer, followed by the freshwater runoff. The winter sea ice and winter oceanographic conditions are described; these force the summer CIL, which is

presented next. The deeper waters, mostly isolated from exchanges with the surface, are presented last along with a summary of major oceanographic surveys.

AIR TEMPERATURE

The air temperature data are the second generation of homogenized surface air temperature data, part of the Adjusted and Homogenized Canadian Climate Data (AHCCD), which accounts for shifts due to the relocation of stations, changes in observing practices and automation (Vincent et al. 2012). The monthly air temperature anomalies for several stations around the Gulf are shown in Figure 4 for 2014 and 2015, as well as the average of all station anomalies.

Figure 5 shows the annual, winter (December-March), and April-November mean air temperature anomalies averaged over all available stations shown in Figure 4 since 1873. Record-high annual and winter temperatures occurred in 2010 and record-high April-November temperatures in 2012. Galbraith et al. (2012) found the average April-November air temperature over the Gulf from Environment Canada's National Climate Data and Information Archive (NCDIA) to be a good proxy for May-November sea-surface temperature over the Gulf (but excluding the estuary) and found within the former a warming trend of 0.9°C per century between 1873 and 2011; the same trend is found here over the selected ACCHD stations between 1873 and 2015 (Figure 5). The NCDIA December-March air temperatures in the western Gulf were found to be highly correlated ($r^2=0.67$) with sea-ice properties, as well as with winter mixed layer volumes (Galbraith et al. 2010). Galbraith et al. (2013) found slightly higher correlations ($r^2=0.72$) with sea-ice using December-February ACCHD averages, possibly because March temperature are of less importance during low sea-ice cover since much of the sea-ice cover decrease has occurred much earlier in February.

Air temperatures were well below normal in February 2015, by 6.5°C at Mont-Joli (coldest since 1923, -2.4 SD), by 7.3°C at Bathurst (1922, -2.7 SD), by 5.1°C at Charlottetown (1923, -2.4 SD), by 5.4°C at Gaspé (1939, -2.0 SD) and by 4.4°C on average over available Gulf stations (coldest since 1993 and 15th lowest since 1873 at -1.6 SD). Overall the winter was cold, with a December-March average air temperature anomaly of -1.5°C (-1.0 SD). August air temperatures were at series record highs at Natashquan (since 1915, +2.9°C, +2.9 SD), Baie-Comeau (since 1965, +2.5°C, +2.6 SD), Mont-Joli (since 1877, +2.3°C, +2.0 SD) and Charlottetown (since 1873, +2.8°C, +3.0 SD). Averaged over all stations, August had the second warmest (after 2012) air temperatures on record (since 1873, +2.2°C, +2.8 SD). April-November air temperatures were normal (anomaly of 0.0°C) and the annual averaged air temperature anomaly was near-normal at -0.4°C overall (-0.4 SD).

PRECIPITATION AND FRESHWATER RUNOFF

Freshwater runoff data for the St. Lawrence River are updated monthly (Figure 6, lower curve) using the water level method from Bourgault and Koutitonsky (1999) and are available from the [St. Lawrence Global Observatory](#). A hydrological watershed model was used to estimate the monthly runoff since 1948 for all other major rivers flowing into the Gulf of St. Lawrence, with discharge locations as shown in Figure 7. The precipitation data (NCEP reanalysis, six hourly intervals) used as input in the model were obtained from the NOAA-CIRES Climate Diagnostics Center (Boulder, Colorado, USA; Kalnay et al. 1996). The data were interpolated to a ¼° resolution grid and the water routed to river mouths using a simple algorithm described here. When air temperatures were below freezing, the water was accumulated as snow in the watershed and later melted as a function of warming temperatures. Water regulation is modelled for three rivers that flow into the estuary (Saguenay, Manicouagan, Outardes) for which the annual runoff is redistributed following the climatology of the true regulated runoffs for

12 months thereafter. Runoffs were summed for each region shown and the climatology established for the 1981–2010 period. The waters that flow into the Estuary (region 1, Figure 7.) were added to the St. Lawrence River runoff measured at Québec City to produce the RIVSUM II index, although no advection lags were introduced (Figure 6, upper curve).

Monthly anomalies of the summed runoffs for 2014 and 2015 are shown in Figure 8. Rivers other than the St. Lawrence contribute about $5\,000\text{ m}^3\text{ s}^{-1}$ runoff to the Estuary, the equivalent of 40% of the St. Lawrence River, while the other tributaries distributed along the border of the GSL provide an additional $3\,500\text{ m}^3\text{ s}^{-1}$ in freshwater runoff to the system. River regulation has a strong impact on the relative contributions of sources. For example, in May 2015 the higher-than-average river runoff into the Estuary (an effect of the heavy precipitation in 2014 and river regulation) was almost as important as the below-normal St. Lawrence run-off. The 2015 simulation shows that rivers in regions 2, 3, 4 and 5 behaved similarly, with below normal runoff in winter and above normal in June, and through to August in most regions. The long-term time series are shown, summed by large basins, in Figure 9. Broad long-term patterns of runoff over the large basins were similar to that of the St. Lawrence River but interannual variability is low in the Northeast basin and Magdalen Shallows basin. The average run-off into the Estuary was above-normal at +2.7 SD, the highest since 1954. The annual average runoff of the St. Lawrence River measured at Québec City and RIVSUM II both show a general downward trend from the mid-1970s until 2001, an upwards trend between 2001 and 2011 and were respectively below-normal and normal in 2015 (Figure 9) at $11\,100\text{ m}^3\text{ s}^{-1}$ (-1.0 SD) and $17\,000\text{ m}^3\text{ s}^{-1}$ (+0.0 SD). Runoff was low from March through May, consistent with the very cold air temperatures. The spring freshet was below-normal at -1.1 SD in April for the St. Lawrence River and -0.5 SD in May for RIVSUM II, but its timing was normal (Figure 6). The fall freshet was also above normal and later than normal.

SURFACE LAYER

The surface layer conditions of the Gulf are monitored by several complementary methods. The shipboard thermosalinograph network (Galbraith et al. 2002) consists of temperature-salinity sensors (SBE-21; Sea-Bird Electronics Inc., Bellevue, WA) that have been installed on various ships starting with the commercial ship Cicero of Oceanex Inc. in 1999 (retired in 2006) and on the Cabot from 2006 to fall 2013. The Oceanex Connaigra, was outfitted with a thermosalinograph in early 2015.

The second data source is the thermograph network (Gilbert et al. 2004, Galbraith et al. 2007), which consists of a number of stations with moored instruments recording water temperature every 30 minutes (Figure 10). Most instruments are installed on Coast Guard buoys that are deployed in the ice-free season, but a few stations are monitored year-round. The data are typically only available after the instruments are recovered except for oceanographic buoys that transmit data in real-time. Data from Shediac station acquired by the DFO Gulf Region are also included here. The network provides valuable near-surface temperature data at fixed sites and at short sampling intervals, but usually not in real-time nor during winter months.

The third data source are 1 km resolution monthly composite Sea Surface Temperature (SST) generated using National Oceanic and Atmospheric Administration (NOAA) and European Organisation for the Exploitation of Meteorological Satellites (EUMETSAT) Advanced Very High Resolution Radiometer (AVHRR) satellite images available from the Maurice Lamontagne Institute sea surface temperature processing facility (details in Galbraith and Larouche 2011, and Galbraith et al. 2012). These data are available for the period of 1985-2013. AVHRR composites of 1.5-km resolution provided by the Bedford Institute of Oceanography (BIO) Operational Remote Sensing group complete the data set. Monthly climatologies for the period

of 1998–2012 common to both products were compared at the 1.5-km pixel level for cross-calibration. The BIO product is adjusted to the MLI product climatology as $SST_{IML} = 0.9794 S_{BIO} - 0.13$ (-0.13°C adjustment at 0°C ; -0.54°C at 20°C). This is in part explained by the fact that the MLI product used all available SST images while the BIO product uses only daytime passes, introducing a slight diurnal bias. This adjustment has decreased somewhat the 2014 record high temperatures reported in Galbraith et al. 2015.

SST SEASONAL CYCLE CLIMATOLOGY

The May to November cycle of weekly averaged surface temperature is illustrated in Figure 11 using a 1985–2010 climatology based on AVHRR remote sensing data for ice-free months complemented by 2001–2010 thermosalinograph data for the winter months. Galbraith et al. (2012) have shown that Gulf-averaged air temperature and SST monthly climatologies match up quite well with SST lagging air temperature by half a month. Maximum sea-surface temperatures are reached on average during the second week of August but that can vary by a few weeks from year to year. The maximum surface temperature averages 15.6°C over the Gulf during the second week of August (1985–2010), but there are spatial differences: temperatures on the Magdalen Shallows are the warmest in the Gulf, averaging 18.1°C over that area, and the coolest are at the head of the St. Lawrence Estuary and upwelling areas along the lower north shore.

Figure 12 shows a mean annual cycle of water temperature at a depth of 8 m along the Montréal to St. John’s shipping route based on thermosalinograph data collected from 2000 to 2015. Data were used from all instrumented ships that were within the main shipping route area to fill data gaps. The data were averaged for each day of the year at intervals of 0.1 degree of longitude to create a composite along the ship track. The most striking feature is the area at the head of the Laurentian Trough (69.5°W), where strong vertical mixing leads to cold summer water temperatures (around 5°C to 6°C and sometimes lower) and winter temperatures that are always above freezing (see also Figure 11). The climatology shows the progression to winter conditions, first reaching near-freezing temperatures in the Estuary and then progressing eastward with time, usually reaching Cabot Strait by the end of the winter.

Temperature anomaly time series and the 2000–2015 climatologies were constructed for selected sections that are crossed by the ship (Figure 13). Although the anomalies are quite similar between the two sections, the near-surface temperature climatology at Tadoussac (head of the Laurentian Trough) contrasts with that nearby in the Estuary, as noted above. Winter temperatures are on average 0.7°C warmer at the Tadoussac section; the maximum monthly mean temperature in summer is only 7.1°C compared with 8.6°C at the nearby Estuary section and up to 13.2°C at the Mont-Louis section. The table in Figure 13 provides a quick reference to the interannual near-surface temperature variations at the selected sections as well as monthly averages for the year in review.

SST IN 2015

Thermosalinograph data show that near-freezing surface layer conditions disappeared earlier than normal in the Estuary and lasted longer in the Gulf near Cabot Strait (Figure 12). The 2015 monthly mean sea-surface temperatures from AVHRR imagery are shown in Figure 14 as colour-coded maps and the corresponding temperature anomaly maps are shown in Figure 15 referenced to 1985–2010 monthly climatologies. Missing anomaly pixels are due to incomplete climatologies during the ice covered winter months. The SST information is summarized in Figure 16, showing the 2015 monthly average temperatures versus the climatology spatially averaged over the Gulf and over each of the eight regions delimited by the areas shown in Figure 2. The information also appears again in tabular form in Figure 17 with the same

averaging regions and further into sub-regions of the Estuary as shown in Figure 18. Figure 16 displays anomalies expressed in degrees while Figure 17 displays average temperatures.

Near-surface water temperatures were generally below normal until July and above normal from August to September 2015, leading to a near-normal May–November average (+0.3°C, +0.5 SD). Record highs were nevertheless reached in September averaged over the Gulf (14.3°C, above normal by +1.8°C and 2.3 SD) and in the following regions: Estuary (+1.9°C, +2.3 SD), Northwest Gulf (+1.9°C, +1.9 SD), Anticosti Channel (+2.1°C, +2.1 SD) and Magdalen Shallows (+1.4°C, +2.0 SD). Figures 19 and 20 show the 1985–2015 time series of monthly surface temperature anomalies spatially averaged over the Gulf of St. Lawrence and over the eight regions of the Gulf.

Sea-surface temperature monthly climatologies and time series were also extracted for more specific regions of the Gulf. The monthly average SST for the St. Lawrence Estuary as a whole (region 1) is repeated in Figure 21 along with averages for the proposed Manicouagan Marine Protected Area (MPA), the proposed St. Lawrence Estuary MPA, and the Saguenay – St. Lawrence Marine Park. The overall pattern is similar across regions, but there are differences associated with episodic local events such as eddies and upwellings. The climatology averages also differ, for example the Manicouagan maximum monthly average temperature is 1.0°C warmer than for the Estuary as a whole.

The Magdalen Shallows, excluding Northumberland Strait, is divided into western and eastern areas as shown in Figure 22. The monthly average SST for the Magdalen Shallows as a whole (region 8) is repeated in Figure 23 along with averages for the western and eastern areas. Climatologies differ by roughly 0.5°C to 1°C between the western and eastern regions. Temperatures were below-normal to normal from May to July and normal to above-normal from August until November.

The number of weeks in the year that the mean weekly temperature is above 10°C for each pixel (Figure 24) integrates summer surface temperature conditions into a single map displaying the length of the warm season. The average number of weeks with mean weekly temperature above 10°C are shown for each region as time series in Figure 25. The Estuary, Northwest Gulf, Anticosti Channel and Mecatina Trough had longer than normal warm seasons (from +0.8 to +1.5 SD, about two weeks longer), while the rest were near-normal.

Seasonal trends in relation to air temperature are examined by first displaying weekly averaged AVHRR SST in the GSL for all years between 1985 and 2015 (Figure 26) with years on the x-axis and week of the year on the y-axis (See Galbraith & Larouche 2013 for a full description). Isotherms show the first and last occurrences of weekly temperature averages of 12°C over the years. These temperatures are chosen to be representative of spring (and fall) transitions to (and from) typical summer temperatures. Although the selected temperature is arbitrary, the results that follow are not particularly sensitive to the exact temperature chosen because the surface mixed layer tends to warm and cool linearly in spring and fall (e.g. Figure 11). The Gulf has experienced earlier summer onset and later fall cooling between 1985 and 2015, with trends of -0.57 and +0.57 weeks per decade respectively. In 2015, the timing of summer onset was near-normal while fall cooling was later than normal (+1.7 weeks, +1.4 SD). The inter-annual variability in the time of year when the 12°C threshold is crossed is correlated with June–July average air temperature for the summer onset (1.1 week sooner per 1°C increase; $R^2=0.60$) and with September average air temperature for the fall (0.8 week later per 1°C increase; $R^2=0.48$). These air temperature averages, shown in Figure 26, can be used as proxies prior to 1985. The implication is that the Gulf of Lawrence warm season will be longer by about 2 weeks for each 1°C of warming associated with climate change.

Thermograph network observations are compared to daily average temperatures calculated using all available data for each day of the year at each station and depth (Figures 27-29). The seasonal cycle of near-surface temperature is measured by shallow instruments, while Cold Intermediate Layer warming from spring to fall is captured by instruments moored between 30 and 120 m depth. Monthly average temperatures are also shown, with the magnitude of their anomaly colour-coded. Salinities are shown in a similar fashion in Figure 30. The average monthly temperatures for each station at shallow sampling depths (< 20 m) for 2014 and 2015 are also shown in Figure 31, while Figure 32 shows information for sensors moored deeper than 20 m and Figure 33 shows the history of monthly averaged temperature anomalies for selected stations.

Monthly shallow-water anomalies were fairly consistent across all stations of each of the three regions listed in Figure 31. As with AVHRR data sources and in spite of different climatological periods, the months of June and July shows colder-than-normal conditions at many stations, while August and September show widespread warm anomalies in the Estuary and Northwest Gulf.

The Île Shag (10 m) station shows bottom temperatures close to Îles-de-la-Madeleine that are important to the lobster fishery. Winter temperatures were below normal at this station (Figure 29 and Figure 33). The Île Shag panel (Figure 29) shows with a red line the span of historical dates when spring temperature increased over 1.5°C, a temperature associated with increased lobster mobility. In 2015, this had not yet occurred by the end of the record on May 8th; a series record since measurements began there in 1994. Station La Perle is also relevant to the lobster fishery because it is located in deeper waters (26 m) where the fishery tends to start. Because the thermograph is attached to a Coast Guard buoy, even the bottom temperature is usually already above 1.5°C by the time it get deployed in spring. However, in 2015 this threshold was only reached after the deployment, on June 2nd. This is the latest date on record. The lobster fishery began on May 14th and must therefore have been in cold waters (<1.5°C).

SEA ICE

Ice volume is estimated from three gridded databases of ice cover and ice categories obtained from the Canadian Ice Service (CIS). Weekly Geographic Information System (GIS) charts covering the period 1969-2015 and daily charts covering the period 2009-2015 were gridded on a 0.01° latitude by 0.015° longitude grid (approximately 1 km resolution), and 5-km resolution gridded daily files were obtained directly from the CIS covering the period 1998-2008. Some of the analyses described below were done using the weekly data exclusively, for long-term consistency, while for others daily data were used when available with results filtered using a 3-day running mean in order to make them more comparable to results calculated from weekly data.

Ice typically forms first in December in the St. Lawrence estuary and in shallow waters along New Brunswick, Prince Edward Island and the lower north shore and melts last in the northeast Gulf where the ice season duration tends to be longest apart from shallow bays elsewhere (Figure 34). Offshore sea ice is typically produced in the northern parts of the Gulf and drifts towards Îles-de-la-Madeleine and Cabot Strait during the ice season. The maximum estimated ice volume in 2015 occurred the week of March 9th and is compared with the 1981-2010 climatology in Figure 35 (upper panels). The 1981-2010 climatology and 2015 distribution of the thickest ice recorded during the season at any location is also shown in Figure 35 (lower panels); the climatological thick areas in the northeast are mostly associated with ice that has

entered the Gulf through the Strait of Belle Isle and are pushed by the wind either on the lower north shore or on the coast of Newfoundland.

Figure 36 shows the daily evolution of the estimated sea-ice volume in relation to the climatology and historical extremes. It clearly shows how the high interannual variability in ice cover leads to weak normalized anomalies even in cases of near-absence of sea-ice. Figure 37 shows the estimated seasonal maximum ice volumes within the Gulf as well as on the Scotian Shelf. The volume shown on the bottom panel of Figure 37 corresponds to that found seaward of Cabot Strait (defined by its narrowest crossing). It would represent the volume of ice exported from the Gulf provided that no melt had already occurred. The combined Gulf and Scotian Shelf ice volume shown separately as top and bottom panels of Figure 37 is indicative of the total volume of ice produced in the Gulf, including the advection out of the Gulf, but it also includes the thicker sea ice that drifts into the Gulf from the Strait of Belle Isle.

Figure 38 shows the day of first and last occurrence of ice in each of the regions of the Gulf of St. Lawrence as well as duration of the ice season and maximum observed volume during each season.

Figure 39 shows the time series of seasonal maximum ice volume and area (excluding thin new ice), ice season duration and December-to-March air temperature anomaly (from Figure 5). The figure shows declining trends in ice cover severity since 1990 with rebounds in 2003 and 2014. The correlation between annual maximum ice volume (including the cover present on the Scotian Shelf) and the December-February air temperature averaged over five Western Gulf stations (Sept-Îles, Mont-Joli, Gaspé, Charlottetown and Îles-de-la-Madeleine) accounted for 72% of the variance using the 1969–2012 time series (Galbraith et al. 2013). Figure 39 shows a similar comparison using ice volume and the ACCHD December-to-March air temperature anomaly from Figure 5 yielding $R^2 = 0.74$. The correlation between air temperature and the ice parameters season duration and area are also very high ($R^2 = 0.76-0.80$). Correlation coefficients are slightly higher when using January to February air temperatures, perhaps because March air temperatures have no effect on ice cover that has almost disappeared by then during very mild winters. Sensitivity of the ice cover to climate change can be estimated using past co-variations between winter air temperature and sea-ice parameters, which indicate losses of 17 km³, 30,000 km² and 14 days of sea-ice season for each 1°C increase in winter air temperature.

In 2015, the seasonal maximum ice volume based on weekly ice charts was 86 km³ (Figure 38), slightly above-normal (+0.6 SD) in spite of below-normal winter air temperatures (-1.0 SD). This contrasts to the four of the six lowest maximum ice volumes of the time series that have occurred in the previous six years. Ice was exported from the Gulf of St. Lawrence onto the Scotian Shelf in greater volumes than the preceding winter. The sea-ice cover throughout the season was typically below the 1981-2010 climatology until the second week of February, and above-normal thereafter (Figure 36). The seasonal maximum was reached at a near-normal time of year in mid-March. Thus, the very cold air temperatures of February (-4.5°C anomaly, coldest since 1993) were sufficient to create the above-normal ice cover within a period of roughly one month, as the ice season began late (Figures 34 and 38). The sea-ice retreat was later than usual on the Magdalen Shallows and Cabot Strait, on average by 18 and 21 days respectively (Figure 38) and by more than 5 weeks in places (Figure 34). This included areas around the Îles-de-la-Madeleine where sea-ice delayed the start of the lobster season to May 14th. Fortunately, the late ice retreat also caused a delay in spring warming of the surface layer in the affected areas such that warming water temperatures coincided with the opening of the fishery (Figure 29, thermograph data at Île Shag and La Perle).

WINTER WATER MASSES

A wintertime survey of the Gulf of St. Lawrence waters (0–200 m) has been undertaken in early March since 1996 using a Canadian Coast Guard helicopter. This has added a considerable amount of data to the previously very sparse winter data for the region. The survey, sampling methods, and results of the cold-water volume analysis in the Gulf and the estimate of the water volume advected into the Gulf via the Strait of Belle Isle over the winter are described in Galbraith (2006) and in Galbraith et al. (2006). Figures 40 and 41 show gridded interpolations of near-surface temperature, temperature above freezing, salinity, cold layer thickness and bottom contacts, and thickness of the Labrador Shelf water intrusion for 2015 as well as climatological means. Stations were only sampled from the ice in March 2015 such that ice-free areas are not represented in the analysis; the ice cover was however very widespread at that time of year (Figure 35).

During winters prior to 2010, the surface mixed layer was usually very close (within 0.1°C) to the freezing point in most regions of the Gulf but thickness of the surface layer varied, leaving only variability in the cold-water volume between mild and severe winters. This was not the case in 2010 for the first time since the inception of the winter survey, when the mixed layer was on average 1°C above freezing. Similar conditions to those of 2010 were observed in March 2011, although not quite as warm. The winter surface mixed layer returned to near-normal conditions in 2012, as observed prior to 2010, whereby waters were near freezing at the end of winter over a large portion of the Gulf. Conditions in March 2015 were similarly cold (Figure 40), consistent with the almost total ice cover. Areas missed by our sampling in the northwest Gulf because of thin ice were areas where ice was actively being produced and transported away by winds, and are assumed to have been similarly cold.

During typical winters, surface waters in the temperature range of ~ 0°C to -1°C are only found on the northeast side of Cabot Strait. Some of these warm waters have presumably entered the Gulf during winter and flowed northward along the west coast of Newfoundland, however it is also possible that local waters could have simply not cooled close to freezing. There was such an area of limited extent in 2015 (Figure 40) and the drifted-in ice cover allowed us to sample in that area. Near-freezing waters with salinities of around 32 are responsible for the (local) formation of the CIL since that is roughly the salinity at the temperature minimum during summer. These are coded in blue in the salinity panel of Figure 40 and are typically found to the north and east of Anticosti Island. Surface salinities were similar to the climatology in this part of the Gulf during the winter of 2015.

Near-freezing waters with salinity >32.35 (colour-coded in violet) are considered to be too saline to have been formed from waters originating within the Gulf (Galbraith 2006) and are presumed to have been advected from the Labrador Shelf through the Strait of Belle Isle. These waters were absent at the surface in Mécatina Trough (Figure 40) in March 2015. A T-S water mass criterion from Galbraith (2006) was used to identify intruding Labrador Shelf waters that have exhibited no evidence of mixing with warm and saline deep Gulf water. These waters only occupied a thin layer within Mécatina Trough in March 2015 (top-right panel of Figure 41). The recent history of Labrador Shelf water intrusions is shown in Figure 42, where its volume is shown as well as the fraction it represents of all the cold-water volume in the Gulf. This volume was at a series low in March 2015, at 230 km³ (-1.2 SD) representing only 2% (-1.3 SD) of the cold water (T < -1°C) in the Gulf. In fact, the bottom waters in Mécatina Trough were unusually warm in March 2015 (as will be described with Figure 60 in a later section).

The thermograph network also provides some information on the winter intrusion of Labrador Shelf waters. There are large differences in springtime bottom temperature at the Strait of Belle Isle (71 m) station depending on how late the cold inflow of Labrador Shelf Water persists

(Figure 33). Deep temperatures in the Strait of Belle Isle were below -1°C up to May 20th (Figure 28), which could be associated with prolonged entry of Labrador Shelf waters into the Gulf.

The cold mixed layer depth typically reaches about 75 m in the Gulf and is usually delimited by the -1°C isotherm because the mixed layer is typically near-freezing and deeper waters are much warmer (Galbraith 2006). In March 2010 and 2011 much of the mixed layer was warmer than -1°C such that the criterion of $T < 0^{\circ}\text{C}$ was also introduced (see middle panels of Figure 41). The cold surface layer is the product of local formation as well as cold waters advected from the Labrador Shelf, and can consist either of a single water mass or of layers of increasing salinity with depth. Integrating the cold layer depth over the area of the Gulf (excluding the Estuary and the Strait of Belle Isle) yields a cold-water ($< -1^{\circ}\text{C}$) volume of $13\,300\text{ km}^3$ in 2015 (Figure 43), 0.5 SD above the 1996–2015 average and similar to the volumes observed in 2001, 2002 and 2004. The time series of winter cold-water ($< -1^{\circ}\text{C}$) volume observed in the Gulf is shown in Figure 49. The mixed layer volume increases only to $14\,200\text{ km}^3$ when water temperatures $< 0^{\circ}\text{C}$ are considered which is close to the 1996–2015 average. This last volume of cold water corresponds to 42% of the total water volume of the Gulf ($33\,500\text{ km}^3$, excluding the Estuary).

COLD INTERMEDIATE LAYER

PREDICTION FROM THE MARCH SURVEY

The summer CIL minimum temperature index (Gilbert and Pettigrew 1997) has been found to be highly correlated with the Gulf (excluding the estuary) volume of cold water ($< -1^{\circ}\text{C}$) measured the previous March when much of the mixed layer is near-freezing (Galbraith 2006, updated relation in right panel of Figure 43). This is expected because the CIL is the remnant of the winter cold surface layer. A measurement of the volume of cold water present in March is therefore a valuable tool for forecasting the coming summer CIL conditions. The winter mixed layer in 2015 was thick and near freezing throughout the Gulf, up to Cabot Strait, after four consecutive winters with warmer conditions. The overall thickness and volume of the layer colder than -1°C was 0.5 SD above normal in 2015 in spite of the record low volume of Labrador Shelf Water that usually also contributes towards the overall volume. The Cold Intermediate Layer for summer 2015 was therefore forecasted to be a bit warmer than in 2014, with a Gilbert and Pettigrew (1997) index of around -0.4°C compared to -0.5°C in 2014 (Galbraith et al. 2015).

AUGUST CIL BASED ON THE MULTI-SPECIES SURVEY

The CIL minimum temperature, thickness and volume for $T < 0^{\circ}\text{C}$ and $< 1^{\circ}\text{C}$ were estimated using temperature profiles from all sources for August and September. Most data are from the multi-species surveys in September for the Magdalen Shallows and August for the rest of the Gulf. Using all available temperature profiles, each 1-m depth layer of the Gulf was spatially interpolated for temperature, with the interpolated field bound between the minimum and maximum values observed within each of the different regions of the Gulf (Figure 2) to avoid spurious extrapolations. The CIL thickness at each grid point is simply the sum of depth bins below the threshold temperature, and the CIL minimum temperature is only defined at grid points where temperature rises by at least 0.5°C at depths greater than that of the minimum, or if the grid point minimum temperature is below the CIL spatial average of the Gulf.

Figure 44 shows the gridded interpolation of the CIL thickness $< 1^{\circ}\text{C}$ and $< 0^{\circ}\text{C}$ and the CIL minimum temperature for August–September 2015 as well their 1985–2010 climatology (1994–2010 for Mécatina Trough). The CIL thickness for $T < 0^{\circ}\text{C}$ and $T < 1^{\circ}\text{C}$ decreased to below-normal values since 2014, with conditions similar to 2010 (not shown). Similar maps were produced for

all years back to 1971 (although some years have no data in some regions), allowing the calculation of volumes for each region for each year as well as the climatologies shown on the left side of Figure 44. The 2015 CIL water mass was thinner and warmer than the 1985-2010 climatologies, with particularly warm conditions in the Estuary, with minimum temperatures above 1°C in the western half.

The time series of the regional August–September CIL volumes are shown in Figure 45 (for <0°C and <1°C). All regions except Cabot Strait show decreased CIL volumes in 2015 compared to 2014. Figure 46 shows the total volume of CIL water (<0°C and <1°C) and the average CIL core temperature from the August–September interpolated grids (e.g., Figure 44). The CIL areal minimum temperature average and volume shown in Figure 46 exclude data from Mécatina Trough which has very different water masses from the rest of the Gulf; it is influenced by inflow through the Strait of Belle Isle and is therefore not indicative of the climate in the rest of the Gulf. The CIL volume as defined by $T < 1^\circ\text{C}$ decreased significantly (to -1.5 SD) compared to 2014 conditions (-0.4 SD) and reached a volume similar to 2010 (-1.3 SD). The volume delimited by 0°C also decreased to a below-normal value (-0.9 SD).

The time series of the CIL regional average minimum core temperatures are shown in Figure 47. All regions, again except for Cabot Strait, show an increase in core temperature. The 2015 average temperature minimum (excluding Mecatina Trough, the Strait of Belle Isle and the Magdalen Shallows) was 0.1°C, an increase of 0.2°C over 2014, and is shown in Figure 46 (bottom panel, green line). The overall 2015 CIL water mass properties are similar to observations of 2010.

NOVEMBER CIL CONDITIONS IN THE ST. LAWRENCE ESTUARY

The AZMP November survey provides a high-resolution conductivity-temperature-depth (CTD) sampling grid in the St. Lawrence estuary since 2006 although measurements are sparser in some years. This allows a higher resolution display of the CIL minimum temperature in the Estuary (Figure 48). The data also show the temporal warming (Figure 45) and thinning (Figure 47) of the CIL since the August survey. The CIL was warmer in November 2015 than in 2014, so much so that none of it was below 1°C. Figure 47 shows that the fairly rapid increase of the CIL minimum temperature occurring between August and November is fairly constant inter-annually in spite of the differences in August temperature.

GILBERT AND PETTIGREW (1997) CIL INDEX

The Gilbert and Pettigrew (1997) CIL index is defined as the mean of the CIL minimum core temperatures observed between 1 May and 30 September of each year, adjusted to 15 July. It was updated using all available temperature profiles measured within the Gulf between May and September inclusively since 1947 (black line of the bottom panel of Figure 46). As expected, the CIL core temperature interpolated to 15 July is almost always colder than the estimate based on August and September data for which no temporal corrections were made. This is because the CIL is eroded over the summer and therefore its core warms over time.

This CIL index for summer 2015 was -0.28°C, 0.3 SD above normal. The 0.21°C increase from the summer 2014 CIL index is consistent with the decrease in CIL volume between August 2014 and 2015 discussed above and the decrease of 0.2°C in the areal average of the minimum temperature in August. The warm winter conditions from 2010 to 2012 led to CIL indices that were still far below the record high observed in the 1960s and 1980s. The earlier CIL temperature minimums will be re-examined to confirm that they were calculated using data with sufficient vertical resolution to correctly resolve the core minimum temperature. It is also becoming increasingly clear that the winter mixed layer is not the only factor explaining

summertime CIL conditions and that mechanisms having a multi-year cumulative effect are required to explain the interannual autocorrelations observed. For example, this may be linked to temperatures below the CIL, which in warm years may create a higher temperature gradient that leads to higher heat fluxes and faster summertime CIL warming rates.

As a summary, Figure 49 shows selected time series of winter and summertime CIL conditions (June and September bottom temperatures also related to the CIL are outlined below) and highlights the strong correlations between these various time series. Surprisingly, the CIL had warmer-than-normal conditions in August whereas winter air temperatures were colder and the seasonal maximum sea-ice cover larger than normal. The August CIL was warmer and thinner in 2015 than in 2014 with conditions similar to those of 2010. The Gilbert & Pettigrew index which considers data from earlier in the season was near-normal and similar to the 2004 index.

MAGDALEN SHALLOWS JUNE SURVEY

A long-standing assessment survey covering the Magdalen Shallows has taken place in June for mackerel assessments and was since merged with the June AZMP survey. This survey provides good coverage of the temperature conditions that are greatly influenced by the cold intermediate layer that reaches the bottom at roughly half of the surface area at this time of time.

Near-surface waters warm quickly in June, mid-way between the winter minimum and the annual maximum in early August. This can introduce a bias if the survey dates are not the same each year. To account for this, the seasonal warming observed at the Shediac Valley AZMP monitoring station was evaluated. A linear regression was performed of temperature versus time for each meter of the water column for each year with monitoring data at Shediac Valley between May and July. Visual inspection showed that the depth-dependent warming rate was fairly constant for all years and an average was computed for every depth. Warming is maximal at the surface at 18°C per 100 days and, in spite of some uncertainties between 30 and 55 m, decreases almost proportionally with depth to reach 2°C per 100 days at 40 m, followed by a further linear decrease to reach 1°C per 100 days at 82 m (Galbraith and Grégoire 2015).

All available temperature profiles taken in June from a given year are binned at 1 m depth intervals (or interpolated if the resolution is too coarse) and then adjusted according to the sampling date to offset them to June 15th according to the depth-dependent warming rate extracted from Shediac Valley monitoring data. An interpolation scheme is used to estimate temperature at each 1 m depth layer on a 2 km resolution grid. Figure 50 shows temperatures and anomalies at depths of 20, 30 and 50 m. Figure 51 shows averages over the grids at 0, 10, 20, 30, 50 and 75 m for all years when interpolation was possible, as well as SST June averages since 1985, for both western and eastern regions of the Magdalen Shallows (Figure 22). Temperatures varied about the mean from below-normal to above-normal at 20, 30 and 50 m (Figure 50), as were the layer area averages (Figure 51).

BOTTOM WATER TEMPERATURES ON THE MAGDALEN SHALLOWS

Bottom temperature is also estimated at each point of the grids constructed from the June survey by looking up the interpolated temperature at the depth level corresponding to a bathymetry grid provided by the Canadian Hydrographic Service with some corrections applied (Dutil et al. 2012). The method is fully described in Tamdrari et al. (2012). A climatology was constructed by averaging all available temperature grids between 1981 and 2010 and anomaly grids were computed for each year. The June bottom temperature climatology as well as the 2015 reconstructed temperature and anomaly fields are shown in Figure 52. The same method was applied using the available CTD data from August and September, thus including the

multispecies surveys for the northern Gulf in August and for the Magdalen Shallows in September. These results are also shown in Figure 52. While much of the deeper bottom water temperatures are climatologically still below 0°C in June, a remnant from the winter near-freezing mixed layer that reached the bottom, most of the area usually warms to below 1°C by August-September. Temperature anomalies in coastal shallow waters range from <-2.5°C to >+2.5°C, but anomalies tend to be of smaller magnitude in deeper waters.

Time series of the bottom area covered by water in various temperature intervals were estimated from the gridded data for the June surveys as well as for the September multispecies survey on the Magdalen Shallows (Figure 53). The time series of areas of the Magdalen Shallows covered by water colder than 0, 1, 2, and 3°C in June and September are also shown in Figure 49 as part of the CIL summary. Unlike the very cold conditions observed on the bottom in 2008, only a small area of the bottom of the Magdalen Shallows was covered by water with temperatures <-1°C in June 2015; these are however colder conditions than during the 2010-2013 period when no bottom waters were that cold. The area covered by water temperatures <1°C in September had reached a low not seen since 1982 in 2012 but rebounded to near-normal in 2014 and 2015. Areas with T < 0°C, < 1°C, < 2°C and < 3°C were all near-normal in September 2015 (Figure 49). The thermograph network (Figure 29) also showed bottom temperatures at Shediac Valley (86 m) to be near normal (using a different reference period) for most of June to October.

DEEP WATERS (>150 M)

The deeper water layer (>150 m) below the CIL originates at the entrance of the Laurentian Channel at the continental shelf and circulates towards the heads of the Laurentian, Anticosti, and Esquiman channels without much exchange with the upper layers. The layer from 150 to 540 m is characterized by temperatures between 1 and >7°C and salinities between 32.5 and 35 (except for Mécatina Trough where near-freezing waters may fill the basin to 235 m in winter and usually persist throughout the summer). Interdecadal changes in temperature, salinity, and dissolved oxygen of the deep waters entering the Gulf at the continental shelf are related to the varying proportion of the source cold-fresh and high dissolved oxygen Labrador Current water and warm-salty and low dissolved oxygen slope water (McLellan 1957, Lauzier and Trites 1958, Gilbert et al. 2005). These waters travel from the mouth of the Laurentian Channel to the Estuary in roughly three to four years (Gilbert 2004), decreasing in dissolved oxygen from in situ respiration and oxidation of organic material as they progress to the channel heads. The lowest levels of dissolved oxygen (around 20 percent saturation in recent years) are therefore found in the deep waters at the head of the Laurentian Channel in the Estuary.

BOTTOM WATER TEMPERATURES IN AUGUST AND SEPTEMBER

The same method used to calculate bottom water temperature on the Magdalen Shallows was applied to the entire Gulf by combining all available CTD data from August and September, thus including the multispecies surveys for the northern Gulf in August and for the Magdalen Shallows in September into a single map (Figure 54). Most of the northeastern Gulf had above normal bottom temperatures, with large areas of Anticosti and Esquiman Channels above 6°C.

Time series of the bottom area covered by water in various temperature intervals were also estimated for the other regions of the Gulf based on August-September temperature profile data (Figures 55 and 56). Many areas had bottom waters colder than 0°C, and Mécatina Trough had bottom waters colder than -1°C. The figures also show compression of the bottom habitat area in the temperature range of 5–6°C in 1992. In 2012, a return of >6°C temperatures to the sea floor was observed. The bottom area covered by waters warmer than 6°C increased again in

2015 in Anticosti Channel, Esquiman Channel and Central Gulf, and reached again a record value in Anticosti Channel and Esquiman Channel while reducing bottom habitat area in the temperature range of 5–6°C.

The warm waters found at the bottom of Esquiman Channel and elsewhere are associated with the deep temperature maximum evident in the temperature profiles in these areas (e.g. Figure 3). The progression from a cold anomaly within the Gulf in 2009 to current conditions of the deep temperature maximum is shown on Figure 57. In 2012 and again in 2015, temperatures above 7°C were recorded in the Gulf near Cabot Strait. The Gulf-wide average and regional areal averages are shown in Figure 58. The deep maximum temperature Gulf-wide average was at a series record high in 2015, at 6.19°C, as were the regional averages for the northwest Gulf, Anticosti Channel and Esquiman Channel.

TEMPERATURE AND SALINITY MONTHLY MEANS

Monthly temperature and salinity averages were constructed for various depths using a method used by Petrie et al. (1996) but using the geographical regions shown in Figure 2. In this method, all available data obtained during the same month within a region and close to each depth bin are first averaged together for each year. Monthly averages from all available years and their standard deviations are then computed. This two-fold averaging process reduces the bias that occurs when the numbers of profiles in any given year are different. These monthly averages were further averaged into regional yearly time series that are presented in Figure 58 for 200 and 300 m. The 300 m observations in particular suggest that temperature anomalies are advected up-channel from Cabot Strait to the northwestern Gulf in two to three years, consistent with the findings of Gilbert (2004). The regional averages are weighted into a Gulf-wide average in accordance to the surface area of each region at the specified depth. These Gulf-wide averages are shown for 200 and 300 m in Figure 58 as well as for 150, 200, and 300 m in Figure 59. Linear trends in temperature and salinity at 300 m of 2.2°C and 0.3 per century, respectively are shown on Figure 59 (See also Galbraith et al. 2013 for other long term trends).

In 2015, the gulf-wide average salinities increased to above normal at all depths shown in Figures 58 and 59. Temperature at 200 m increased overall to reach a record-high of 5.6°C (+2.7 SD). It increased to regional record highs in the Northwest Gulf (5.2°C, +2.4 SD), Anticosti Channel (5.6°C, +2.8 SD), Esquiman Channel (5.9°C, +2.3 SD), and remained well above-normal in central Gulf (5.8°C, +2.5 SD, second highest) and Cabot Strait (6.2°C, +2.2 SD, third highest). Temperature at 250 m increased overall to reach 6.1°C (+2.8 SD); the highest on record. Temperature at 300 m increased overall to reach the record-high of 6.0°C (+3.4 SD). It increased to regional record highs in the Estuary (5.4°C, +1.8 SD), Northwest Gulf (5.8°C, +3.0 SD), Anticosti Channel (6.4°C, +3.2 SD), Esquiman Channel (6.3°C, +2.8 SD), and remained well above-normal in central Gulf (6.3°C, +3.2 SD, second highest) and Cabot Strait (6.2°C, +2.1 SD, third highest).

The warm anomaly present since 2010 at Cabot Strait (record in 2012) has been progressing up the channel towards the Estuary since then, but waters that have followed into the gulf have also remained very warm such that the average overall temperature may continue to increase (Figure 57).

DISSOLVED OXYGEN AND HYPOXIA IN THE ST. LAWRENCE ESTUARY

Figure 59 shows an update of the Gilbert et al. (2005) oxygen time series of the mean dissolved oxygen value at depths ≥ 295 m in the St. Lawrence Estuary. The value of $100 \mu\text{mol l}^{-1}$ corresponds approximately to 30% saturation, below which is considered to be hypoxic. Since some of the variability is associated with changing water masses, the temperature at 300 m in

the Estuary is also shown. The deep waters of the Estuary were briefly hypoxic in the early 1960s and have consistently been hypoxic since 1984. Dissolved oxygen decreased to its lowest annual average in 2015, at $54.5 \mu\text{mol l}^{-1}$ (-1.6 SD), corresponding to 18% saturation.

Based on interdecadal variability, the inflow of warmer waters to the Estuary is expected to deteriorate the hypoxic conditions since these waters are typically poorer in dissolved oxygen (McLellan 1957, Lauzier and Trites 1958, Gilbert et al. 2005). A change of dissolved oxygen of $147.4 \mu\text{mol l}^{-1}$ is accounted for by a 10.09°C temperature difference in source water masses in Gilbert et al. 2005, implying that a decrease of $1.46 \mu\text{mol l}^{-1}$ would be expected for each 0.1°C temperature increase (at Cabot Strait). Recent interannual variability in the Gilbert et al. 2005 updated time series did not show changes in dissolved oxygen that would have been expected to be associated with the increases in temperature. However during the last two years, the dissolved oxygen concentration decrease ($-11.7 \mu\text{mol l}^{-1}$) has been greater than expected considering the observed warming of Estuary bottom waters. The correlation between the temperature and oxygen timeseries shown on the bottom panel of Figure 63 explains 74% of the variance ($R^2 = 0.74$) and other factors can cause oxygen variability, such as interannual changes in the vertical flux of organic matter to the bottom waters of the Lower St. Lawrence Estuary.

SEASONAL AND REGIONAL AVERAGE TEMPERATURE STRUCTURE

In order to show the seasonal progression of the vertical temperature structure, regional averages are shown in Figures 60 to 63 based on the profiles collected during the March helicopter survey, the June AZMP and mackerel surveys, the August multi-species survey (September survey for the Magdalen Shallows), and the October-November AZMP survey. All additional archived CTD data for those months were also used, including a NOVA autonomous profiler deployed in June that was active until January 2016. The temperature scale was adjusted to highlight the CIL and deep-water features; the display of surface temperature variability is best suited to other tools such as remote sensing and thermographs. Average discrete depth layer conditions are summarized for the months of the 2014 and 2015 AZMP surveys in Figure 64 for temperature and in Figure 65 for salinity and 0-50 m stratification. For each survey the anomalies were computed relative to monthly temperature and salinity 1981-2010 climatologies calculated for each region, shown in grey as the mean value ± 0.5 SD in Figures 60 to 63.

The March water temperature conditions are shown in Figure 60 but caution is needed in interpreting the profiles. Indeed, regional averaging of winter profiles does not work very well in the northeast Gulf (regions 3 and 4) because very different water masses are present in the area such as the cold Labrador Shelf intrusion with saltier and warmer deeper waters of Anticosti Channel or Esquiman Channel. For example, the sudden temperature increase near the bottom of Mécatina Trough in 2015 resulted from the deepest cast used in each of the averages, which contained warmer waters. Large changes near 200 m are due to our usual sampling cutoff near 200 m for the March airborne survey, with some casts being slightly deeper than others. The highlights of March water temperatures shown in Figure 60 include the previously discussed winter mixed layer, with below-normal temperatures and above-normal thickness. The thermocline was much shallower than usual in most regions, associated with temperatures well above normal at 200 m. Waters deeper than 100 m in Mécatina Trough were much warmer than normal, indicating no deep renewal from a Labrador Shelf intrusion.

Temperatures in June and August 2015 (Figures. 58 and 59 and summary in Figure 64) were characterized by CIL conditions that were below normal in thickness. The CIL temperature minimum was usually high in the Estuary. Deep-water temperatures were above normal in all

regions along the Laurentian Channel, with most regions showing increases compared with 2014 conditions in waters shallower than 250 m depth. Temperatures at the depth of the temperature maximum (200 to >250 m) remained above normal in Esquiman Channel and central Gulf, exceeding 6°C at depth, presumably advected in from the Cabot Strait recent record-high conditions. Deep waters in Mécatina Trough were colder in June than in March, indicating a later-than-usual intrusion from the Labrador Shelf, but returned to warmer conditions by August, then cold again in the fall (see also Figure 64). These changes indicate much more variability than is usually observed, with the warmer and saltier waters corresponding more to Esquiman Channel waters than typical Mécatina Trough waters. Waters beneath the CIL were much warmer and saltier than normal in the Estuary in November (Figure 63), indicating enhanced deep circulation into the Estuary.

CURRENTS AND TRANSPORTS

Currents and transports are derived from a numerical model of the Gulf of St. Lawrence, Scotian Shelf, and Gulf of Maine. The model is prognostic, i.e., it allows for evolving temperature and salinity fields. It has a spatial resolution of 1/12° with 46 depth-levels in the vertical. The atmospheric forcing is taken from the Global Environmental Multiscale (GEM) model running at the Canadian Meteorological Center (CMC). Freshwater runoff is obtained from observed data and the hydrological model, as discussed in the freshwater runoff section. A simulation was run for 2006–2015 from which transports were calculated. The reader is reminded that the results outlined below are not measurements but simulations and improvements in the model may lead to changes in the transport values.

Figures 66–68 show seasonal depth-averaged currents for 0–20 m, 20–100 m, and 100 m to the bottom for 2015. Currents are strongest in the surface mixed layer, generally 0–20 m, except in winter months when the 20–100 m and the 100 m to bottom averages are almost as high (note the different scale for this depth). Currents are also strongest along the slopes of the deep channels. The Anticosti Gyre is always evident but strongest during winter months, when it even extends strongly into the bottom-average currents.

Monthly averaged transports across seven sections of the Gulf of St. Lawrence are shown in Figure 69 for sections with estuarine circulation, and in Figure 70 for sections where only net transports are relevant. In Figure 69, the net transport integrates both up and downstream circulation and, for example, corresponds to freshwater runoff at the Pointe-des-Monts section. The outflow transport integrates all currents heading toward the ocean, while the estuarine ratio corresponds to the outflow divided by the net transports.

Transports through sections under the direct estuarine influence of the St. Lawrence River (e.g., Pointe-des-Monts) have a more direct response to change in freshwater runoff while others (e.g., Cabot Strait, Bradelle Bank) have a different response, presumably due to redistribution of circulation in the GSL under varying runoff. The estuarine circulation ratio is determined by the mixing intensities within the estuary and is greatly influenced by stratification. It is on average greatest during winter months and weakest during the spring freshet. In fact, it is sufficiently reduced in spring that the overall outward transport at Pointe-des-Monts reaches its minimum value in June even though this month corresponds to the third highest net transport of the year, i.e. the estuary becomes sufficiently stratified that fresh water runoff tends to slip on top of the denser salty waters underneath. In 2015, the estuarine ratio at Pointe-des-Monts was above-normal in late winter and early spring. The below-normal spring freshet led to above-normal Estuarine ratio and, perhaps paradoxically, above-normal outward transport at the Pointe-des-Monts section (e.g. enhanced estuarine entrainment).

HIGH FREQUENCY SAMPLING AZMP STATIONS

Sampling by the Maurice Lamontagne Institute began in 1991 at a station offshore of Rimouski (48° 40' N 68° 35' W, 320 m depth; Plourde et al. 2009), typically once a week during summer and less often during spring and fall and almost never in winter (Figure 71). In 2013, following several analyses that identified good correlations and correspondences between the prior AZMP Anticosti Gyre and Gaspé Current stations with the Rimouski station, it was decided to drop sampling efforts at these logistically difficult stations and integrate the Rimouski station officially in the AZMP program. The AZMP station in the Shediac Valley (47° 46.8' N, 64° 01.8' W, 84 m depth) is sampled on a regular basis by the Bedford Institute of Oceanography as well as occasionally by DFO Gulf Region and by the Maurice Lamontagne Institute during their Gulf-wide surveys (Figure 71). This station has been sampled irregularly since 1947, nearly every year since 1957, and more regularly during the summer months since 1999 when the AZMP program began. However, observations were mostly limited to temperature and salinity prior to 1999.

Isotherms and isohalines as well as monthly averages of layer temperature and salinity, stratification, and CIL core temperature and thickness at <1°C are shown for 2011-2015 for the Rimouski station in Figure 72 and for the Shediac Valley station in Figure 73. The scorecard climatologies are calculated from 1991-2010 data for Rimouski station, and for 1981-2015 for Shediac Valley (given the sparseness of data prior to 1999).

At the Rimouski station in 2015, the CIL typically had much below-normal thickness and above-normal minimum temperature, with higher anomalies than those prevailing in the Gulf. At 200-300 m, the gradual shift of cold-fresh waters present in 2010 to warmer-saltier waters advected from Cabot Strait lead to a shift to warm anomalies by May 2013 and series records in temperature (5.55°C) observed in September of 2015. The thermograph network also shows a Rimouski station series record of the daily average temperature (since 2005) of 5.57°C occurring in September, and a record-high monthly average of 5.52°C (Figures 27 and 33).

A mooring measuring temperature and salinity at multiple depths was deployed at Shediac Valley station in June and rotated in October such that the data from June to September are currently available. Because of the sparse sampling at this station, the monthly averages at 10, 20, 30 and 75 m of Figure 73 were calculated using the mooring data rather than the monitoring sorties data. This eliminated strong anomalies that would have been estimated for the shallower depths but did not alter the anomalies significantly at 75 m. Temperatures were generally near-normal at Shediac Valley station over the season.

Figure 74 shows the interannual variability of some bulk layer averages from May to October for the two stations. Bulk surface layer temperature, salinity and CIL minimum temperature were above normal at Rimouski station while stratification was below normal. Near-bottom temperature (290 m) was at a record high. Bulk surface layer (0-50 m) temperature and salinity, as well as bottom temperature, were above-normal at Shediac Valley station in 2015. Since these bulk layer averages are calculated from profile data, the mooring data were not used here and the results at Shediac Valley are likely aliased. An automatic CTD is planned for deployment in summer 2016 and will yield much more reliable results.

OUTLOOK FOR 2015

Air temperatures were respectively 2.5°C and 2.1°C above-normal over the Gulf in January and February 2016, but below-normal by 1.4°C in March. This was the setting for the March 2016 survey, which provides an outlook for CIL conditions expected for the remainder of 2016. Figure 75 shows the surface mixed layer temperature, salinity, and thickness (at $T < -1^{\circ}\text{C}$ and $T < 0^{\circ}\text{C}$),

as well as the thickness and extent of the cold and saline layer that has intruded into the Gulf from the Labrador shelf. A large portion of the winter mixed layer was warm, above -1°C . The overall thickness and volume of the layer colder than -1°C was 0.6 SD below normal and the Cold Intermediate Layer for summer 2016 is therefore forecasted to be warmer than in 2015, with a Gilbert and Pettigrew (1997) index of around $+0.07^{\circ}\text{C}$ compared to -0.28°C in 2015.

Concerning deep waters, recall that record high temperatures were recorded in Cabot Strait in 2012 and again in 2014, and that overall the Gulf waters below 150 m were in 2015 at a 100-year record high. There were 14 stations sampled in March 2016 with some deep-water temperatures greater than 6°C , located from Cabot Strait up to Centre Gulf. One station had its deep temperature maximum reaching 7.17°C . This signifies the continuation of warmer than normal conditions at depth.

SUMMARY

Figure 76 summarizes SST, summertime CIL and deep-water average temperatures. For May-November SST, a proxy is used prior to 1985 using the April-November air temperature anomaly averaged over all stations of Figure 4 except the two from the Estuary, similar to the index developed in Galbraith et al. (2012). Figure 76 shows a decrease from 2014 values for May-November average SST, but increases for the average temperature at 200 m and 300m, as well as for the CIL temperature minimum. The SST was near-normal, temperature at 200 m and 300 m were the highest on record (5.6°C , $+2.7$ SD and 6.1°C , $+3.4$ SD). The CIL temperature minimum was above-normal ($+0.5$ SD) in contrast to the colder than normal winter air temperatures (-1.5°C , -1.0 SD).

Another summary of the temperature state of the Gulf of St. Lawrence over a shorter time span (since 1971) allows the inclusion of more data sets, and three sets of four time series are chosen to represent surface, intermediate and deep conditions (Figure 77). Here, sea-ice is grouped as an intermediate feature since all are associated with winter formation. Figure 77 shows the sums of these three sets of anomalies representing the state of different parts of the system and is reproduced on Figure 78 with each time series contribution shown as stacked bars (Petrie et al. 2007). These composite indices measure the overall state of the climate system with positive values representing warm conditions and negative representing cold conditions. The plot also indicates the degree of correlation between the various measures of the environment. In 2015, the surface index decreased to the 5th largest in the series, the intermediate index was near-normal and the deep index increased to a record high value.

KEY FINDINGS

- The annual average runoff from the St. Lawrence River measured at Québec City and RIVSUM II was below-normal and near-normal in 2015 ($11\ 100\ \text{m}^3\text{s}^{-1}$, -1.0 SD and $17\ 000\ \text{m}^3\text{s}^{-1}$, $+0.1$ SD respectively). The spring freshet was below-normal at -1.1 SD and -0.5 SD, but timing was normal.
- The estuarine ratio at Pointe-des-Monts was above-normal in late winter and early spring. The below-normal spring freshet led to above-normal Estuarine ratio and, perhaps paradoxically, above-normal outward transport at the Pointe-des-Monts section.
- April-November air temperatures were normal with an anomaly of 0.0°C . Air temperatures in August were the second warmest on record (since 1873, $+2.2^{\circ}\text{C}$, $+2.8$ SD) when averaged over all stations, including series record highs at four stations.

-
- Winter (December-March) air temperatures were below normal by -1.5°C (-1.0 SD), the coldest since 1993.
 - Annual mean air temperature anomaly in 2015 were near normal over the Gulf (-0.4°C , -0.4 SD).
 - The winter surface mixed cold layer ($<- 1^{\circ}\text{C}$) volume of $13\,300\text{ km}^3$ was 0.5 SD above the 1996–2015 average. The Labrador Shelf water intrusion into Mécatina Trough was at a series low in March 2015, representing only 2% (-1.3 SD) of the cold water in the Gulf.
 - Sea ice maximum volume was slightly above-normal ($+0.6$ SD) at 86 km^3 . Most of it was formed during the month of February, coldest since 1993.
 - The August cold intermediate layer (CIL) showed warmer ($+0.8$ SD) and thinner (-1.5 SD for volume colder than 1°C) than normal conditions in spite of the cold winter. The Gilbert & Pettigrew minimum temperature index, which includes data over a longer season, was however near-normal ($+0.3$ SD).
 - In 2015, the timing of summer onset was near-normal while post-season cooling was later than normal ($+1.7$ weeks, $+1.4$ SD). The Estuary, Northwest Gulf, Anticosti Channel and Mecatina Trough had longer than normal seasons with surface temperature above 10°C (from $+0.8$ to $+1.5$ SD, about two weeks longer), while the rest were near-normal.
 - May–November sea-surface temperatures averaged over the Gulf were generally below normal until July and above normal from in August and September 2015, leading to a near-normal May–November average ($+0.3^{\circ}\text{C}$, $+0.5$ SD). Record highs were nevertheless reached in September averaged over the Gulf ($T=14.3^{\circ}\text{C}$, above normal by $+1.8^{\circ}\text{C}$ and 2.3 SD) and in the following regions: Estuary ($+1.9^{\circ}\text{C}$, $+2.3$ SD), Northwest Gulf ($+1.9^{\circ}\text{C}$, $+1.9$ SD), Anticosti Channel ($+2.1^{\circ}\text{C}$, $+2.1$ SD) and Magdalen Shallows ($+1.4^{\circ}\text{C}$, $+2.0$ SD).
 - Water masses in Mécatina Trough were exchanged more frequently than usual, beginning with a renewal from a Labrador Shelf intrusion that came in only after the March survey.
 - Deep water temperatures have been increasing overall in the Gulf, with inward advection from Cabot Strait where temperature had reached a record high (since 1915) in 2012 at 200 m. Temperature averaged over the Gulf at depths from 150 to 300 m all show record highs in 2015 and stand above 6°C at 250 and 300 m for the first time since 1915.
 - Bottom area covered by waters warmer than 6°C increased in 2015 in Anticosti Channel, Esquiman Channel and Central Gulf, and reached a record value in Anticosti Channel and Esquiman Channel while reducing its bottom habitat area in the temperature range of 5 – 6°C .

ACKNOWLEDGEMENTS

We are grateful to the people responsible for CTD data acquisition during the surveys used in this report:

- Rimouski station monitoring: Roger Pigeon, Félix St-Pierre, Michel Rousseau, Sylvain Chartrand, Pierre Joly, Lily St-Amand, Line McLaughlin, Marie-Lyne Dubé, Michel Starr, Yves Gagnon, Rémi Desmarais, François Villeneuve, Caroline Lafleur, Jean-François St-Pierre, Michael Scarratt, Peter Galbraith, Bernard Pelchat, Isabelle St-Pierre, Laure Devine.
- March 2015 helicopter survey: Peter Galbraith, Rémi Desmarais; helicopter pilot Michel Dubé; aircraft technician Barry Conrad.

-
- June AZMP transects: Yves Gagnon, Michel Rousseau, Sylvain Chartrand, Marie-Lyne Dubé, François Villeneuve, Kim Émond, Johanne Guérin, Benoît Légaré, Isabelle St-Pierre, Roger Pigeon, Linda Girard; the officers and crew of the CCGS Teleost.
 - August Multi-species survey: Sylvain Chartrand, Michel Rousseau, Bernard Pettigrew, Caroline Lafleur; the officers and crew of the CCGS Teleost.
 - October-November AZMP survey: Pierre Joly, Yves Gagnon, Félix St-Pierre, Jean-François St-Pierre, François Villeneuve, Sonia Michaud, Caroline Lafleur, Jean-Pierre Allard, Michel Starr, Marie-Lyne Dubé, Laure Devine, Lily St-Amand, Roger Pigeon, Joana Roma, Jory Cabrol, Angélique Ollier, Roxanne Sage; the officers and crew of the CCGS Hudson.
 - September Multi-species survey: Luc Savoie for providing the CTD data.
 - Northumberland Strait survey: Chief scientists Mark Hanson and Joël Chassé.
 - Data management: Laure Devine, Caroline Lafleur, Isabelle St-Pierre.
 - CTD maintenance: Roger Pigeon, Félix St-Pierre, Michel Rousseau, Sylvain Chartrand.

Data from the following sources are also gratefully acknowledged:

- Air temperature: Environment Canada.
- Sea-ice: Canadian Ice Service, Environment Canada. Processing of GIS files by Paul Nicot.
- Runoff at Québec City: Denis Lefavre.
- Runoff from hydrological modelling: Joël Chassé and Diane Lavoie.
- Thermograph network: Bernard Pettigrew, Rémi Desmarais, Félix St-Pierre.
- Historical AVHRR SST remote sensing (IML): Pierre Larouche, Bernard Pettigrew.
- AVHRR SST remote sensing (BIO): Carla Caverhill.

All figures were made using the free software Gri (Kelley and Galbraith 2000).

We are grateful to David Hebert and Eugene Colbourne for reviewing the manuscript and providing insightful comments.

REFERENCES

- Benoît, H.P., Savenkoff, C., Ouellet, P., Galbraith, P.S., Chassé, J. and Fréchet, A. 2012. Impacts of fishing and climate-driven changes in exploited marine populations and communities with implications for management, in State-of-the-Ocean Report for the Gulf of St. Lawrence Integrated Management (GOSLIM) Area, H. P. Benoît, J. A. Gagné, C. Savenkoff, P. Ouellet and M.-N. Bourassa, Eds. Can. Man. Rep. Fish. Aquat. Sci. 2986: viii + 73 pp.
- Bourgault, D. and Koutitonsky, V.G. 1999. Real-time monitoring of the freshwater discharge at the head of the St. Lawrence Estuary. *Atmos. Ocean*, 37 (2): 203–220.
- Colbourne, E., Holden, J., Senciall, D., Bailey, W., Craig, J. and Snook, S. 2015. [Physical Oceanographic Conditions on the Newfoundland and Labrador Shelf during 2014](#). DFO Can. Sci. Advis. Sec. Res. Doc. 2015/053. v+ 37 p.
- Cyr, F., Bourgault, D. and Galbraith, P.S. 2011. Interior versus boundary mixing of a cold intermediate layer. *J. Geophys. Res. (Oceans)*, 116, C12029, doi:10.1029/2011JC007359.

-
- Dutil, J.-D., Proulx, S., Galbraith, P.S., Chassé, J., Lambert, N. and Laurian, C. 2012. Coastal and epipelagic habitats of the estuary and Gulf of St. Lawrence. *Can. Tech. Rep. Fish. Aquat. Sci.* 3009: ix + 87 p.
- Galbraith, P.S. 2006. Winter water masses in the Gulf of St. Lawrence. *J. Geophys. Res.*, 111, C06022, doi:10.1029/2005JC003159.
- Galbraith, P. S., and Grégoire, F. 2015. [Habitat thermique du maquereau bleu; profondeur de l'isotherme de 8 °C dans le sud du golfe du Saint-Laurent entre 1960 et 2014](#). *Secr. can. de consult. sci. du MPO. Doc. de rech.* 2014/116. v + 13 p.
- Galbraith, P.S. and Larouche, P. 2011. Sea-surface temperature in Hudson Bay and Hudson Strait in relation to air temperature and ice cover breakup, 1985-2009. *J. Mar. Systems*, 87, 66-78.
- Galbraith, P.S. and Larouche, P. 2013. Trends and variability in eastern Canada sea-surface temperatures. Ch. 1 (p. 1-18) In: *Aspects of climate change in the Northwest Atlantic off Canada* [Loder, J.W., G. Han, P.S. Galbraith, J. Chassé and A. van der Baaren (Eds.)]. *Can. Tech. Rep. Fish. Aquat. Sci.* 3045: x + 190 p.
- Galbraith, P.S., Saucier, F.J., Michaud, N., Lefavre, D., Corriveau, R., Roy, F., Pigeon, R. and Cantin, S. 2002. [Shipborne monitoring of near-surface temperature and salinity in the Estuary and Gulf of St. Lawrence](#). *Atlantic Zone Monitoring Program Bulletin*, Dept. of Fisheries and Oceans Canada. No. 2: 26–30.
- Galbraith, P.S., Desmarais, R., Pigeon, R. and Cantin, S. 2006. [Ten years of monitoring winter water masses in the Gulf of St. Lawrence by helicopter](#). *Atlantic Zone Monitoring Program Bulletin*, Dept. of Fisheries and Oceans Canada. No. 5: 32–35.
- Galbraith, P.S., Gilbert, D., Lafleur, C., Larouche, P., Pettigrew, B. 2007. [Physical oceanographic conditions in the Gulf of St. Lawrence in 2006](#). *DFO Can. Sci. Advis. Sec. Res. Doc.* 2007/024, iv + 51 pp.
- Galbraith, P. S., Larouche, P., Gilbert, D., Chassé, J. and Petrie, B. 2010. [Trends in sea-surface and CIL temperatures in the Gulf of St. Lawrence in relation to air temperature](#). *Atlantic Zone Monitoring Program Bulletin*, 9: 20-23.
- Galbraith P.S., Larouche, P., Chassé, J., Petrie, B. 2012. Sea-surface temperature in relation to air temperature in the Gulf of St. Lawrence: interdecadal variability and long term trends. *Deep Sea Res. II*, V77–80, 10–20.
- Galbraith. P.S., Hebert, D., Colbourne, E. and Pettipas, R. 2013. Trends and variability in eastern Canada sub-surface ocean temperatures and implications for sea ice. Ch.5 In: *Aspects of climate change in the Northwest Atlantic off Canada* [Loder, J.W., G. Han, P.S. Galbraith, J. Chassé and A. van der Baaren (Eds.)]. *Can. Tech. Rep. Fish. Aquat. Sci.* 3045: x + 192 p.
- Galbraith, P.S., Chassé, J., Nicot, P., Caverhill, C., Gilbert, D., Pettigrew, B., Lefavre, D., Brickman, D., Devine, L., and Lafleur, C. 2015. [Physical Oceanographic Conditions in the Gulf of St. Lawrence in 2014](#). *DFO Can. Sci. Advis. Sec. Res. Doc.* 2015/032. v + 82 p.
- Gilbert, D. 2004. Propagation of temperature signals from the northwest Atlantic continental shelf edge into the Laurentian Channel. *ICES CM*, 2004/N:7, 12 pp.
- Gilbert, D. and Pettigrew, B. 1997. Interannual variability (1948-1994) of the CIL core temperature in the Gulf of St. Lawrence. *Can. J. Fish. Aquat. Sci.*, 54 (Suppl. 1): 57–67.

-
- Gilbert, D., Galbraith, P.S., Lafleur, C. and Pettigrew, B. 2004. [Physical oceanographic conditions in the Gulf of St. Lawrence in 2003](#). DFO Can. Sci. Advis. Sec. Res. Doc. 2004/061, 63 pp.
- Gilbert, D., Sundby, B., Gobeil, C., Mucci, A. and Tremblay, G-H. 2005. A seventy-two-year record of diminishing deep-water oxygen in the St. Lawrence estuary: The northwest Atlantic connection. *Limnol. Oceanogr.*, 50(5): 1654–1666.
- Hammill, M.O. and Galbraith, P.S. 2012. Changes in seasonal sea-ice cover and its effect on marine mammals, in State-of-the-Ocean Report for the Gulf of St. Lawrence Integrated Management (GOSLIM) Area, H. P. Benoît, J. A. Gagné, C. Savenkoff, P. Ouellet and M.-N. Bourassa, Eds. *Can. Man. Rep. Fish. Aquat. Sci.* 2986: viii + 73 pp.
- Hebert, D., Pettipas, R., Brickman, D., and Dever, M. 2015. Meteorological, Sea Ice and [Physical Oceanographic Conditions on the Scotian Shelf and in the Gulf of Maine during 2014](#). DFO Can. Sci. Advis. Sec. Res. Doc. 2015/040. v + 49 p.
- Kalnay, E., Kanamitsu, M., Kistler, R., Collins, W., Deaven, D., Gandin, L., Iredell, M., Saha, S., White, G., Woollen, J., Zhu, Y., Chelliah, M., Ebisuzaki, W., Higgins, W., Janowiak, J., Mo, K., Ropelewski, C., Wang, J., Leetmaa, A., Reynolds, R. Jenne, R. and Josephé, D. 1996. The NCEP/NCAR 40-year reanalysis project. *Bull. Am. Meteorol. Soc.* 77, 437–470.
- Kelley, D.E. and Galbraith, P.S. 2000. Gri: A language for scientific illustration, *Linux J.*, 75, 92–101.
- Lauzier, L.M. and Trites, R.W. 1958. The deep waters of the Laurentian Channel. *J. Fish. Res. Board Can.* 15: 1247–1257.
- McLellan, H.J. 1957. On the distinctness and origin of the slope water off the Scotian Shelf and its easterly flow south of the Grand Banks. *J. Fish. Res. Board Can.* 14: 213–239.
- Petrie, B., Drinkwater, K., Sandström, A., Pettipas, R., Gregory, D., Gilbert, D. and Sekhon, P. 1996. Temperature, salinity and sigma-t atlas for the Gulf of St. Lawrence. *Can. Tech. Rep. Hydrogr. Ocean Sci.*, 178: v + 256 pp.
- Petrie, B., Pettipas, R.G. and Petrie, W.M. 2007. [An overview of meteorological, sea ice and sea surface temperature conditions off eastern Canada during 2006](#). DFO Can. Sci. Advis. Sec. Res. Doc. 2007/022.
- Plourde, S., Joly, P., St-Amand, L. and Starr, M. 2009. La station de monitoring de Rimouski : plus de 400 visites et 18 ans de monitoring et de recherche. *Atlantic Zone Monitoring Program Bulletin*, Dept. of Fisheries and Oceans Canada. No. 8: 51-55.
- Tamdrari, H., Castonguay, M., Brêthes, J.-C., Galbraith, P.S. and Duplisea, D.E. 2012. The dispersal pattern and behaviour of cod in the northern Gulf of St. Lawrence: results from tagging experiments, *Can. J. Fish. Aquat. Sci.*, 69: 112-121.
- Therriault, J.-C., Petrie, B., Pépin, P., Gagnon, J., Gregory, D., Helbig, J., Herman, A., Lefavre, D., Mitchell, M., Pelchat, B., Runge, J. and Sameoto, D. 1998. Proposal for a Northwest Atlantic zonal monitoring program. *Can. Tech. Rep. Hydrogr. Ocean Sci.*, 194: vii + 57 pp.
- Vincent, L. A., Wang, X.L., Milewska, E.J., Wan, H., Yang, F. and Swail, V. 2012. A second generation of homogenized Canadian monthly surface air temperature for climate trend analysis. *J. Geophys. Res.* 117, D18110, doi:10.1029/2012JD017859.

FIGURES

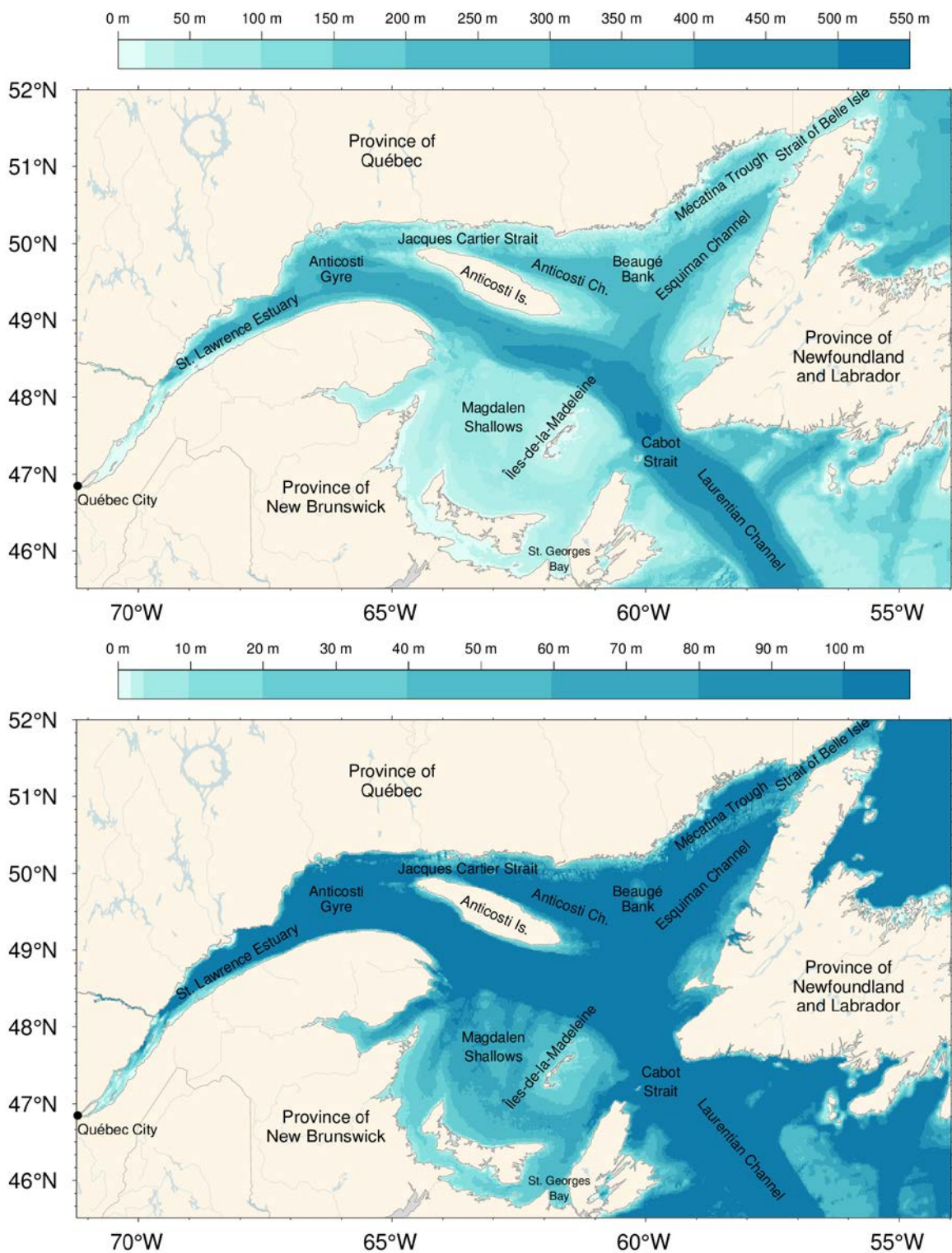


Figure 1. The Gulf of St. Lawrence. Locations discussed in the text are indicated. Bathymetry datasets used are from the Canadian Hydrographic Service to the west of $56^{\circ}47' W$ (with some corrections applied to the baie des Chaleurs and Magdalen Shallows) and TOPEX data to the east. Bottom panel shows detail for 0-100 m bathymetry.

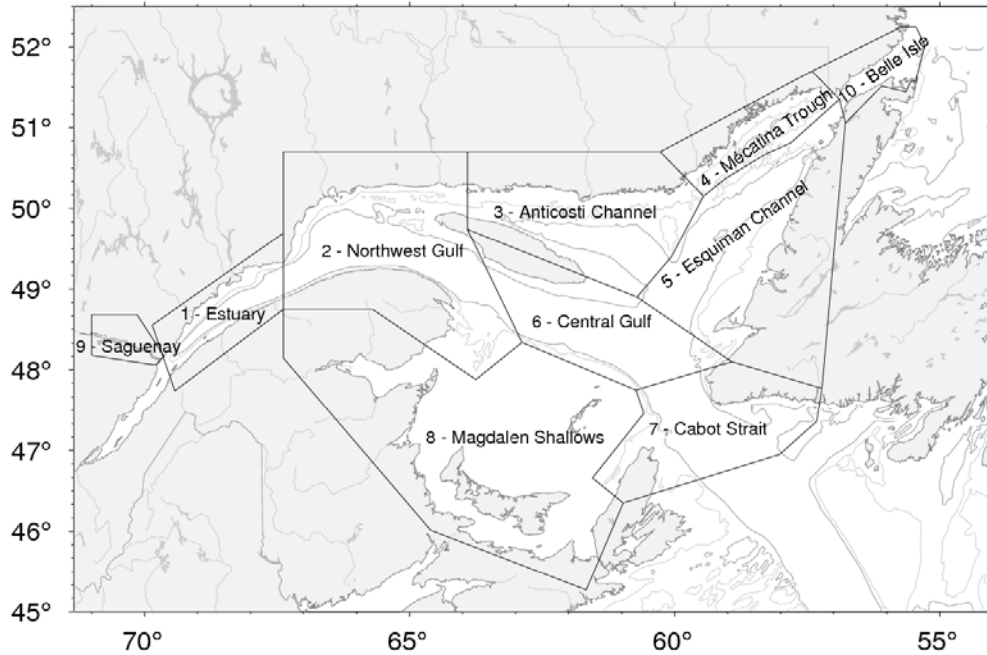


Figure 2. Gulf of St. Lawrence divided into oceanographic regions. The first eight are typically used in this report.

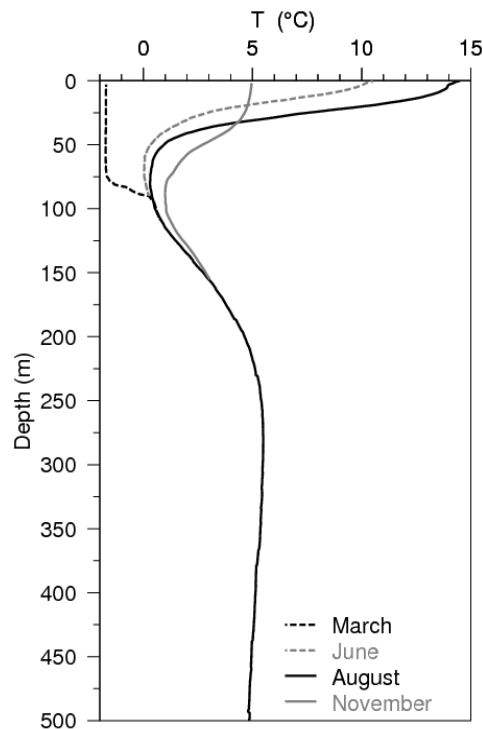


Figure 3. Typical seasonal progression of the depth profile of temperature observed in the Gulf of St. Lawrence. Profiles are averages of observations in August, June and November 2007 in the northern Gulf. The dashed line at left shows a single winter temperature profile (March 2008), with near freezing temperatures in the top 75 m. The cold intermediate layer (CIL) is defined as the part of the water column that is colder than 1°C, although some authors use a different temperature threshold. Figure from Galbraith et al. (2012).

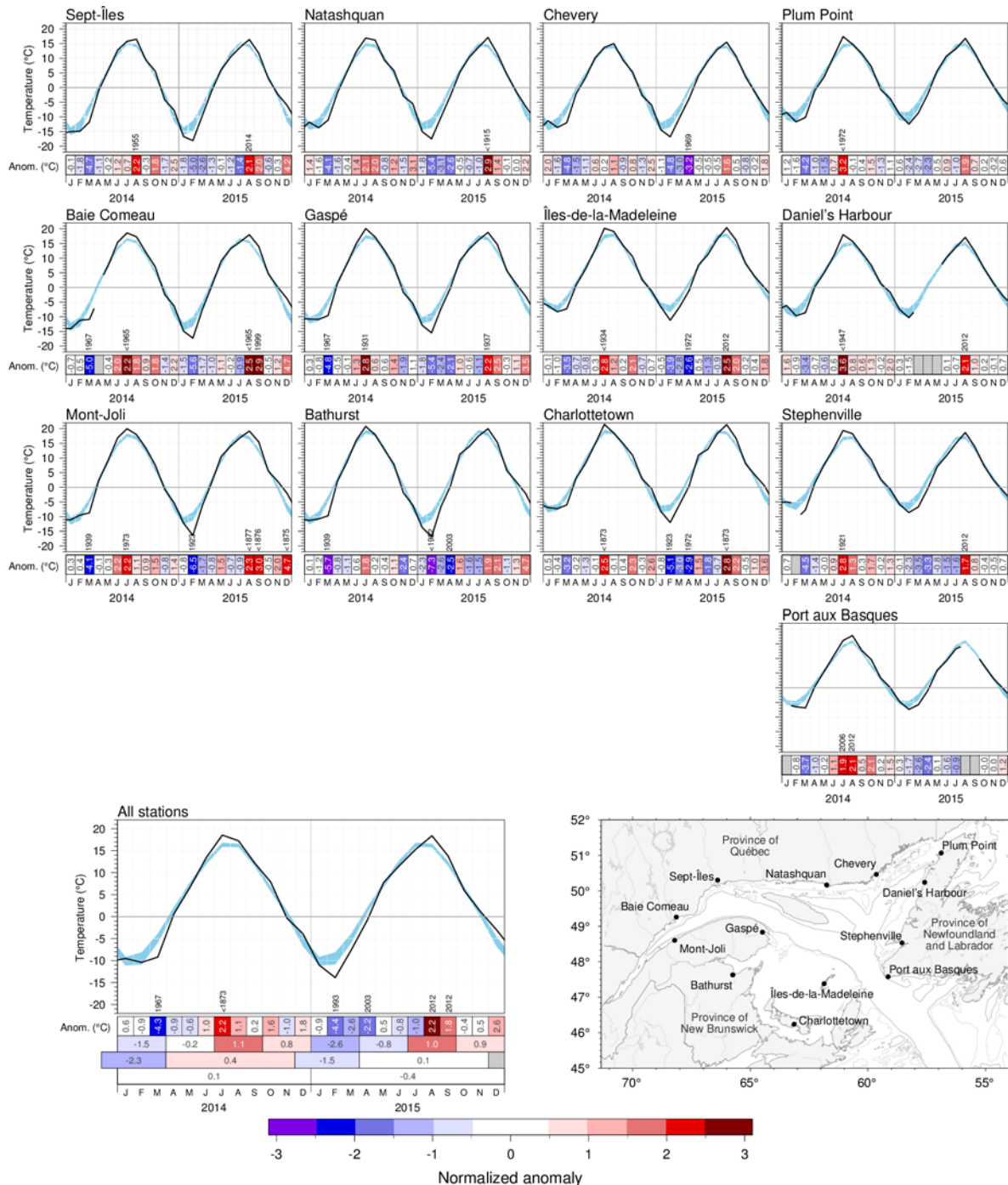


Figure 4. Monthly air temperatures and anomalies for 2014 and 2015 at selected stations around the Gulf as well as the average for all stations. The blue area represents the 1981–2010 climatological monthly mean ± 0.5 SD. Months with 4 or more days of missing data are omitted. The bottom scorecards are colour-coded according to the monthly normalized anomalies based on the 1981–2010 climatologies for each month, but the numbers are the monthly anomalies in $^{\circ}\text{C}$. For anomalies greater than 2 SD from normal, the prior year with a greater anomaly is indicated. Seasonal, December–March, April–November and annual anomalies are included for the all-station average.

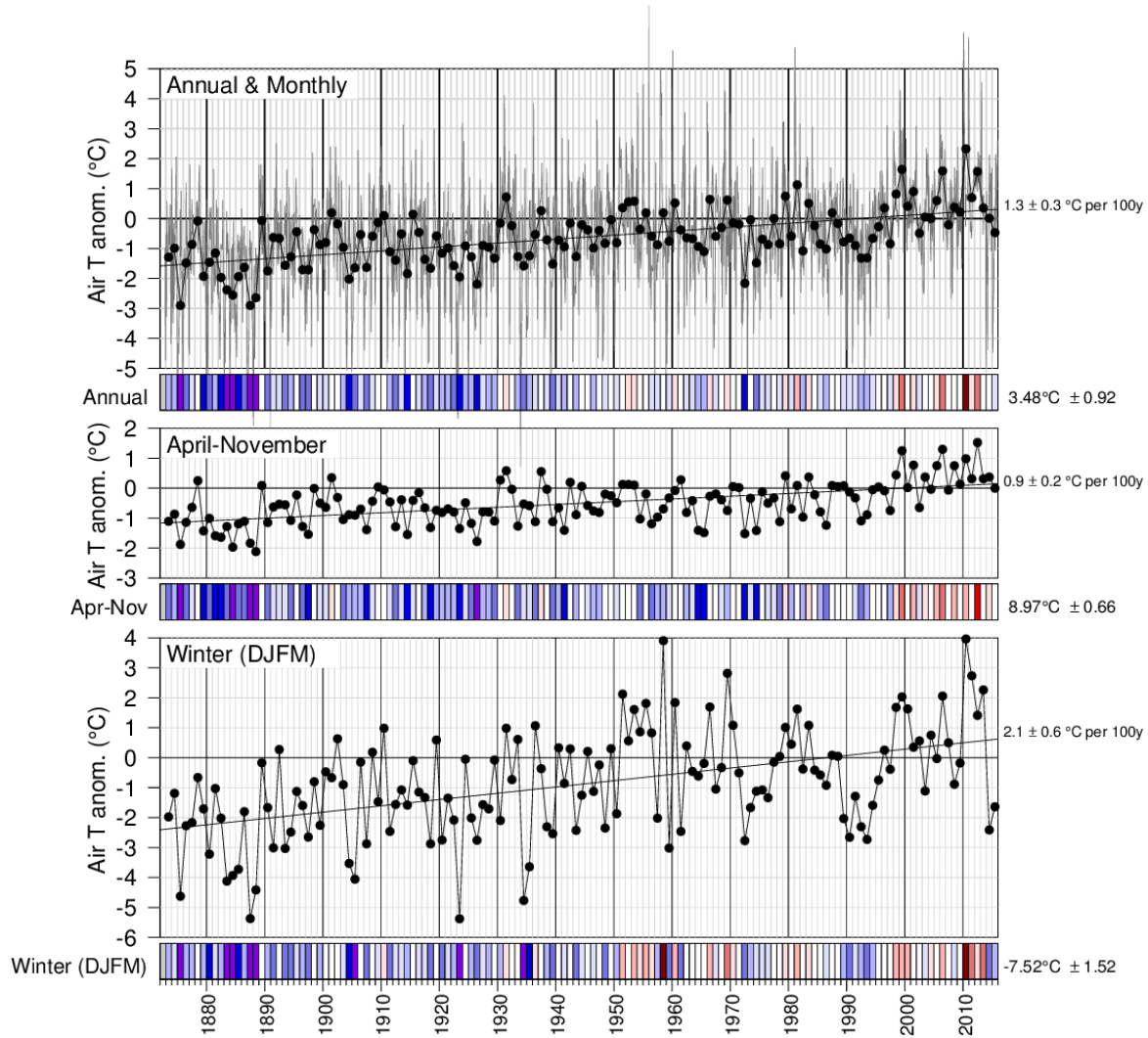


Figure 5 Annual, April–November December–March mean air temperature anomalies averaged for the selected stations around the Gulf from Figure 4. The bottom scorecards are colour-coded according to the normalized anomalies based on the 1981–2010 climatology. Trends plus and minus their 95% confidence intervals are shown. April–November air temperature anomalies tend to be highly-correlated with May–November sea-surface temperature anomalies (Galbraith et al. 2012; Galbraith and Larouche 2013) whereas winter air temperature anomalies correlate highly with sea-ice cover parameters and winter mixed-layer volumes (Galbraith et al. 2010; Galbraith et al. 2013).

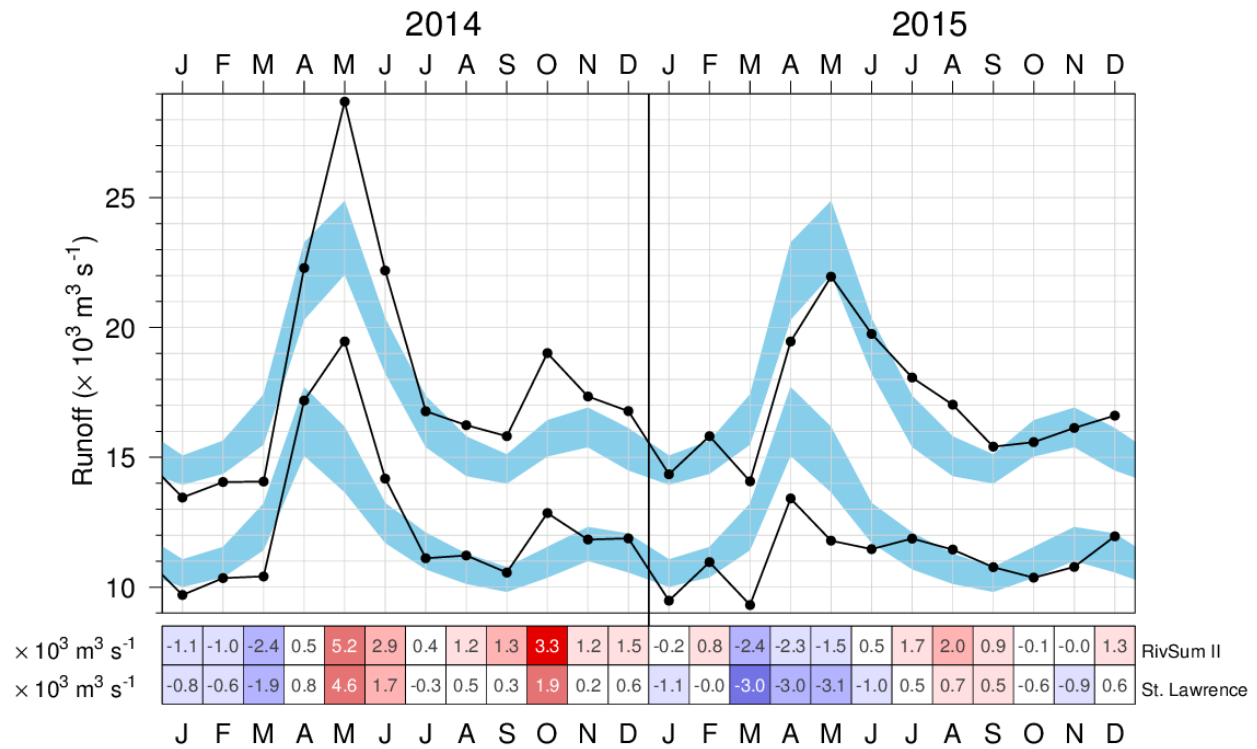


Figure 6. Monthly mean freshwater flow of the St. Lawrence River at Québec City (lower curve) and its sum with rivers flowing into the St. Lawrence Estuary (RIVSUM II, upper curve). The 1981–2010 climatological mean (± 0.5 SD) is shown (blue shading). The scorecards are colour-coded according to the monthly anomalies normalized for each month of the year, but the numbers are the actual monthly anomalies in $10^3 \text{ m}^3 \text{ s}^{-1}$.

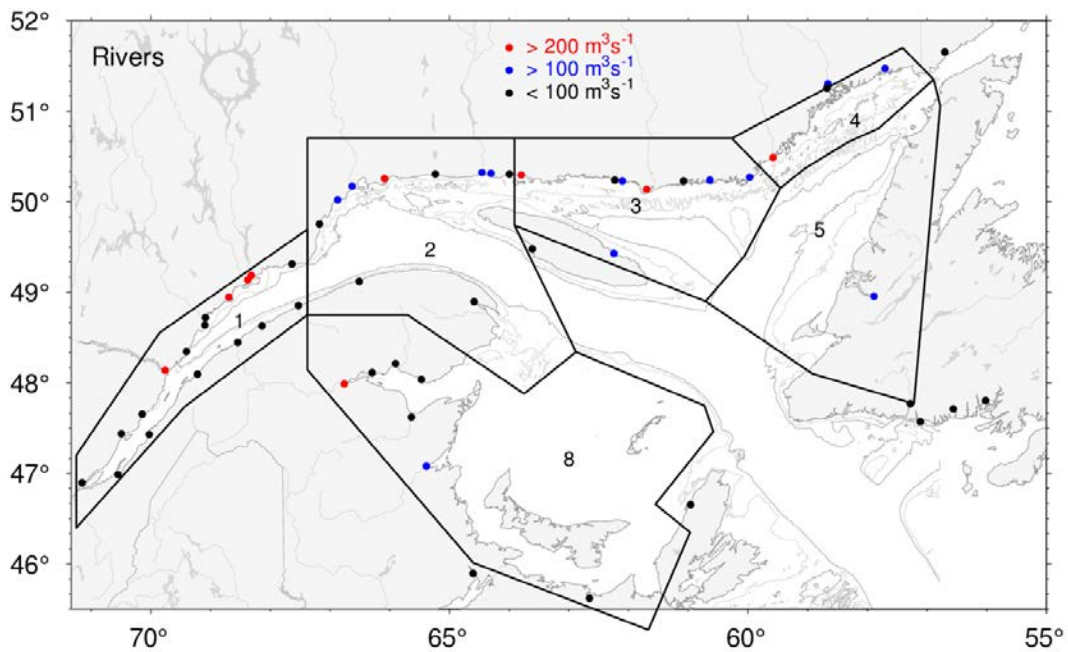


Figure 7. River discharge locations for the regional sums of runoffs listed in Table 2. Red and blue dots indicate rivers that have climatological mean runoff greater than $200 \text{ m}^3 \text{ s}^{-1}$ and between 100 and $200 \text{ m}^3 \text{ s}^{-1}$, respectively.

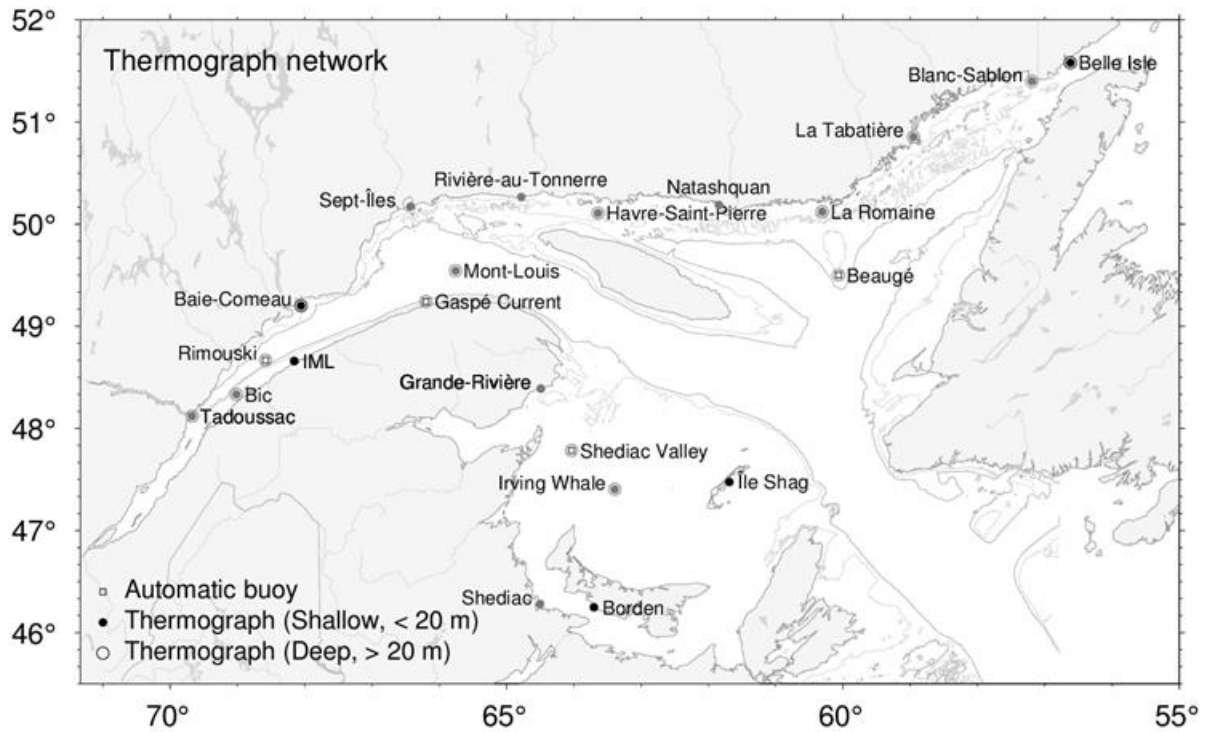


Figure 10. Locations of the Maurice Lamontagne Institute thermograph network stations in 2015, including oceanographic buoys that transmit data in real time (squares). Deep and shallow instruments are denoted by open circles and dots, while seasonal and year-round deployments are denoted by gray and black symbols. Shédiac station from DFO Gulf Region is also shown.

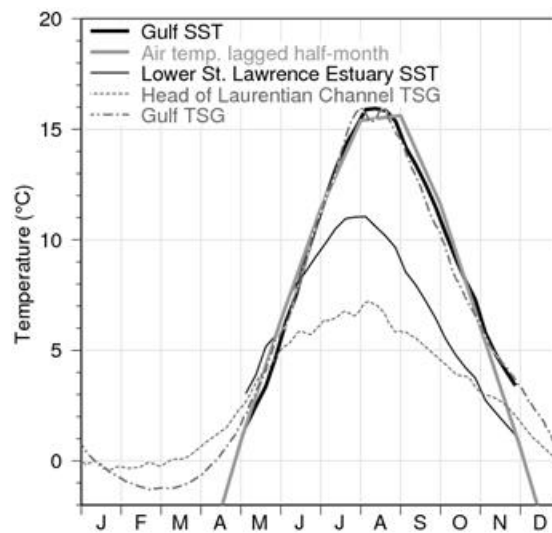


Figure 11. Sea-surface temperature climatological seasonal cycle in the Gulf of St. Lawrence. AVHRR temperature weekly averages for 1985 to 2010 are shown from May to November (ice-free months) for the entire Gulf (thick black line) and the cooler Lower St. Lawrence Estuary (thin black line), defined as the area west of the Pointe-des-Monts section and east of approx 69°30'W. Thermosalinograph data averages for 2000 to 2010 are shown for the head of the Laurentian Channel (at 69°30'W, grey dashed line) and for the average over the Gulf waters along the main shipping route between the Pointe-des-Monts and Cabot Strait sections (gray dash-dotted line). Monthly air temperature averaged over eight stations in the Gulf of St. Lawrence are shown offset by 2 weeks into the future (thick grey line; winter months not shown). Figure from Galbraith et al. (2012).

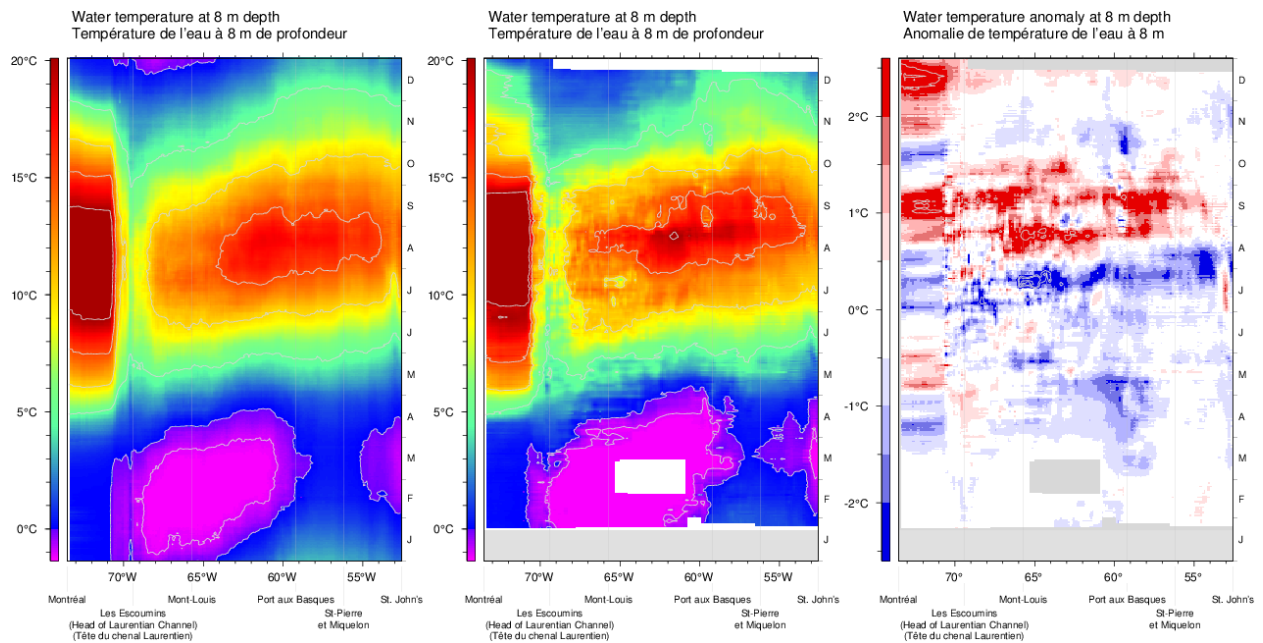


Figure 12. Thermosalinograph data at 8 m depth along the Montréal to St. John's shipping route: composite mean annual cycle of the water temperature for the 2000–2015 period (left panel), composite annual cycle of the water temperature for 2015 (middle panel), and water temperature anomaly for 2015 relative to the 2000–2015 composite (right panel).

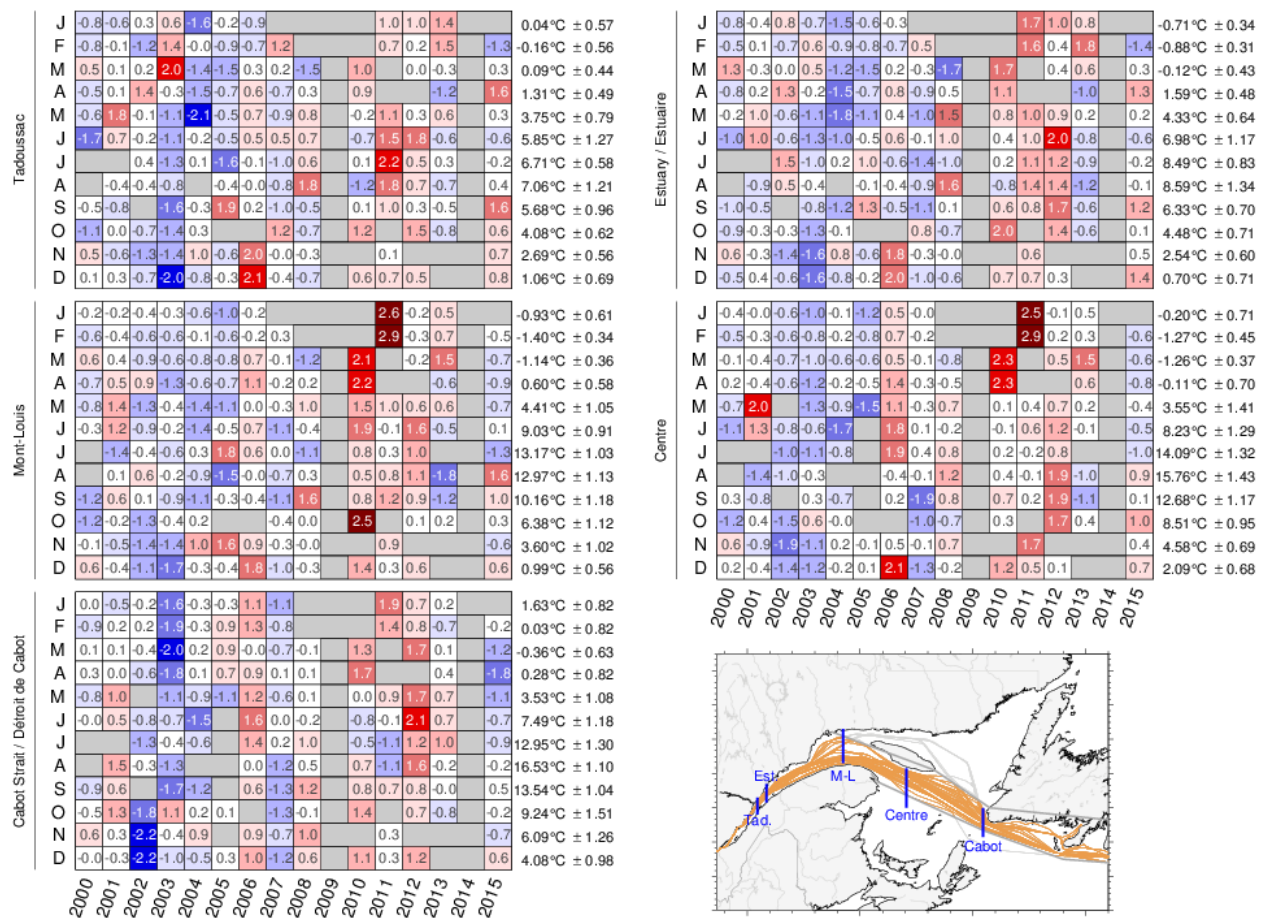


Figure 13. Thermosaligraph near-surface temperature monthly anomalies for various sections along the main shipping lane. The numbers on the right are the 2000–2015 climatological means and standard deviations. The numbers in the boxes are normalized anomalies. The map shows all TSG data sampled in 2015. Those drawn in colour are within the main shipping corridor and are used in this report. Monthly average anomalies of temperatures measured close to the indicated blue section lines are shown in the other scorecard panels.

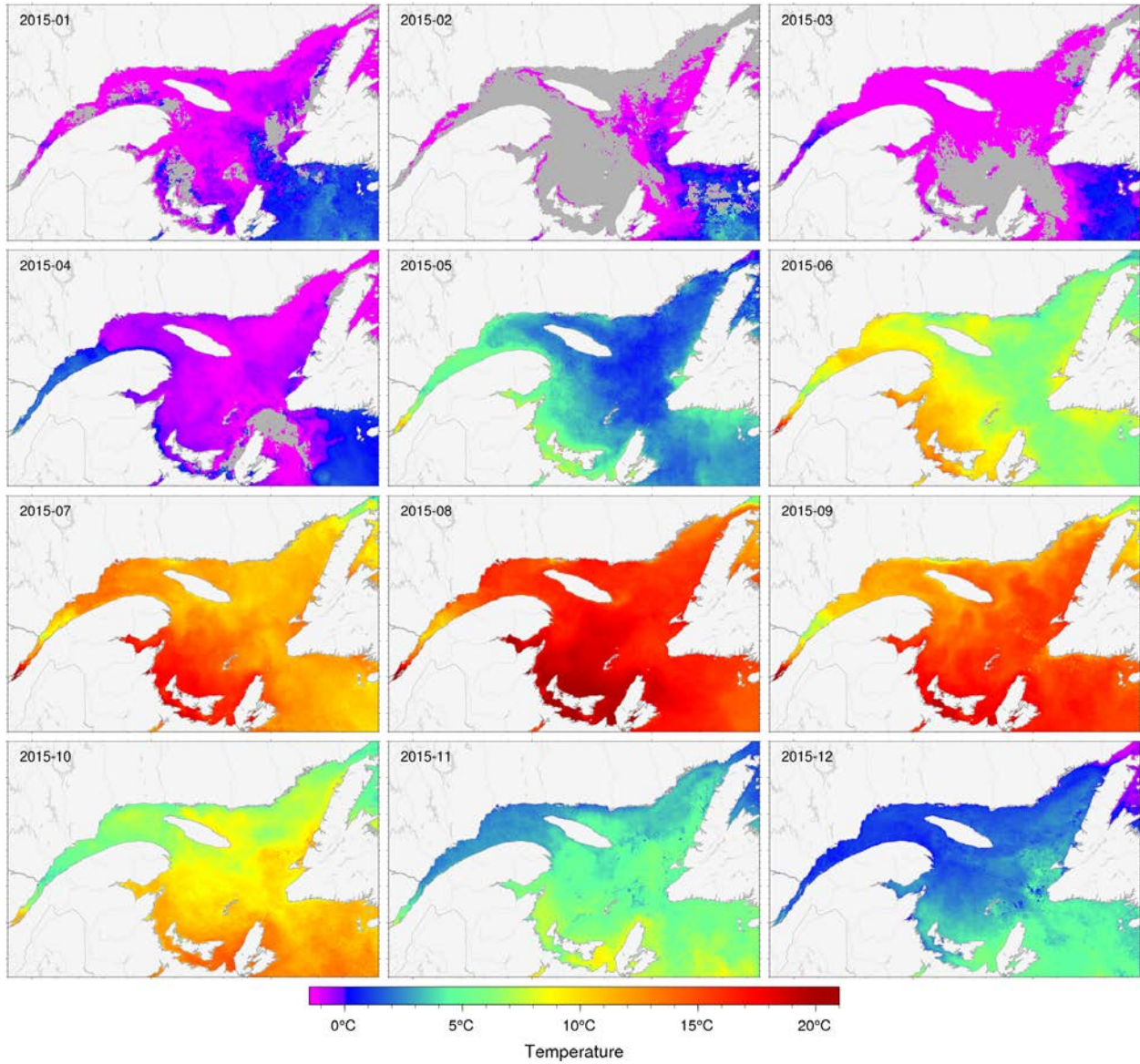


Figure 14. Sea-surface temperature monthly averages for 2015 as observed with AVHRR remote sensing. Grey areas have no data for the period due to ice cover or clouds.

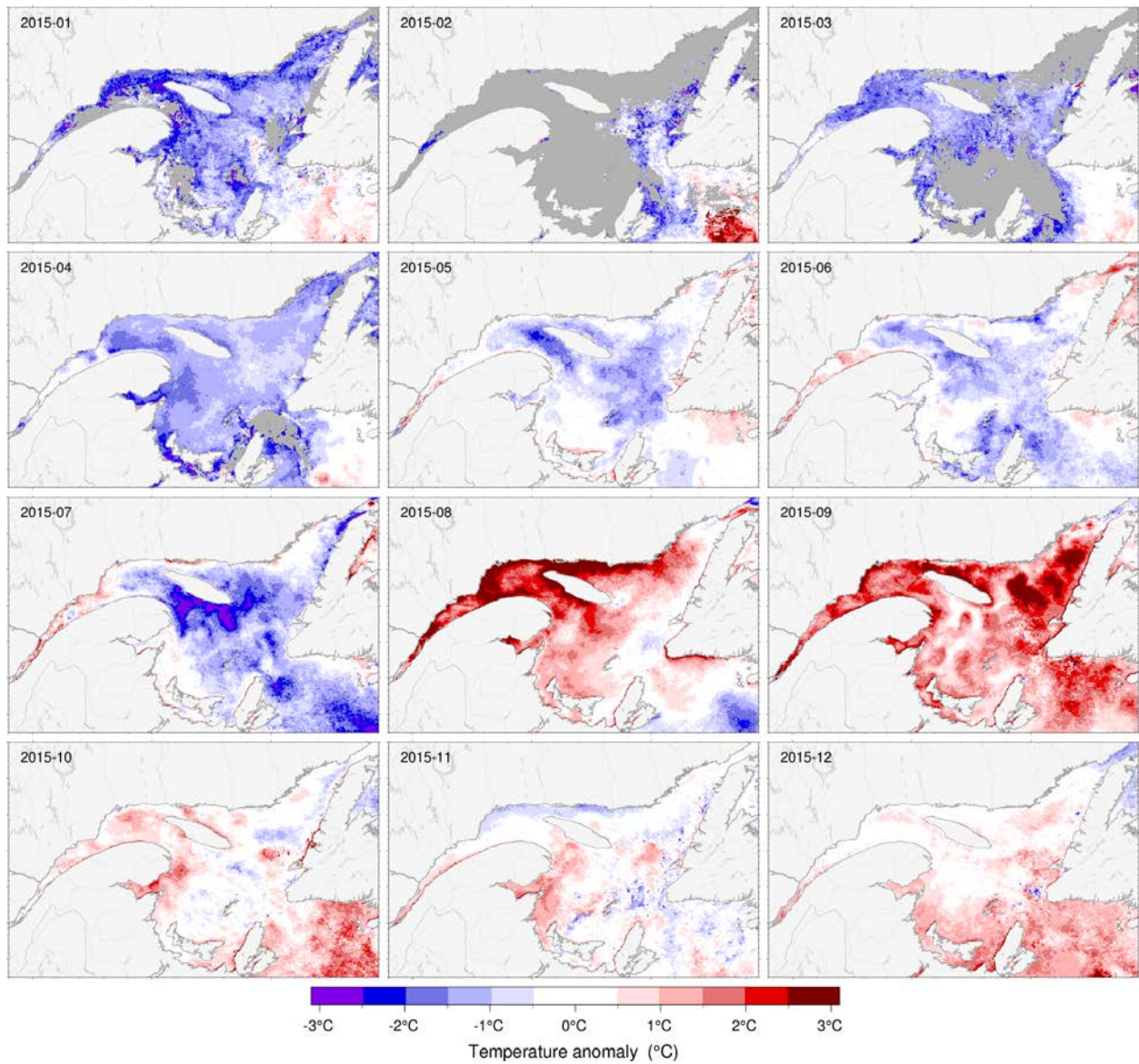


Figure 15. Sea-surface temperature monthly anomalies for 2015 based on monthly climatologies calculated for the 1985–2010 period observed with AVHRR remote sensing. Gray area either had sea-ice cover or missing climatologies due to recurrent sea-ice cover.

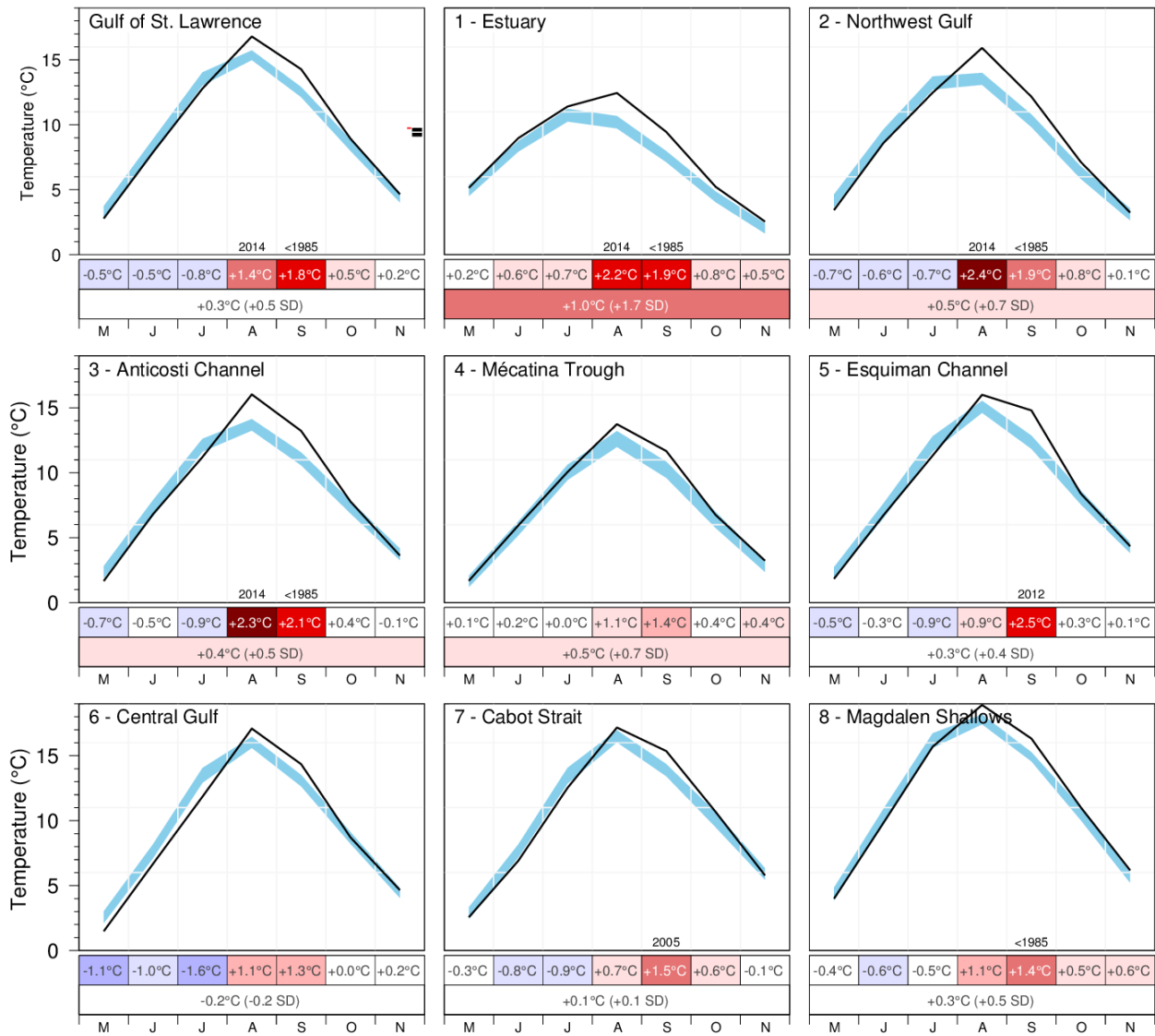


Figure 16. AVHRR SST May to November monthly averages over the Gulf and over the eight regions of the Gulf. The blue area represents the 1981–2010 climatological monthly mean \pm 0.5 SD. The scorecards are colour-coded according to the monthly normalized anomalies based on the 1985–2010 climatologies for each month, but the numbers are the monthly average temperature anomalies.

GSL		3.6	9.9	14.8	17.4	12.9	9.1	4.6							2.8	7.9	12.8	16.8	14.3	8.9	4.6	
1 - Estuary		6.1	11.3	9.5	14.1	8.1	5.4	2.0							5.2	9.0	11.4	12.4	9.4	5.2	2.5	
2 - Northwest Gulf	-0.6	5.1	11.6	14.2	17.1	11.3	6.8	3.4							-0.6	3.4	8.6	12.5	15.9	12.2	7.1	3.2
3 - Anticosti Channel		2.2	8.7	14.3	16.1	11.1	7.1	4.2							1.7	6.8	11.2	16.0	13.2	7.8	3.6	
4 - Mécatina Trough		1.5	5.6	9.8	13.8	10.2	8.2	3.1							1.7	5.9	10.1	13.7	11.7	6.8	3.2	
5 - Esquiman Channel		2.7	8.2	13.8	16.8	12.7	8.8	4.6							1.8	6.7	11.3	16.0	14.8	8.4	4.3	
6 - Central Gulf		2.8	9.1	15.4	17.7	13.0	9.3	4.7							1.5	6.7	11.8	17.1	14.3	8.7	4.6	
7 - Cabot Strait		3.5	9.2	14.5	18.9	14.5	11.4	6.0							2.6	6.9	12.5	17.2	15.4	10.7	5.6	
8 - Magdalen Shallows		4.3	11.4	17.2	18.5	15.1	11.1	5.3							4.0	9.8	15.7	18.9	16.3	11.0	6.0	
SSLMP (Estuary)		5.8	9.8	7.9	11.0	7.4	5.5	2.2							5.0	7.7	10.1	11.4	8.7	4.8	2.7	
St. Lawrence Estuary MPA		6.1	10.9	9.3	12.8	8.0	5.5	2.1							5.5	8.7	10.9	12.0	9.4	5.3	2.9	
Manicouagan MPA		6.8	12.3	9.9	15.9	8.8	6.0	2.3							5.8	9.4	12.9	13.7	10.6	5.5	2.4	
		A	M	J	J	A	S	O	N	D		J	F	M	A	M	J	J	A	S	O	N
		2014										2015										

Figure 17. AVHRR SST May to November monthly anomalies averaged over the Gulf, the eight regions of the Gulf, and management regions of the St. Lawrence Estuary for 2014 and 2015 (April results are also shown for the Northwest Gulf). The scorecards are colour-coded according to the monthly normalized anomalies based on the 1985–2010 climatologies for each month, but the numbers are the monthly average temperatures.

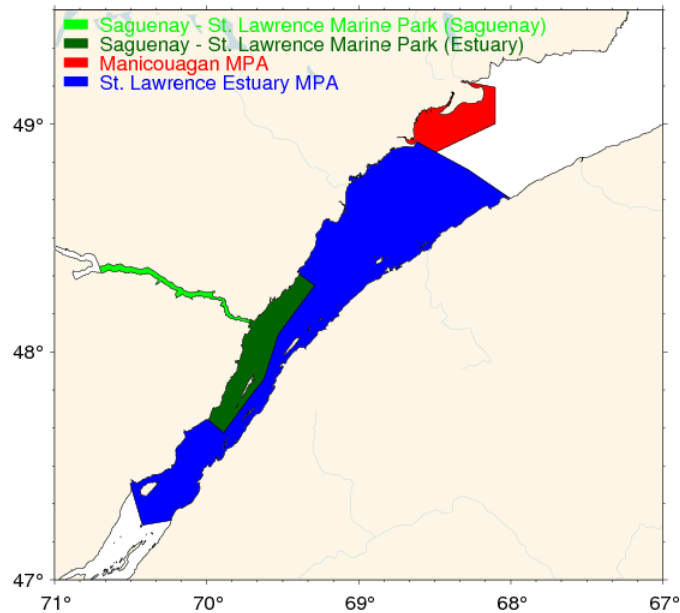


Figure 18. Map showing the proposed Manicouagan MPA, the proposed St. Lawrence Estuary MPA, and the Saguenay – St. Lawrence Marine Park for the purpose of SST extraction from NOAA imagery (Figure 17).

		1985-2010 Mean and Standard Deviation																				1985-2010 Mean and Standard Deviation											
		1985	1986	1987	1988	1989	1990	1991	1992	1993	1994	1995	1996	1997	1998	1999	2000	2001	2002	2003	2004		2005	2006	2007	2008	2009	2010	2011	2012	2013	2014	2015
GSL SST Anomaly	M	2.5	3.7	2.9	3.4	2.3	1.9	2.3	2.6	2.5	3.6	3.8	3.2	2.8	4.7	4.0	3.4	4.5	2.9	2.7	2.6	3.6	5.6	3.2	4.2	3.4	4.1	3.5	4.6	3.4	3.6	2.8	3.31°C ± 0.86
	J	7.0	6.8	8.7	7.2	8.8	7.0	7.7	7.3	7.9	8.7	9.4	9.4	7.8	9.4	9.8	8.3	9.8	8.2	8.4	7.4	8.9	10.4	8.6	8.5	9.0	8.3	8.2	9.4	8.4	9.9	7.9	8.42°C ± 0.97
	J	12.2	12.1	13.7	13.1	13.6	11.9	12.2	11.5	12.2	14.4	14.7	13.6	13.3	14.1	14.9	14.1	14.2	13.3	13.6	13.9	14.0	15.2	14.1	14.7	13.3	14.2	13.0	15.1	13.7	14.8	12.8	13.54°C ± 1.00
	A	15.0	14.2	14.8	15.3	14.5	14.7	14.2	13.5	15.5	15.6	16.0	16.2	15.0	15.2	15.8	16.5	15.9	15.7	15.5	15.9	15.0	15.7	14.8	15.9	16.2	16.4	15.4	17.3	15.3	17.4	16.8	15.36°C ± 0.74
	S	12.4	11.3	12.1	11.9	11.2	12.4	11.3	12.3	12.5	12.9	12.1	13.8	12.9	12.9	14.1	13.0	13.4	12.1	12.8	11.7	13.6	13.2	11.6	13.1	12.2	13.0	12.6	14.0	12.5	12.9	14.3	12.52°C ± 0.77
	O	7.8	7.3	8.3	7.3	5.9	8.7	8.5	7.5	8.3	9.0	9.1	8.6	8.6	7.8	8.8	8.4	9.5	8.2	9.9	8.9	9.2	9.7	8.4	8.7	7.8	9.3	8.6	8.8	9.4	9.1	8.9	8.43°C ± 0.87
	N	3.8	3.4	3.4	3.7	3.7	3.2	4.7	3.3	4.0	5.3	5.4	4.9	4.8	4.6	4.4	4.6	4.5	3.5	4.1	4.5	5.2	5.6	5.0	5.4	4.7	5.3	5.5	5.3	5.2	4.6	4.7	4.41°C ± 0.75
M-N	8.7	8.4	9.1	8.8	8.6	8.5	8.7	8.3	9.0	9.9	10.1	9.9	9.3	9.8	10.3	9.8	10.2	9.1	9.6	9.3	9.9	10.8	9.4	10.1	9.5	10.1	9.5	10.7	9.7	10.3	9.7	9.43°C ± 0.67	
1 - Estuary	M		5.3	4.7	5.2	3.5	4.6		3.9	4.4	6.5	4.9	4.8	4.7	5.6	6.1	4.9	6.7	4.6	4.1	4.0	3.9	5.7	5.0	5.5	4.1	6.0	4.6	5.5	4.7	6.1	5.2	4.95°C ± 0.86
	J	7.6	6.2	7.5	8.0	7.9	7.4	8.1	7.4	9.0	9.0	8.5	8.8	8.2	9.7	8.6	8.0	9.7	8.5	8.1	7.9	8.2	9.7	9.1	8.7	8.1	9.0	8.9	9.6	7.7	11.3	9.0	8.34°C ± 0.81
	J	9.2	9.2	10.4	11.3	10.2	9.1	9.2	9.4	12.6	11.5	12.2	11.3	10.2	10.2	10.0	11.9	10.8	11.3	11.2	11.6	11.2	11.3	11.0	11.2	10.5	11.1	11.6	12.1	9.5	9.5	11.4	10.74°C ± 0.98
	A	9.8	9.1	9.8	10.6	8.1	9.7	10.1	8.5	11.8	10.3	11.1	10.6	9.5	9.0	10.4	11.5	10.4	10.6	11.2	9.5	9.5	10.7	9.6	11.9	11.0	10.6	11.4	12.3	8.9	14.1	12.4	10.20°C ± 0.95
	S	8.2	6.5	6.7	6.4	6.5	7.4	6.3	6.8	7.8	7.7	7.1	8.9	8.4	9.0	9.0	7.3	7.5	8.2	7.2	6.9	8.1	8.0	6.5	8.0	7.2	8.5	8.0	8.1	7.6	8.1	9.4	7.55°C ± 0.84
	O	4.2	3.8	4.2	3.4	2.4	3.8	3.5	3.3	3.7	5.7	4.9	4.0	5.0	4.2	5.3	4.2	4.8	5.0	4.7	4.8	5.6	5.2	5.4	4.4	4.7	5.6	5.3	5.4	5.3	5.4	5.2	4.46°C ± 0.82
	N	1.6	1.3	1.2	1.2	0.9	0.8	2.3	1.0	1.1	3.8	2.2	1.6	2.5	2.1	2.2	2.2	2.3	1.6	1.4	2.5	2.9	3.3	2.5	2.4	3.0	2.5	3.0	2.6	2.3	2.0	2.5	2.02°C ± 0.77
M-N	5.9	6.3	6.6	5.6	6.1		5.8	7.2	7.8	7.3	7.2	6.9	7.1	7.4	7.2	7.5	7.1	6.8	6.7	7.0	7.7	7.0	7.5	7.0	7.6	7.5	7.9	6.6	8.1	7.9	6.93°C ± 0.59		
2 - Northwest Gulf	A		0.7	1.3	0.1	0.4	0.6	0.4	0.6	0.5	0.1	1.2	0.8	0.6	1.2	1.6	0.7	0.5	0.7	0.1	0.2	-0.2	1.5	0.6	1.1	0.7	1.2	0.5	0.8	0.9	-0.6	-0.6	0.69°C ± 0.46
	M	2.7	5.4	3.7	4.3	2.9	3.2	2.7	3.6	3.6	4.8	4.7	3.8	3.9	5.9	5.0	3.7	5.9	3.5	4.0	3.0	3.9	5.8	3.8	5.3	3.4	5.0	4.0	4.5	4.3	5.1	3.4	4.14°C ± 0.99
	J	8.4	6.8	8.7	7.8	9.8	8.0	8.2	8.1	9.5	10.1	10.5	10.5	8.8	10.2	10.1	8.8	10.1	8.6	9.3	8.1	9.8	10.8	8.9	8.8	9.2	9.8	9.3	10.2	8.3	11.6	8.6	9.14°C ± 1.00
	J	12.2	11.4	12.8	13.8	13.2	11.4	11.4	11.2	13.4	13.8	15.1	13.3	12.9	13.5	13.5	14.1	13.4	13.0	13.0	13.8	14.3	14.5	13.7	13.6	13.1	14.3	13.5	14.3	12.3	14.2	12.5	13.22°C ± 1.01
	A	13.4	12.7	12.3	14.0	12.1	13.3	13.0	11.5	15.3	13.0	14.6	13.9	13.1	13.5	14.0	15.1	13.3	13.8	14.0	13.5	12.8	13.4	12.8	14.9	14.5	14.2	14.2	15.7	12.6	17.1	15.9	13.54°C ± 0.92
	S	11.2	9.0	9.2	9.1	9.3	10.1	9.6	10.2	10.5	10.0	10.3	11.7	11.5	12.2	11.9	10.2	10.5	9.9	10.2	9.1	10.9	10.3	8.7	11.4	9.7	11.4	10.6	11.4	10.2	11.3	12.2	10.31°C ± 0.97
	O	5.6	5.4	5.7	5.1	3.9	5.7	5.9	5.1	5.3	8.1	6.7	6.5	7.4	6.3	7.4	6.1	6.6	6.0	7.4	7.0	7.2	7.0	6.4	6.4	6.8	7.4	7.4	6.3	8.0	6.8	7.1	6.32°C ± 0.95
N	2.5	1.9	1.9	2.1	1.9	1.8	3.6	1.9	2.2	4.8	3.3	3.2	3.4	3.7	3.1	3.2	2.9	2.5	2.3	4.0	4.3	4.6	3.8	3.6	3.9	4.0	4.3	3.4	3.8	3.4	3.2	3.10°C ± 0.91	
M-N	8.0	7.5	7.8	8.0	7.6	7.7	7.8	7.4	8.6	9.2	9.3	9.0	8.7	9.3	9.3	8.7	9.0	8.2	8.6	8.3	9.0	9.5	8.3	9.2	8.6	9.4	9.1	9.4	8.5	9.9	9.0	8.54°C ± 0.67	
3 - Anticosti Channel	M	1.9	2.5	1.9	2.4	1.4	0.5	1.4	1.6	1.6	2.5	3.0	2.8	1.6	3.7	2.8	2.1	3.5	2.1	1.4	1.8	2.7	4.9	1.9	3.5	2.0	3.4	2.0	3.1	2.2	2.2	1.7	2.35°C ± 0.92
	J	5.7	5.0	7.9	6.3	8.2	4.7	6.1	6.0	7.0	7.1	8.0	8.7	7.0	8.5	8.4	6.6	8.7	7.5	7.3	6.5	8.7	9.7	6.9	7.4	8.4	7.0	7.1	8.0	7.1	8.7	6.8	7.28°C ± 1.24
	J	11.0	10.9	12.4	11.5	12.4	10.0	10.5	10.3	10.9	12.2	13.1	12.5	12.0	12.8	12.8	12.7	12.3	12.2	12.0	13.0	12.8	13.9	13.0	13.3	12.2	12.3	12.3	13.4	11.5	14.3	11.2	12.12°C ± 0.98
	A	13.1	13.1	13.2	13.6	12.5	12.5	12.6	12.0	13.8	13.3	13.9	14.7	13.4	13.2	14.2	15.1	13.8	14.2	14.6	13.9	12.4	14.1	13.8	15.3	14.6	15.0	14.6	15.7	13.6	16.1	16.0	13.69°C ± 0.88
	S	11.3	10.1	10.8	9.8	10.2	10.0	9.6	10.3	10.1	11.4	11.3	12.5	11.8	11.9	13.2	10.8	11.8	10.8	10.7	10.3	12.3	12.2	10.0	12.0	10.4	12.2	10.6	12.6	11.3	11.1	13.2	11.07°C ± 0.99
	O	6.2	6.5	7.5	6.5	4.8	7.2	7.1	6.6	5.7	8.3	8.2	7.4	8.0	6.9	7.9	6.8	8.5	7.0	8.0	8.3	8.5	8.7	7.4	8.0	6.8	8.4	7.1	6.8	8.9	7.1	7.8	7.35°C ± 0.96
	N	2.5	2.3	2.8	3.3	2.8	2.8	4.0	2.9	2.8	4.5	4.9	4.0	3.9	3.2	3.3	3.8	4.0	3.1	3.5	4.2	5.1	5.5	4.0	5.2	3.4	4.9	4.6	4.5	4.6	4.2	3.6	3.72°C ± 0.89
M-N	7.4	7.2	8.1	7.6	7.5	6.8	7.3	7.1	7.4	8.4	8.9	8.9	8.3	8.6	8.9	8.3	8.9	8.2	8.2	8.3	8.9	9.9	8.1	9.2	8.3	9.0	8.3	9.2	8.5	9.1	8.6	8.22°C ± 0.76	
4 - Mécatina Trough	M	1.6	1.4	1.4	2.4	0.2	-0.5	1.1	1.2	0.9	1.7	1.5	2.1	1.2	1.6	2.3	2.0	2.8	1.3	1.6	1.2	3.1	4.0	1.3	2.0	1.5	1.8	1.8	2.2	1.8	1.5	1.7	1.64°C ± 0.88
	J	5.2	3.7	6.9	4.6	5.6	3.8	4.6	4.5	5.0	6.2	6.3	5.8	5.5	6.5	6.8	6.6	5.8	6.4	5.7	5.4	7.2	7.3	5.7	5.5	7.5	4.3	5.8	6.7	6.2	5.6	5.9	5.71°C ± 1.06
	J	8.2	9.3	10.7	8.9	9.9	9.4	8.5	7.0	7.9	10.7	11.0	10.2	10.4	10.7	11.2	11.3	10.1	9.9	10.5	10.0	10.1	12.0	10.6	11.4	10.1	10.7	9.9	11.8	10.2	9.8	10.1	10.03°C ± 1.17
	A	11.3	11.8	12.9	12.0	12.0	11.3	10.6	9.7	10.7	12.1	13.4	14.1	12.5	12.0	14.4	13.9	13.5	12.9	13.3	13.2	12.3	14.2	12.7	13.7	13.1	13.8	12.7	14.5	13.3	13.8	13.7	12.60°C ± 1.22
	S	9.3	8.9	10.2	10.2	8.3	10.5	7.4	9.3	9.2	10.6	9.6	10.8	9.4	8.7	12.5	11.5	12.0	10.0	11.6	10.5	11.7	11.5	10.0	11.8	10.1	10.5	9.9	12.1	11.0	10.2	11.7	10.23°C ± 1.24
	O	5.4	4.7	6.7	5.8	4.7	7.8	6.2	6.0	6.5	5.7	7.5	5.0	6.2	5.4	6.5	7.5	7.8	5.1	8.8	6.6	7.5	8.1	5.2	7.5	4.0	7.4	6.2	7.1	5.8	8.2	6.8	6.37°C ± 1.23
	N	1.3	1.9	2.8	3.3	1.8	1.8	2.6	2.2	3.0	3.9	4.6	2.5	2.2	2.3	2.8	2.5	3.2	1.5	3.7	3.0	3.0	3.5	3.0	4.2	2.1	3.8	2.5	3.1	2.9	3.1	3.2	2.79°C ± 0.85
M-N	6.0	5.9	7.4	6.7	6.1	6.3	5.9	5.7	6.2	7.3	7.7	7.2	6.8	6.7	8.1	7.9	7.9	6.7	7.9	7.1	7.8	8.7	7.0	8.0	6.9	7.5	7.0	8.2	7.3	7.5	7.6	7.05°C ± 0.81	

Figure 19. AVHRR SST May to November monthly anomalies averaged over the Gulf of St. Lawrence and over the first four regions of the Gulf. The score

5 - Esquiman Channel	M	2.0	2.4	2.1	2.8	0.8	0.9	1.5	1.5	1.5	2.6	2.7	2.3	1.6	3.0	3.0	2.6	3.3	1.7	1.8	1.8	3.2	4.6	2.4	3.1	1.9	3.1	2.4	3.6	2.6	2.7	1.8	2.31°C ± 0.84
	J	5.8	5.4	7.6	6.1	7.2	5.0	5.8	5.7	6.3	6.5	8.1	7.5	6.4	8.6	8.5	7.0	8.8	7.0	7.3	5.8	8.0	9.1	7.8	7.4	8.1	6.6	6.7	7.7	7.1	8.2	6.7	7.06°C ± 1.13
	J	11.1	11.7	13.1	10.8	12.8	10.6	10.8	9.8	12.1	12.9	12.0	12.0	13.1	14.4	12.4	12.8	12.1	12.3	12.9	12.3	14.5	13.1	13.7	12.1	12.4	11.5	14.5	12.4	13.8	11.3	12.22°C ± 1.18	
	A	14.6	14.3	15.1	15.0	14.3	13.9	13.6	12.8	13.8	15.4	15.4	16.1	14.6	14.7	15.4	16.6	15.7	15.5	15.3	16.2	14.7	16.0	14.9	15.9	16.0	16.2	15.2	17.0	15.2	16.8	16.0	15.08°C ± 0.92
	S	11.7	10.9	12.5	12.5	10.6	12.5	10.5	11.8	11.8	12.9	11.4	13.7	12.1	11.4	14.1	13.8	13.3	11.5	13.4	12.0	13.5	13.5	11.8	13.2	12.0	12.6	12.5	14.8	12.1	12.7	14.8	12.35°C ± 1.01
	O	7.9	6.8	8.3	7.3	5.7	8.5	7.5	7.4	8.2	8.6	8.8	7.7	7.6	7.2	9.1	8.7	9.2	7.0	10.5	8.2	8.2	10.0	8.0	8.6	6.5	9.0	7.1	8.6	8.8	8.8	8.4	8.10°C ± 1.05
	N	3.1	3.6	3.7	4.1	3.4	2.9	4.9	3.0	3.9	5.0	5.9	4.7	4.1	4.7	4.3	4.1	4.0	2.7	4.4	4.3	4.7	5.3	4.5	5.4	3.9	5.4	3.9	5.4	5.1	4.6	4.3	4.23°C ± 0.82
M-N	8.0	7.9	8.9	8.4	7.8	7.8	7.8	7.5	7.9	9.0	9.3	9.2	8.3	8.9	9.8	9.3	9.6	8.2	9.3	8.7	9.2	10.4	8.9	9.6	8.6	9.3	8.4	10.2	9.0	9.7	9.1	8.76°C ± 0.75	
6 - Central Gulf	M	1.8	3.1	2.5	2.5	1.6	1.1	1.8	1.7	2.0	2.2	3.4	2.2	2.1	3.8	2.9	2.7	3.6	1.8	1.8	1.9	3.1	5.2	2.6	3.7	2.4	3.3	2.7	4.0	2.7	2.8	1.5	2.57°C ± 0.90
	J	6.2	6.3	8.7	6.3	8.5	6.0	6.8	6.8	7.1	7.3	9.3	8.5	7.2	8.7	9.0	7.2	9.4	7.2	7.4	6.3	8.2	9.8	7.7	7.7	7.9	7.5	7.5	8.9	7.4	9.1	6.7	7.66°C ± 1.07
	J	12.5	12.1	14.0	12.8	13.9	11.2	12.0	11.8	11.7	13.9	14.7	13.7	13.3	14.3	15.3	13.9	14.4	13.0	12.7	14.0	14.0	15.6	14.0	14.8	13.5	13.9	12.4	15.6	13.4	15.4	11.8	13.49°C ± 1.13
	A	16.0	15.0	15.0	16.3	15.5	14.9	14.4	14.2	15.9	16.3	16.6	17.0	15.9	16.0	16.1	17.4	16.7	16.2	15.8	17.0	15.8	16.6	15.4	16.8	16.9	17.3	15.8	18.1	15.7	17.7	17.1	16.03°C ± 0.85
	S	13.1	12.3	13.0	12.8	11.0	12.7	12.1	13.0	13.0	13.6	12.5	14.6	13.6	13.5	14.6	13.9	13.7	12.2	13.6	11.9	13.6	14.3	11.8	13.2	13.0	13.6	13.5	15.2	12.5	13.0	14.3	13.08°C ± 0.87
	O	7.8	8.0	8.6	7.5	5.9	8.9	8.8	7.9	8.7	9.3	9.2	9.1	8.8	7.9	8.7	8.6	9.3	8.5	10.0	9.2	8.9	10.3	8.5	8.8	7.9	9.8	9.2	9.0	9.7	9.3	8.7	8.67°C ± 0.89
	N	3.8	3.4	3.4	3.7	3.8	3.1	4.7	3.5	4.2	4.6	5.5	5.0	5.0	4.6	4.4	4.8	4.2	3.7	3.9	4.6	5.0	6.0	5.0	5.5	4.9	5.5	6.2	5.7	5.5	4.7	4.7	4.44°C ± 0.76
M-N	8.7	8.6	9.3	8.8	8.6	8.3	8.7	8.4	8.9	9.6	10.2	10.0	9.4	9.8	10.1	9.8	10.2	9.0	9.3	9.3	9.8	11.1	9.3	10.1	9.5	10.1	9.6	10.9	9.6	10.3	9.3	9.42°C ± 0.69	
7 - Cabot Strait	M	1.9	3.3	2.5	3.2	1.7	1.1	1.7	2.1	2.2	3.0	3.3	2.7	2.1	4.2	3.7	3.6	3.7	2.4	2.3	2.3	3.7	5.3	2.8	3.2	3.3	3.5	3.8	5.0	3.3	3.5	2.6	2.88°C ± 0.91
	J	6.3	6.7	7.7	6.5	7.7	6.4	6.3	6.4	6.8	8.1	8.4	8.5	6.8	8.8	9.6	8.1	8.9	7.6	7.6	6.6	8.2	9.5	8.3	7.8	8.2	7.2	7.1	9.3	8.3	9.2	6.9	7.67°C ± 0.99
	J	11.7	11.9	14.0	12.6	13.6	11.9	12.1	11.2	11.5	14.8	13.9	13.5	13.1	14.5	15.6	14.3	14.5	13.1	13.4	13.6	13.6	15.3	13.8	14.9	13.7	14.2	12.1	15.7	14.7	14.5	12.5	13.47°C ± 1.20
	A	15.9	15.2	16.5	15.9	16.1	15.7	14.9	14.6	16.2	17.6	16.9	17.5	15.9	17.1	17.6	17.8	17.3	17.0	16.2	17.5	16.1	16.5	15.5	16.3	17.2	17.8	15.6	18.5	17.3	18.9	17.2	16.50°C ± 0.92
	S	13.5	12.8	14.3	13.3	12.2	14.2	12.2	14.5	14.3	14.8	13.1	14.8	14.0	14.2	15.6	14.3	15.0	13.1	13.5	12.6	15.5	14.4	12.9	14.2	13.4	14.4	14.3	15.2	14.6	14.5	15.4	13.89°C ± 0.93
	O	9.1	8.9	10.0	9.2	7.0	10.7	10.6	8.8	11.7	10.6	10.9	10.5	9.7	9.6	10.2	9.7	11.9	8.8	12.0	9.9	10.8	11.5	9.2	9.9	9.5	11.1	10.0	10.6	10.2	11.4	10.7	10.07°C ± 1.14
	N	5.7	5.4	4.4	5.4	5.1	4.3	5.5	4.5	6.0	6.2	7.0	6.6	7.0	6.9	5.8	6.6	6.1	4.1	5.4	6.3	6.3	7.0	6.0	7.0	6.0	6.9	7.0	7.3	6.2	6.0	5.8	5.90°C ± 0.89
M-N	9.2	9.2	9.9	9.4	9.1	9.2	9.0	8.9	9.8	10.7	10.5	10.6	9.8	10.7	11.2	10.6	11.1	9.4	10.1	9.8	10.6	11.4	9.8	10.5	10.2	10.7	10.0	11.7	10.7	11.1	10.1	10.05°C ± 0.73	
8 - Magdalen Shallows	M	3.6	4.4	3.8	3.9	3.9	2.7	3.6	3.5	3.0	4.4	4.7	4.1	3.7	6.2	5.2	4.4	5.3	4.3	3.7	3.7	4.1	7.0	4.6	5.3	5.3	5.2	4.9	6.0	4.2	4.3	4.0	4.36°C ± 0.97
	J	8.2	9.2	10.6	8.6	10.6	9.7	10.5	9.5	9.3	11.1	11.3	11.6	9.3	10.9	12.1	10.5	11.9	10.0	10.4	9.4	10.0	12.6	10.4	10.7	10.7	10.5	9.7	11.3	10.6	11.4	9.8	10.37°C ± 1.05
	J	14.5	14.2	16.1	15.9	15.9	14.7	15.5	14.2	14.7	18.1	17.6	15.9	15.9	16.6	18.0	16.5	17.1	15.8	16.6	16.0	16.5	17.6	16.6	17.4	15.4	17.0	15.3	17.2	17.1	17.2	15.7	16.17°C ± 1.12
	A	17.4	15.9	17.2	17.7	17.2	17.8	16.8	16.4	18.1	18.5	18.5	18.8	17.7	17.9	18.1	18.2	18.9	18.1	17.3	18.6	18.2	17.9	17.1	17.1	18.5	18.7	17.4	19.6	17.9	18.5	18.9	17.80°C ± 0.75
	S	14.6	13.4	14.1	14.3	14.0	15.1	14.2	15.0	15.5	15.3	14.5	16.0	15.1	15.2	15.9	15.4	16.1	14.8	15.2	14.2	16.2	15.4	14.3	14.9	14.8	14.8	14.8	16.0	14.5	15.1	16.3	14.92°C ± 0.70
	O	10.0	9.3	10.2	8.8	7.8	11.3	11.3	9.5	10.9	10.2	11.1	11.1	10.4	9.6	10.1	10.5	12.0	11.2	11.9	11.0	11.7	11.5	11.0	10.6	9.9	10.9	10.8	11.1	11.5	11.1	11.0	10.54°C ± 0.99
	N	5.3	4.4	4.3	4.6	5.4	4.5	6.0	4.4	5.4	6.4	6.5	6.7	6.1	5.5	5.7	6.0	5.8	4.8	5.2	4.9	6.2	6.3	6.8	6.5	6.2	6.3	7.4	6.6	6.7	5.3	6.2	5.62°C ± 0.79
M-N	10.5	10.1	10.9	10.6	10.7	10.8	11.1	11.0	11.0	12.0	12.0	12.0	11.2	11.7	12.2	11.6	12.5	11.3	11.5	11.1	11.9	12.6	11.5	11.8	11.6	11.9	11.5	12.5	11.8	11.8	11.7	11.40°C ± 0.66	
		1985	1986	1987	1988	1989	1990	1991	1992	1993	1994	1995	1996	1997	1998	1999	2000	2001	2002	2003	2004	2005	2006	2007	2008	2009	2010	2011	2012	2013	2014	2015	

Figure 20. AVHRR SST May to November monthly anomalies averaged over the remaining four regions of the Gulf. The scorecards are colour-coded according to the monthly normalized anomalies based on the 1985–2010 climatologies for each month, but the numbers are the monthly average temperatures in °C. The 1985–2010 mean and standard deviation are indicated for each month on the right side of the table. The May to November average is also included.

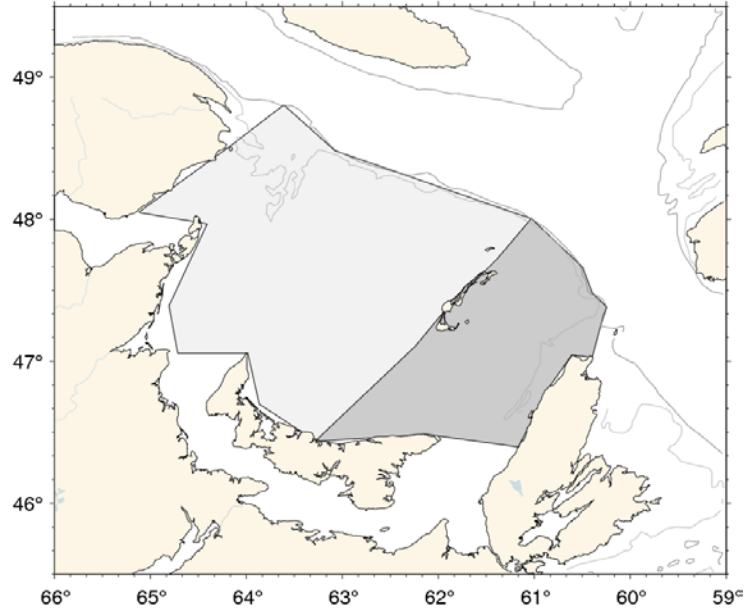


Figure 22. Areas defined as the western and eastern Magdalen Shallows.

		Mean ± S.D.																															
Magdalen Shallows	M	3.6	4.4	3.8	3.9	3.9	2.7	3.6	3.5	3.0	4.4	4.7	4.1	3.7	6.2	5.2	4.4	5.3	4.3	3.7	3.7	4.1	7.0	4.6	5.3	5.3	5.2	4.9	6.0	4.2	4.3	4.0	4.36°C ± 0.97
	J	8.2	9.2	10.6	8.6	10.6	9.7	10.5	9.5	9.3	11.1	11.3	11.6	9.3	10.9	12.1	10.5	11.9	10.0	10.4	9.4	10.0	12.6	10.4	10.7	10.7	10.5	9.7	11.3	10.6	11.4	9.8	10.37°C ± 1.05
	J	14.5	14.2	16.1	15.9	15.9	14.7	15.5	14.2	14.7	18.1	17.6	15.9	15.9	16.6	18.0	16.5	17.1	15.8	16.6	16.0	16.5	17.6	16.6	17.4	15.4	17.0	15.3	17.2	17.1	17.2	15.7	16.17°C ± 1.12
	A	17.4	15.9	17.2	17.7	17.2	17.8	16.8	16.4	18.1	18.5	18.5	18.8	17.7	17.9	18.1	18.2	18.9	18.1	17.3	18.6	18.2	17.9	17.1	17.1	18.5	18.7	17.4	19.6	17.9	18.5	18.9	17.80°C ± 0.75
	S	14.6	13.4	14.1	14.3	14.0	15.1	14.2	15.0	15.5	15.3	14.5	16.0	15.1	15.2	15.9	15.4	16.1	14.8	15.2	14.2	16.2	15.4	14.3	14.9	14.8	14.8	14.8	16.0	14.5	15.1	16.3	14.92°C ± 0.70
	O	10.0	9.3	10.2	8.8	7.8	11.3	11.3	9.5	10.9	10.2	11.1	11.1	10.4	9.6	10.1	10.5	12.0	11.2	11.9	11.0	11.7	11.5	11.0	10.6	9.9	10.9	10.8	11.1	11.5	11.1	11.0	10.54°C ± 0.99
N	5.3	4.4	4.3	4.6	5.4	4.5	6.0	4.4	5.4	6.4	6.5	6.7	6.1	5.5	5.7	6.0	5.8	4.8	5.2	4.9	6.2	6.3	6.8	6.5	6.2	6.3	7.4	6.6	6.7	5.3	6.2	5.62°C ± 0.79	
Eastern Magdalen Shelf	M	2.4	3.5	2.6	3.0	2.8	1.7	2.2	2.3	2.1	3.7	3.5	3.2	2.6	5.2	3.9	3.6	4.2	3.2	2.9	2.6	3.5	6.2	3.3	4.0	4.2	4.2	4.5	5.1	3.5	3.5	2.7	3.33°C ± 0.99
	J	7.1	8.3	9.8	7.3	9.2	8.1	8.6	8.1	7.7	9.8	10.0	10.5	8.0	10.2	11.1	9.3	10.8	9.0	9.0	8.2	8.9	11.5	9.5	9.7	9.6	9.2	8.4	10.7	9.6	10.1	8.1	9.17°C ± 1.13
	J	13.5	13.6	15.7	15.1	15.3	14.1	14.7	13.4	13.4	17.6	16.7	15.1	15.3	16.2	18.1	16.1	16.7	15.4	15.8	15.4	15.6	17.7	15.7	17.2	14.7	16.4	14.0	17.1	16.8	16.5	14.7	15.56°C ± 1.32
	A	17.7	16.1	17.6	17.4	17.4	17.4	16.8	16.4	17.6	19.2	18.6	19.2	17.6	18.3	18.6	18.5	19.2	18.4	17.6	19.0	18.2	18.0	16.9	17.2	18.7	19.2	17.5	19.8	18.4	19.2	18.4	17.95°C ± 0.90
	S	14.6	13.7	14.9	14.6	14.2	15.0	14.2	15.5	15.9	16.0	14.4	16.1	15.3	14.9	16.3	16.0	16.5	15.0	15.4	14.1	16.7	15.5	14.2	15.2	15.0	14.8	15.3	16.3	14.6	14.8	16.2	15.14°C ± 0.79
	O	10.2	9.8	10.7	9.7	8.2	11.2	12.1	9.9	12.4	10.5	11.2	11.7	10.8	9.6	10.4	10.7	12.5	11.1	12.3	11.5	12.3	11.7	11.1	11.2	10.0	11.6	10.8	11.3	11.7	11.0	11.1	10.94°C ± 1.04
N	6.2	4.9	4.4	5.3	5.9	4.3	6.1	4.6	6.0	6.3	6.8	7.4	6.8	5.9	5.9	6.9	6.0	5.2	5.5	5.1	6.2	6.3	7.2	7.1	6.4	6.9	8.0	7.2	6.9	5.3	6.0	5.99°C ± 0.86	
Western Magdalen Shelf	M	3.2	4.0	3.6	3.1	3.4	2.2	3.0	2.9	2.8	3.5	4.3	3.3	3.3	5.8	4.6	3.8	4.7	3.8	3.1	3.3	3.6	6.5	4.0	5.1	4.6	4.5	3.8	5.5	3.6	3.7	3.5	3.85°C ± 0.96
	J	8.0	8.6	10.6	8.0	10.5	9.1	10.0	9.4	8.8	10.4	11.1	11.2	9.0	10.6	11.6	9.8	11.7	9.6	9.8	8.8	9.6	11.9	9.8	10.1	10.2	9.8	9.4	10.8	9.8	10.9	9.6	9.92°C ± 1.06
	J	14.4	13.9	15.8	15.6	15.7	13.8	14.5	13.8	14.1	17.4	17.6	15.4	15.5	16.3	17.5	16.3	16.7	15.3	16.0	15.8	16.3	17.2	16.3	16.9	15.0	16.4	15.0	16.9	16.2	16.9	15.1	15.75°C ± 1.15
	A	17.1	15.4	16.5	17.6	16.7	16.9	16.0	15.6	17.9	17.7	18.1	18.2	17.3	17.3	17.4	18.0	18.3	17.4	16.7	17.9	17.9	17.6	16.4	16.9	18.0	18.3	17.1	19.3	17.1	17.8	18.5	17.27°C ± 0.82
	S	13.9	12.7	13.3	13.7	12.8	14.4	13.4	13.9	14.7	14.4	13.8	15.5	14.8	14.8	15.0	14.6	15.3	13.7	14.3	13.2	15.6	14.7	13.1	14.3	14.0	14.2	14.0	15.6	13.5	14.2	15.3	14.16°C ± 0.79
	O	9.3	8.4	9.4	7.8	6.8	10.5	10.2	8.6	9.7	9.3	10.3	10.4	9.8	9.0	9.3	9.8	10.9	10.4	11.2	10.2	10.6	10.6	9.8	9.7	9.2	10.1	10.0	10.3	10.5	10.0	10.0	9.66°C ± 0.99
N	4.8	3.9	3.6	3.7	4.5	4.1	5.4	3.9	4.7	6.0	5.8	6.2	5.5	5.0	5.0	5.3	5.0	4.4	4.4	4.6	5.8	5.8	6.1	5.9	5.8	5.6	6.8	5.9	6.1	4.4	5.6	5.03°C ± 0.81	
		1985	1986	1987	1988	1989	1990	1991	1992	1993	1994	1995	1996	1997	1998	1999	2000	2001	2002	2003	2004	2005	2006	2007	2008	2009	2010	2011	2012	2013	2014	2015	

Figure 23. AVHRR SST May to November monthly anomalies averaged over the Magdalen Shallows (region 8 of the Gulf) and the eastern and western subregions of the Magdalen Shallows. The scorecards are colour-coded according to the monthly normalized anomalies based on the 1985–2010 climatologies for each month, but the numbers are the monthly average temperatures in °C. The 1985–2010 mean and standard deviation are indicated for each month on the right side of the table.

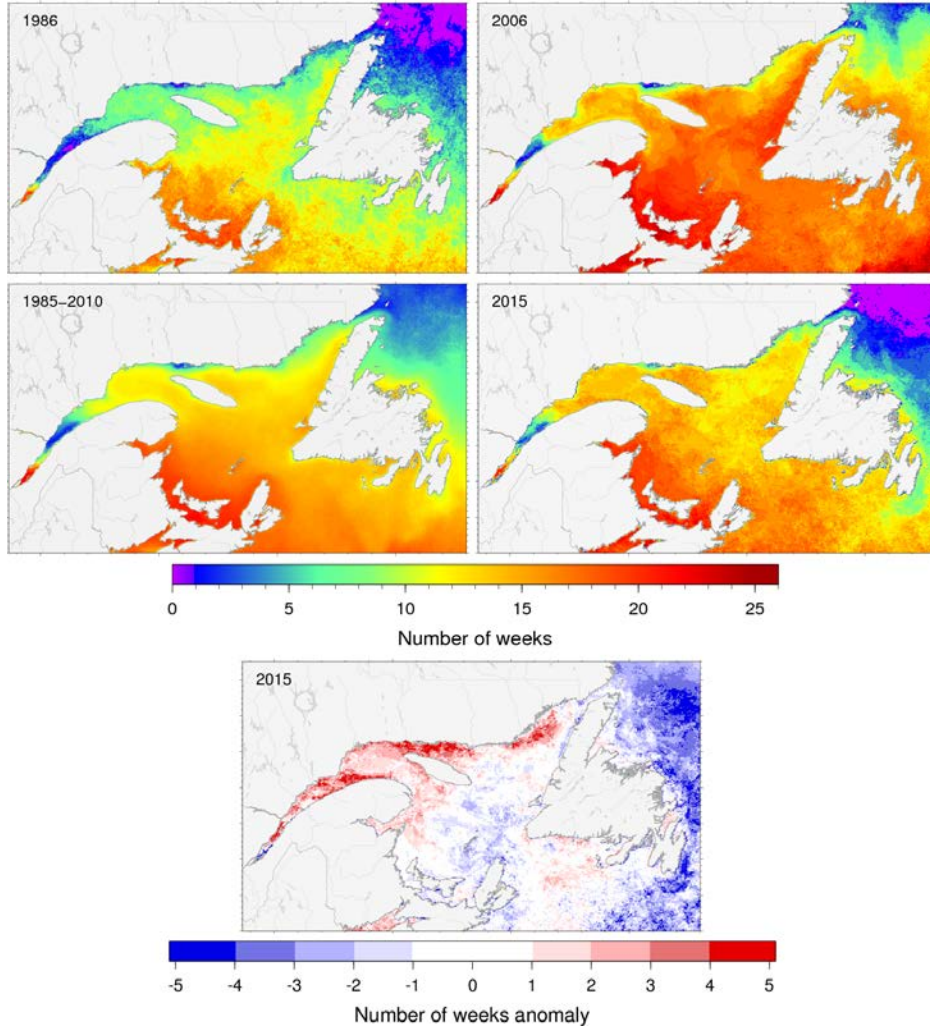


Figure 24. Yearly number of weeks with mean weekly surface temperature >10°C. (Top) Years with the minimum (1986, top left) and maximum (2006, top right) number of weeks are shown along with the 1985–2010 climatological average (lower left) and the chart for 2015. (Bottom) Anomaly for 2015 relative to 1985–2010 climatology, expressed in numbers of weeks.

	1985	1986	1987	1988	1989	1990	1991	1992	1993	1994	1995	1996	1997	1998	1999	2000	2001	2002	2003	2004	2005	2006	2007	2008	2009	2010	2011	2012	2013	2014	2015	
Gulf of St. Lawrence	11.4	10.4	13.0	11.0	12.1	12.0	11.8	10.8	12.4	14.0	14.9	14.8	13.7	14.4	16.2	14.1	15.6	12.7	14.8	13.1	14.2	16.3	13.8	14.4	14.2	14.2	13.7	15.9	14.0	15.0	14.3	13.5 w ± 1.6
1 - Estuary	4.9	3.5	5.1	6.6	5.4	5.5	5.0	5.2	10.1	6.9	7.4	8.1	7.6	7.9	8.2	8.0	7.8	8.1	6.9	5.8	6.7	9.1	6.6	8.7	6.3	8.8	9.1	10.3	4.4	10.0	9.3	6.9 w ± 1.6
2 - Northwest Gulf	11.0	8.0	9.0	9.2	10.7	10.0	9.6	9.4	13.0	12.6	13.6	15.0	12.6	14.6	15.1	12.3	13.1	11.1	12.6	10.5	12.7	13.8	11.6	13.0	11.9	13.9	13.0	14.6	11.5	13.9	14.1	11.9 w ± 1.9
3 - Anticosti Channel	9.5	8.8	11.5	8.9	11.4	7.3	7.7	8.9	9.4	11.4	12.6	13.4	12.0	13.0	15.2	11.3	12.9	11.3	11.9	10.8	13.0	14.6	10.7	11.9	12.7	12.5	10.9	13.2	12.9	12.2	13.0	11.3 w ± 2.0
4 - Mécatina Trough	4.6	5.4	9.0	6.7	5.9	7.7	2.9	2.8	4.2	8.3	7.8	7.8	8.8	8.4	12.5	11.6	10.7	8.0	11.8	9.5	9.7	11.7	8.6	10.2	9.9	9.1	8.3	12.0	10.9	8.7	10.2	8.2 w ± 2.7
5 - Esquiman Channel	9.9	9.4	13.0	10.8	10.9	10.9	8.9	8.2	9.2	12.9	13.1	11.9	12.4	12.6	15.6	13.6	14.5	10.1	15.3	11.8	12.6	16.8	13.1	13.3	13.3	12.6	11.7	15.2	12.7	13.7	12.8	12.2 w ± 2.1
6 - Central Gulf	12.3	10.9	14.2	11.3	12.4	12.2	12.6	11.8	12.8	14.6	15.5	15.4	13.9	14.2	16.7	14.2	16.1	12.4	15.3	13.3	13.8	17.2	13.1	13.9	14.9	13.9	13.5	16.2	14.3	14.9	13.4	13.8 w ± 1.6
7 - Cabot Strait	11.6	11.1	15.0	11.8	12.6	14.4	13.6	11.3	14.1	16.1	16.9	16.1	14.6	15.6	17.3	15.4	18.1	12.5	16.2	14.0	15.6	17.4	15.4	15.4	15.8	15.0	14.6	17.4	15.0	16.8	14.5	14.7 w ± 1.9
8 - Magdalen Shallows	14.8	14.5	16.6	14.1	15.5	16.3	17.6	15.1	16.1	17.5	18.8	18.2	16.8	17.4	18.6	17.6	19.8	17.4	18.1	17.8	17.9	19.5	18.7	18.2	17.7	17.6	17.7	19.0	17.9	18.4	17.3	17.2 w ± 1.5

Figure 25. Yearly number of weeks with mean weekly surface temperature >10°C, averaged for the entire Gulf and each region of the Gulf. The scorecards are colour-coded according to the normalized anomalies based on the 1985–2010 time series, but the numbers are the average number of weeks above 10°C for each year.

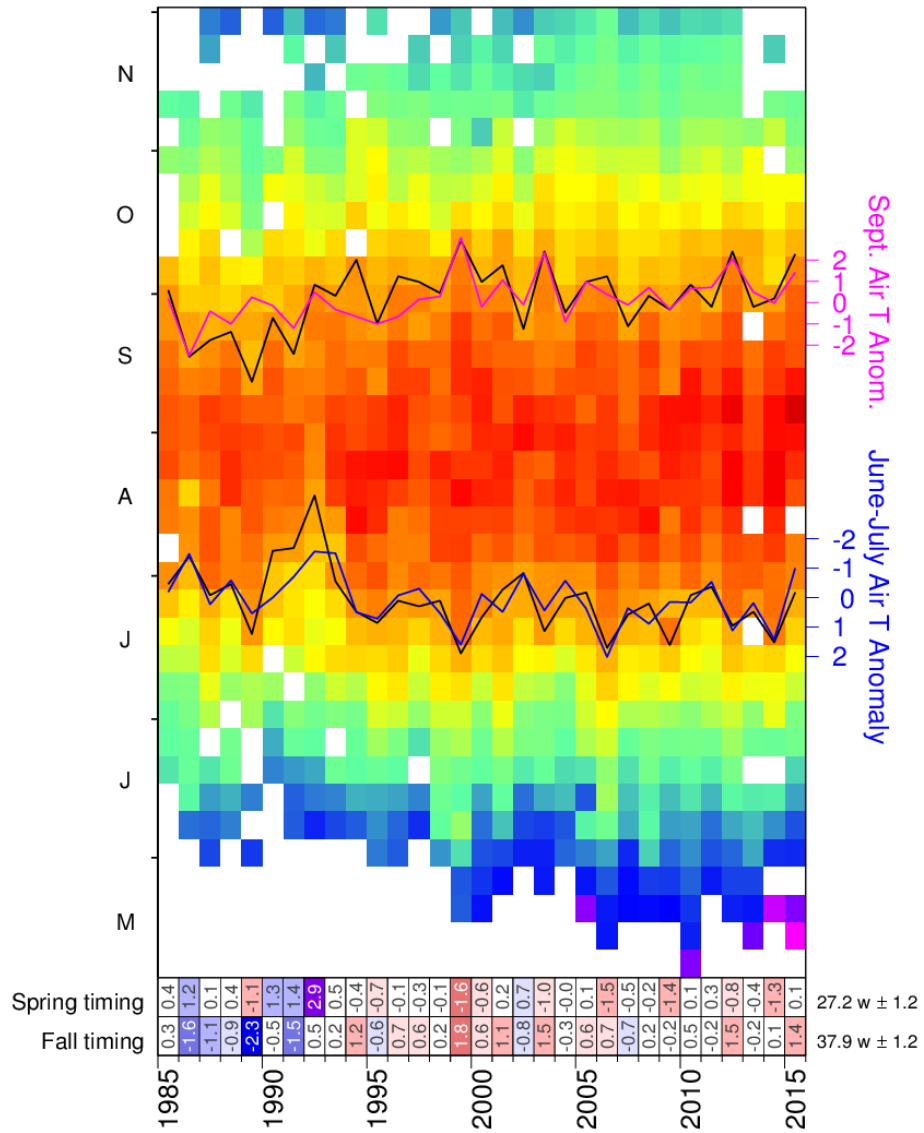


Figure 26. Weekly average SST (1985-2015) matrices for the Gulf of St. Lawrence. Temperature anomaly proxies for the first and last occurrence of the 12°C isotherm based on June-July and September average air temperature are also shown (axes on right). Updated from Galbraith and Larouche 2013.

Estuary and NW Gulf / Estuaire et NO du Golfe

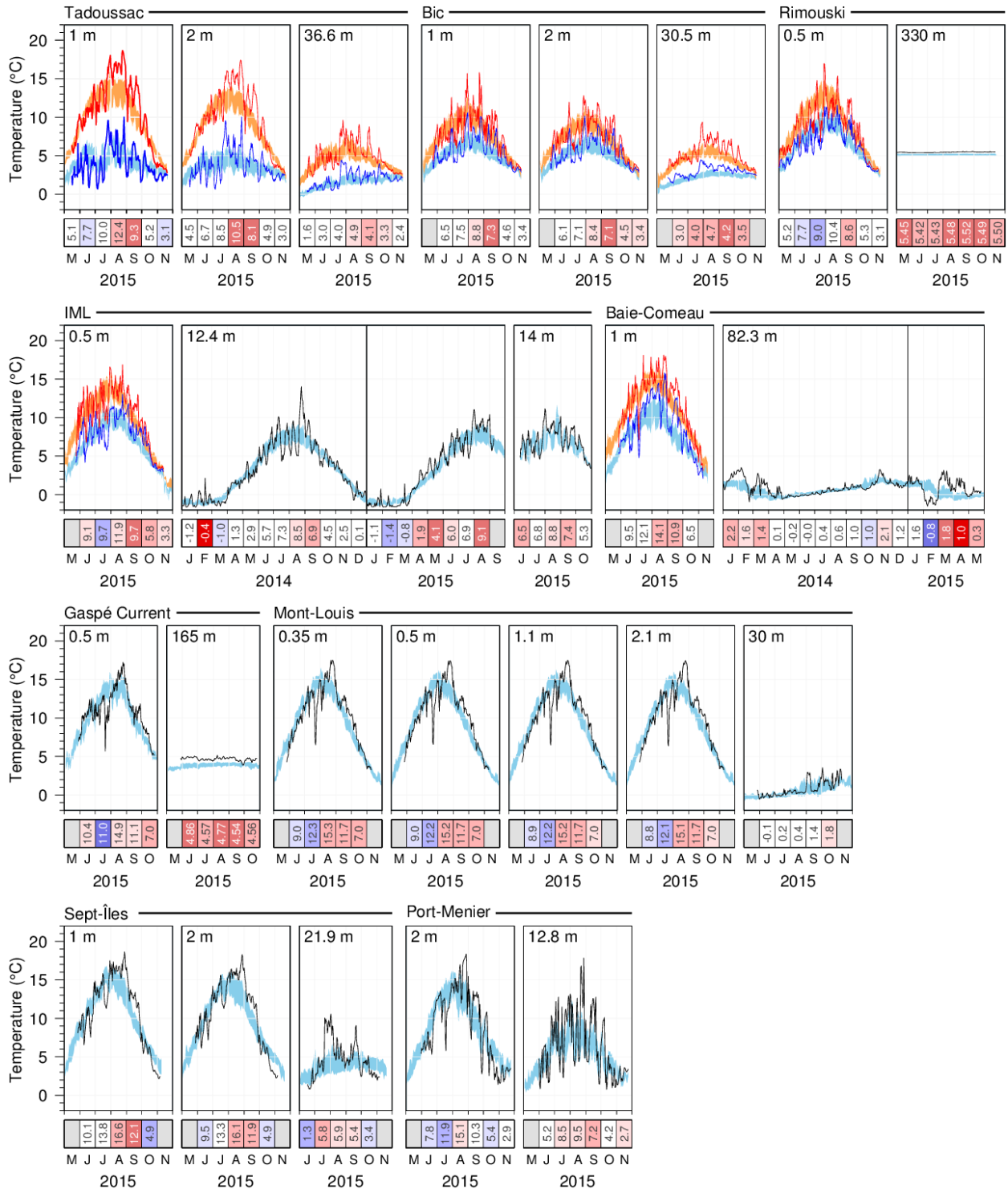


Figure 27. Thermograph network data. Daily mean 2015 temperatures compared with the daily climatology (blue areas are daily averages ± 0.5 SD, orange areas are daily average maximums ± 0.5 SD and bright blue areas are daily average minimums ± 0.5 SD) for stations in the Estuary and northwestern Gulf. Scorecards show monthly average temperature.

Lower North Shore / Basse Côte Nord

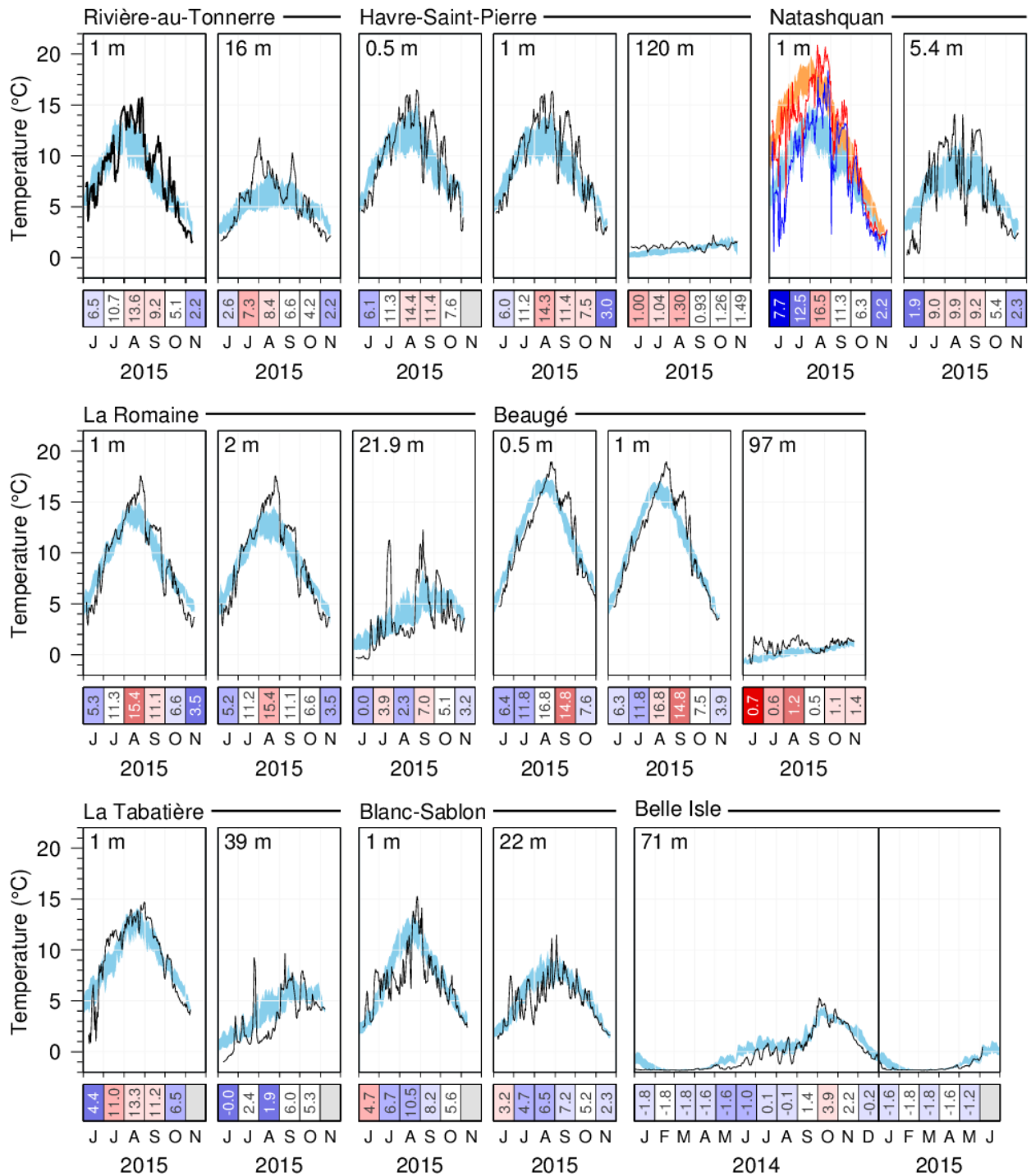


Figure 28. Thermograph network data. Daily mean 2015 temperatures compared with the daily climatology (blue areas are daily averages ± 0.5 SD, orange areas are daily average maximums ± 0.5 SD and bright blue areas are daily average minimums ± 0.5 SD) for stations of the lower north shore.

Southern Gulf / Sud du Golfe

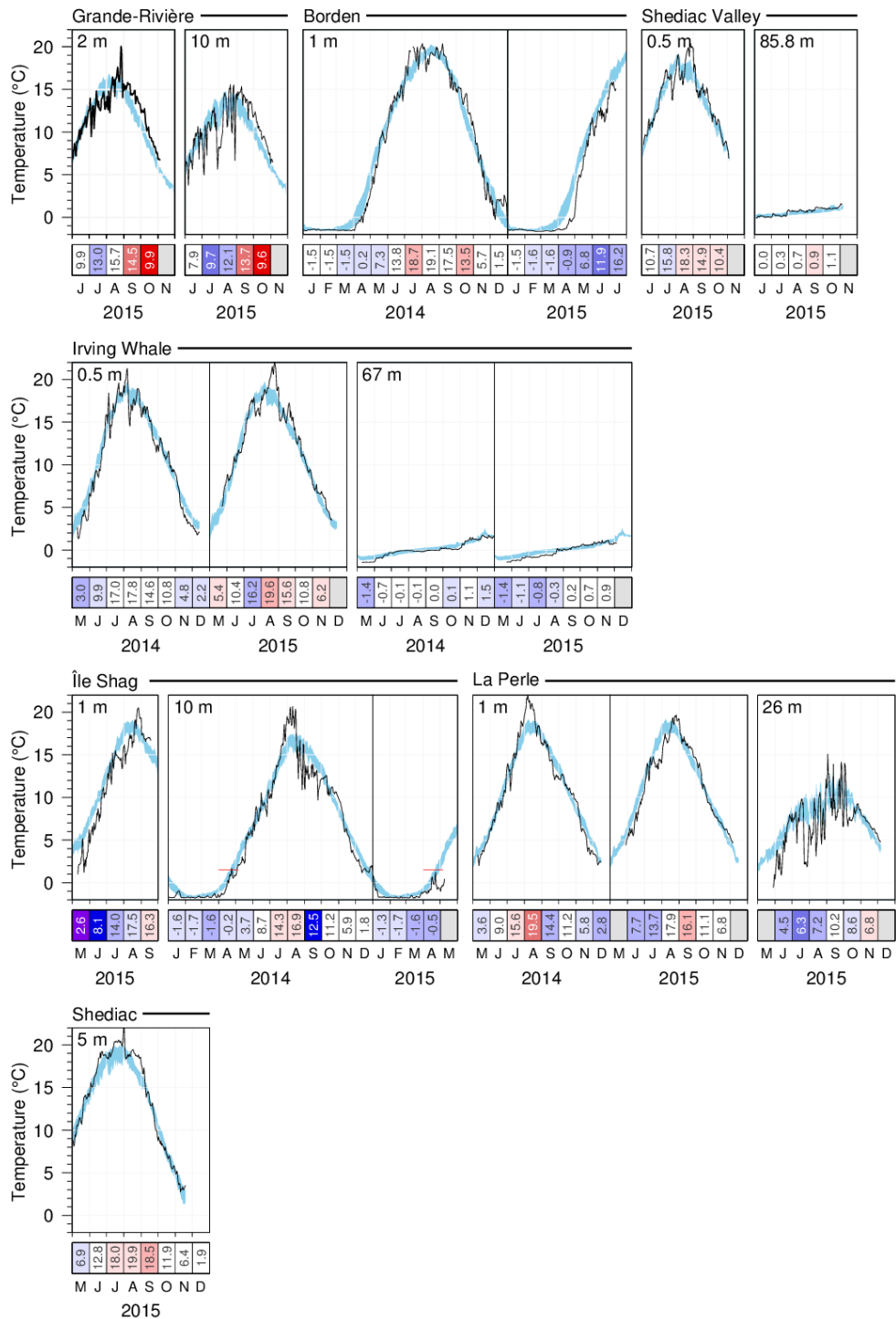


Figure 29. Thermograph network data. Daily mean 2015 temperatures compared with the daily climatology (daily averages ± 0.5 SD; blue area) for stations of the southern Gulf. Data from 2014 are included if they were not all shown in last year's report. Red lines in the Île Shag panel span the historical dates when spring temperature increased over 1.5°C , a temperature associated with increased lobster mobility.

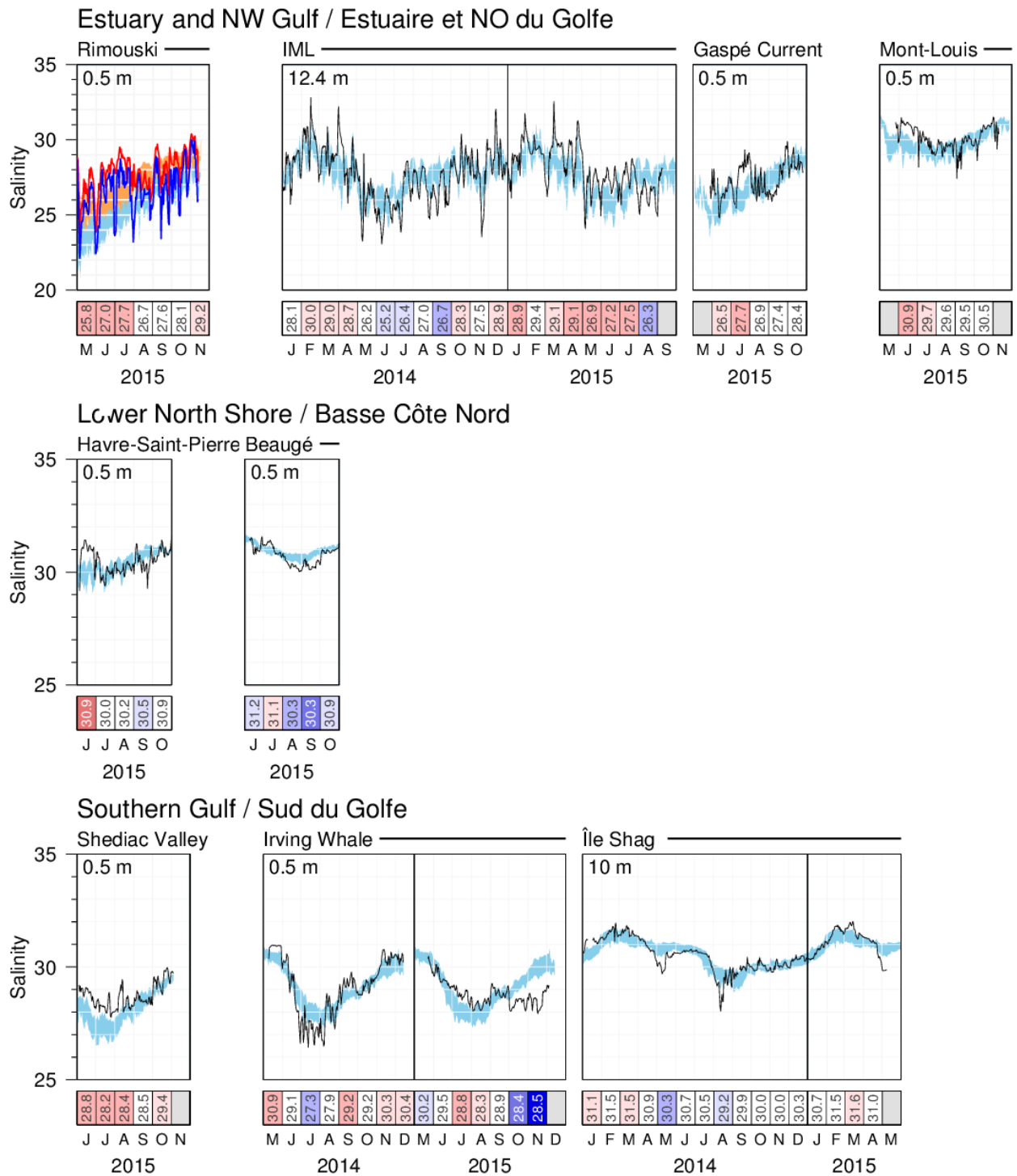


Figure 30. Thermograph network data. Daily mean 2015 salinities compared with the daily climatology (daily averages \pm 0.5 SD; blue area) computed from all available stations.

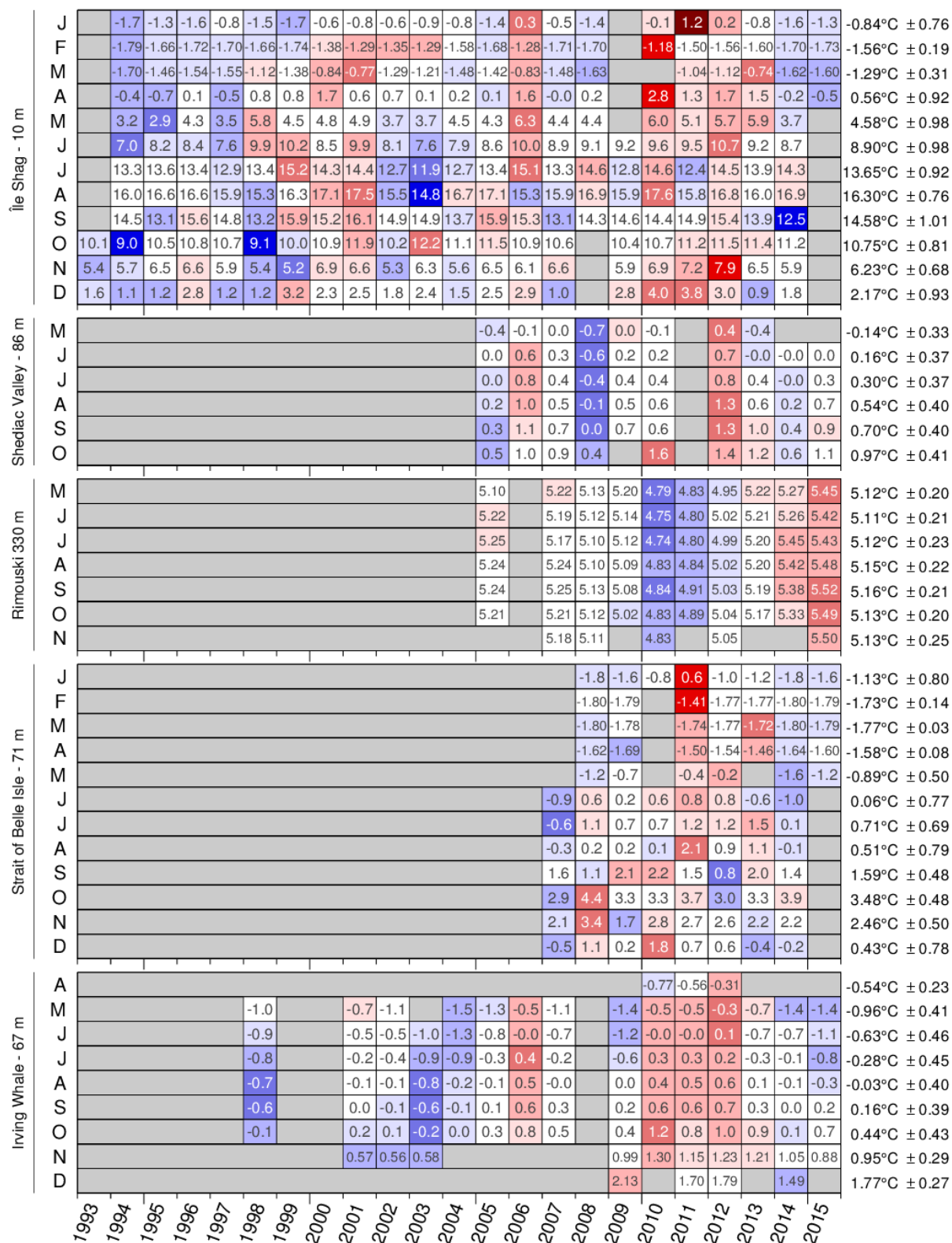


Figure 33. Time series of the monthly averaged temperature anomalies for selected stations of the thermograph network. The colour-coding is according to the temperature anomaly relative to the climatology of each station for each month. Numbers are monthly average temperatures. The mean and standard deviation are indicated for each month on the right side of the figure.

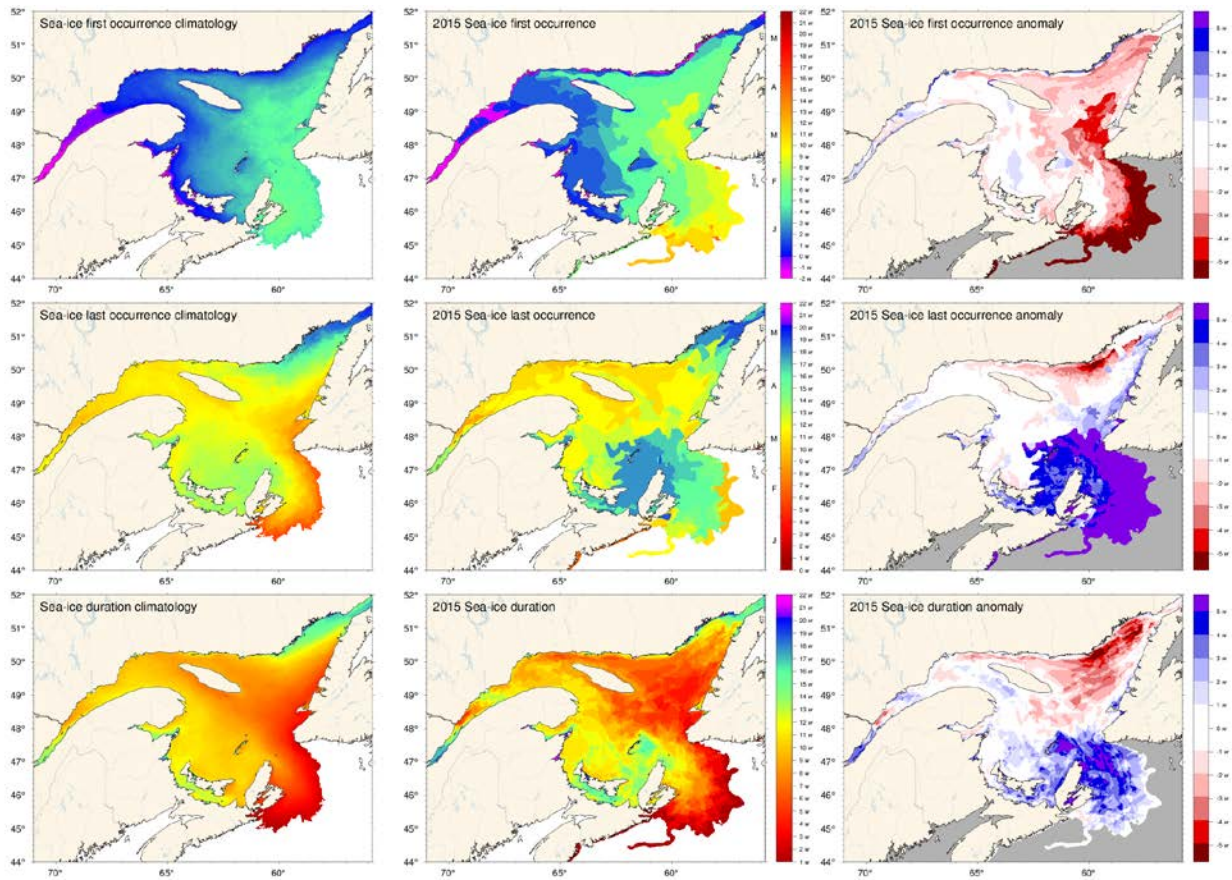


Figure 34. First and last occurrence of ice and ice season duration based on weekly data. The 1981-2010 climatologies are shown (left) as well as the 2015 values (middle) and anomalies (right). First and last occurrence is defined here as the first and last weekly chart in which any amount of ice is recorded for each pixel and are illustrated as day-of-year. Ice duration sums the number of weeks with ice cover for each pixel. Climatologies are shown for pixels that had at least 15 years out of the 30 with occurrence of sea-ice, and therefore also show the area with 50% likelihood of having some sea-ice at any time during any given year.

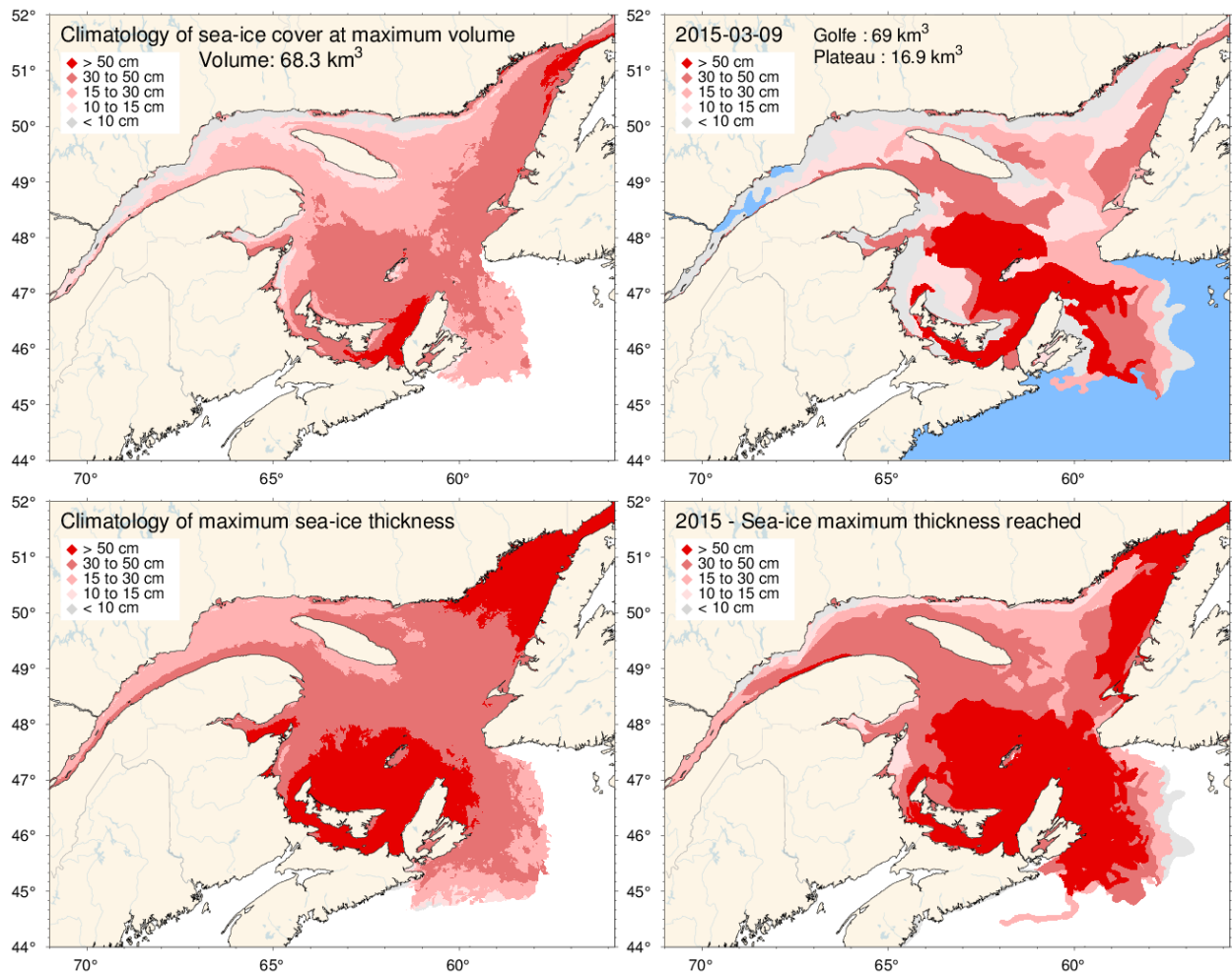


Figure 35. Ice thickness map for 2015 for the week of the year with the maximum annual volume including the portion covering the Scotian Shelf (upper right panel) and similarly for the 1981-2010 climatology of the weekly maximum (upper left panel). Note that these maps reflect the ice thickness distribution on that week, and not the maximum observed at any given location during the year. That information is shown by the lower panels, showing the 1981-2010 climatology and 2015 distribution of the thickest ice recorded during the season at any location.

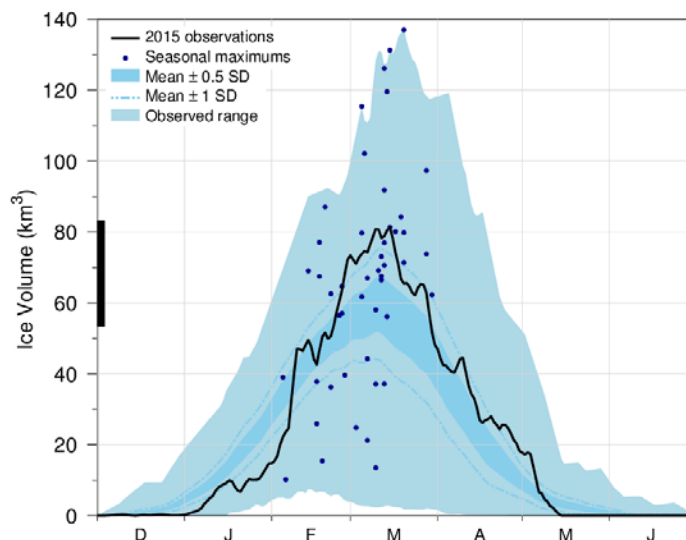


Figure 36. Time series of the 2014-2015 daily mean ice volume for the Gulf of St. Lawrence and Scotian Shelf (black line), the 1981-2010 climatological mean volume plus and minus 0.5 and 1 SD (dark blue area and dashed line), the minimum and maximum span of 1969-2015 observations (light blue) and the date and volumes of 1969-2015 seasonal maximums (blue dots). The black thick line on the left indicates the mean volume plus and minus 0.5 SD of the annual maximum ice volume, which is higher than the peak of the mean daily ice volume distribution.

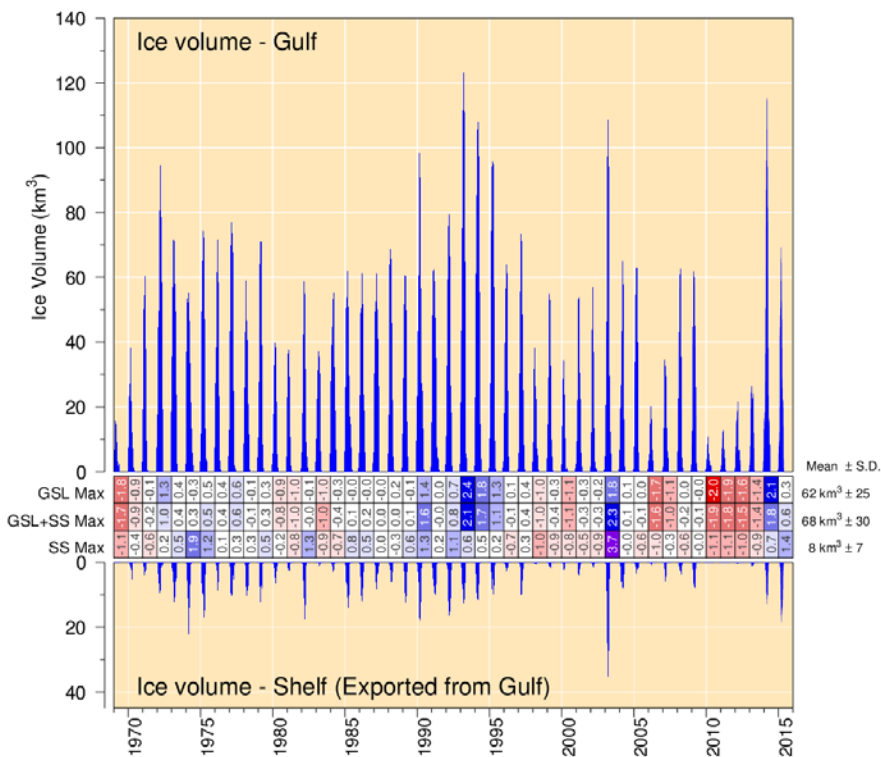


Figure 37. Estimated ice volume in the Gulf of St. Lawrence (upper panel) and on the Scotian Shelf seaward of Cabot Strait (lower panel). Scorecards show numbered normalized anomalies for the Gulf, combined Gulf and Shelf and Shelf-only annual maximum volumes from weekly ice data. The mean and standard deviation are indicated on the right side using the 1981-2010 climatology.

	First occurrence of ice								Mean ± S.D.
	1 - Estuary	2 - Northwest Gulf	3 - Anticosti Channel	4 - Mécatina Trough	5 - Esquiman Channel	6 - Central Gulf	7 - Cabot Strait	8 - Magdalen Shallows	
	17	56	77	43	17	17	17	17	8 ± 10
	17	31	29	52	12	12	12	12	2 ± 10
	-5	25	13	12	11	9	9	9	7 ± 14
	-6	23	16	14	-5	-5	-3	-7	1 ± 12
	-12	10	0	-6	-12	-10	-12	-12	20 ± 13
	4	19	13	8	5	3	-3	-3	20 ± 11
	4	27	23	26	3	7	1	8	29 ± 13
	4	31	12	32	3	-5	-5	-5	3 ± 11
	14	8	9	-12	-1	-14	-14	-14	
	3	26	19	32	3	2	1	1	
	-21	37	12	11	-28	-26	-23	-26	
	5	30	30	27	0	-10	5	-13	
	-7	9	6	30	-5	2	-9	-24	
	10	28	38	28	14	12	10	9	
	8	49	21	40	11	9	2	-11	
	-5	27	17	12	-7	-2	-7	-9	
	-1	17	17	12	-3	-3	-2	-3	
	-9	16	9	4	-15	-7	-14	-19	
	1	31	16	6	-18	-16	-14	-19	
	2	25	20	13	1	1	1	1	
	-9	24	11	4	-7	-6	-8	-11	
	-2	24	11	4	-7	-6	-8	-11	
	-20	2	0	3	-21	-20	-21	-21	
	1	19	10	5	-11	-6	-1	-5	
	-3	20	17	17	-8	-4	-4	-17	
	-2	21	6	2	-8	-5	-3	-21	
	-1	13	8	19	-2	-6	-3	-7	
	5	38	26	11	-2	6	10	3	
	-14	22	17	12	-20	17	2	-21	
	4	35	28	37	13	17	5	0	
	-1	38	34	19	6	13	5	-13	
	1	33	15	26	4	12	2	-1	
	4	39	29	40	12	12	9	1	
	4	47	32	30	7	22	14	2	
	17	37	32	24	17	21	16	2	
	6	25	19	14	-2	3	10	0	
	6	23	44	42	29	34	6	-8	
	6	28	25	21	6	16	2	-3	
	38	60	37	27	12	22	23	21	
	29	37	37	27	12	22	23	21	
	7	44	24	17	7	7	7	7	
	4	22	18	27	14	16	6	-18	
	20	41	22	26	19	-7	-7	-7	
	28	59	39	59	35	34	1	-1	
	17	54	34	61	20	20	3	3	
	14	39	54	40	21	33	14	1	
	-7	30	8	1	-7	-3	-11	-20	
	8	34	34	34	20	27	7	-11	
	8	34	34	34	20	27	7	-11	

	Last occurrence of ice								Mean ± S.D.
	1 - Estuary	2 - Northwest Gulf	3 - Anticosti Channel	4 - Mécatina Trough	5 - Esquiman Channel	6 - Central Gulf	7 - Cabot Strait	8 - Magdalen Shallows	
	95	84	137	86	84	84	84	84	85 ± 12
	103	74	124	129	102	81	88	88	93 ± 13
	104	100	90	90	93	77	83	70	120 ± 24
	142	140	136	135	128	139	114	104	140 ± 19
	127	130	103	124	140	133	91	77	118 ± 25
	113	113	120	168	179	160	96	78	101 ± 15
	127	131	117	140	168	126	91	77	109 ± 16
	105	103	106	127	144	124	104	93	112 ± 15
	113	120	99	130	156	106	92	91	112 ± 15
	117	112	108	136	142	132	96	104	112 ± 15
	117	104	101	83	137	111	96	91	112 ± 15
	111	112	86	103	121	97	85	84	112 ± 15
	81	69	75	68	95	82	65	58	112 ± 15
	107	111	104	123	156	144	83	83	
	120	104	79	89	117	103	99	106	
	141	91	105	132	147	132	103	101	
	106	113	102	153	162	131	85	84	
	113	111	112	133	147	144	90	77	
	131	128	94	124	122	122	116	86	
	113	106	97	109	135	135	85	79	
	108	118	110	125	134	110	90	91	
	109	115	126	159	161	154	94	73	
	123	124	120	127	184	132	92	103	
	136	133	124	139	152	132	105	93	
	129	128	120	133	159	124	112	90	
	120	113	121	146	162	161	113	94	
	126	123	116	138	151	146	121	105	
	115	101	98	102	125	109	97	77	
	127	135	119	131	150	157	97	89	
	108	93	105	103	137	100	94	88	
	109	110	72	124	139	108	93	87	
	91	79	81	83	118	86	85	84	
	116	116	85	129	153	119	84	77	
	96	95	98	93	111	94	87	83	
	109	117	111	145	152	159	96	82	
	116	115	98	120	130	102	95	86	
	114	114	92	92	122	98	93	87	
	89	85	111	118	118	80	78	78	
	91	85	82	131	147	112	84	87	
	112	114	97	117	150	104	97	90	
	109	104	98	118	128	114	87	81	
	86	80	100	107	82	66	56	54	
	86	80	100	107	82	66	56	54	
	84	77	73	100	134	77	75	75	
	110	110	58	107	123	97	61	82	
	115	111	109	154	160	158	95	89	
	130	130	132	132	137	93	88	88	

	Duration of ice season								Mean ± S.D.
	1 - Estuary	2 - Northwest Gulf	3 - Anticosti Channel	4 - Mécatina Trough	5 - Esquiman Channel	6 - Central Gulf	7 - Cabot Strait	8 - Magdalen Shallows	
	79	0	46	63	24	65	68	68	93 ± 14
	92	70	46	63	24	65	68	68	90 ± 19
	110	76	66	79	76	69	75	81	107 ± 29
	149	118	121	118	134	145	118	112	138 ± 26
	140	121	104	131	153	135	104	90	95 ± 36
	110	95	103	159	175	151	101	81	74 ± 31
	123	105	95	135	161	119	91	86	76 ± 28
	122	73	95	96	150	120	110	99	109 ± 22
	110	87	84	105	140	131	98	104	
	139	68	80	70	155	122	115	118	
	107	83	57	76	122	108	81	96	
	89	61	70	39	101	81	75	83	
	98	84	67	96	138	112	74	93	
	113	43	59	50	129	113	98	118	
	147	64	95	100	150	131	110	111	
	123	96	104	130	163	148	100	97	
	131	98	79	118	141	129	129	106	
	112	82	78	97	135	127	88	88	
	118	95	100	122	142	108	99	103	
	130	114	97	115	163	151	116	92	
	123	106	111	123	181	139	92	109	
	40	119	104	123	161	123	110	113	
	132	106	115	132	163	130	118	111	
	122	101	114	125	165	155	117	98	
	122	86	91	127	154	141	112	103	
	122	72	82	88	141	93	96	99	
	124	101	84	95	138	109	88	90	
	110	42	51	56	132	88	90	102	
	109	63	58	59	136	97	92	89	
	80	41	41	31	107	75	77	76	
	113	60	44	100	145	98	71	76	
	80	59	62	70	95	74	72	81	
	104	93	93	129	155	139	87	83	
	109	93	48	71	102	69	90	97	
	109	83	68	72	113	83	92	91	
	52	26	0	71	118	65	77	91	
	71	53	41	99	136	90	64	67	
	103	71	74	101	142	98	83	83	
	106	83	81	88	116	99	82	100	
	63	0	0	10	79	37	38	56	
	62	22	0	13	68	28	46	79	
	68	24	27	22	105	58	70	73	
	97	72	5	58	102	66	41	70	
	123	82	102	135	168	150	107	110	
	123	97	74	95	116	107	82	94	

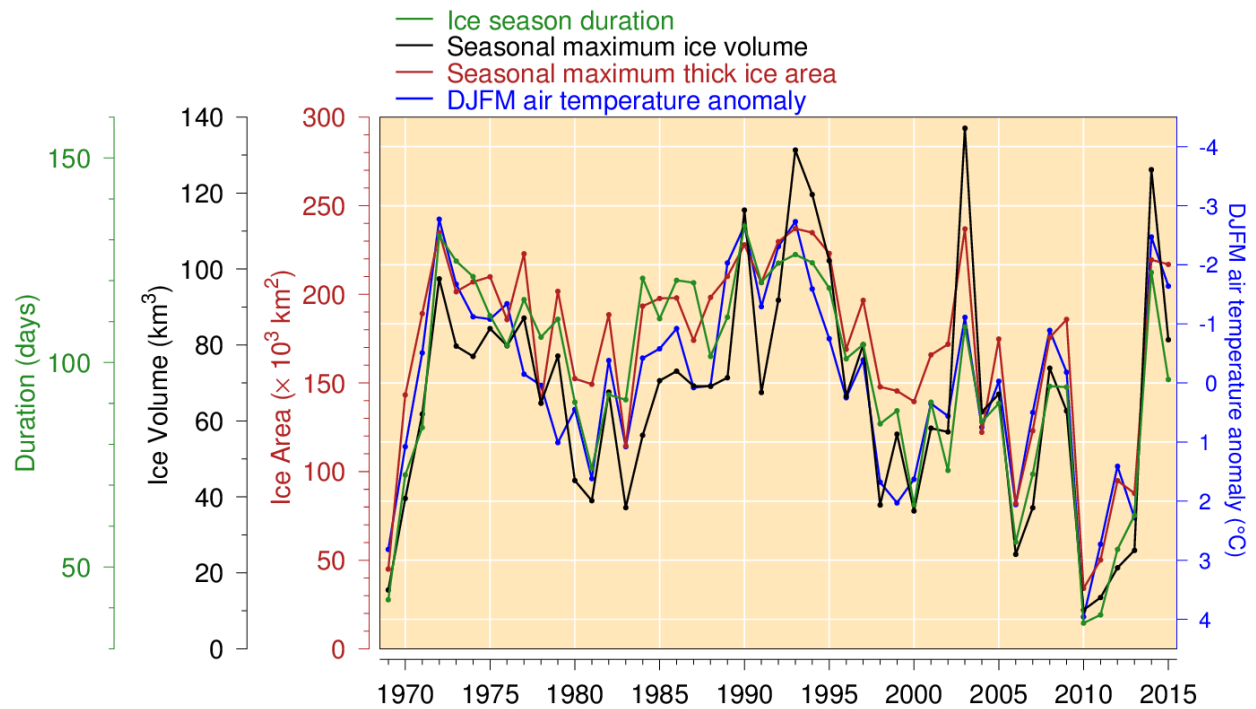


Figure 39. Seasonal maximum ice volume and area including the portion on the Scotian Shelf (excluding ice less than 15 cm thick), ice season duration and December-to-March air temperature anomaly (Figure adapted from Hammill and Galbraith 2012, but here not excluding small floes and adding February and March data to the air temperature anomalies). All sea-ice products are based on weekly data. Linear relations indicate losses of 17 km³, 30,000 km² and 14 days of sea-ice season for each 1°C increase in winter air temperature (R^2 of 0.74, 0.80 and 0.76 respectively).

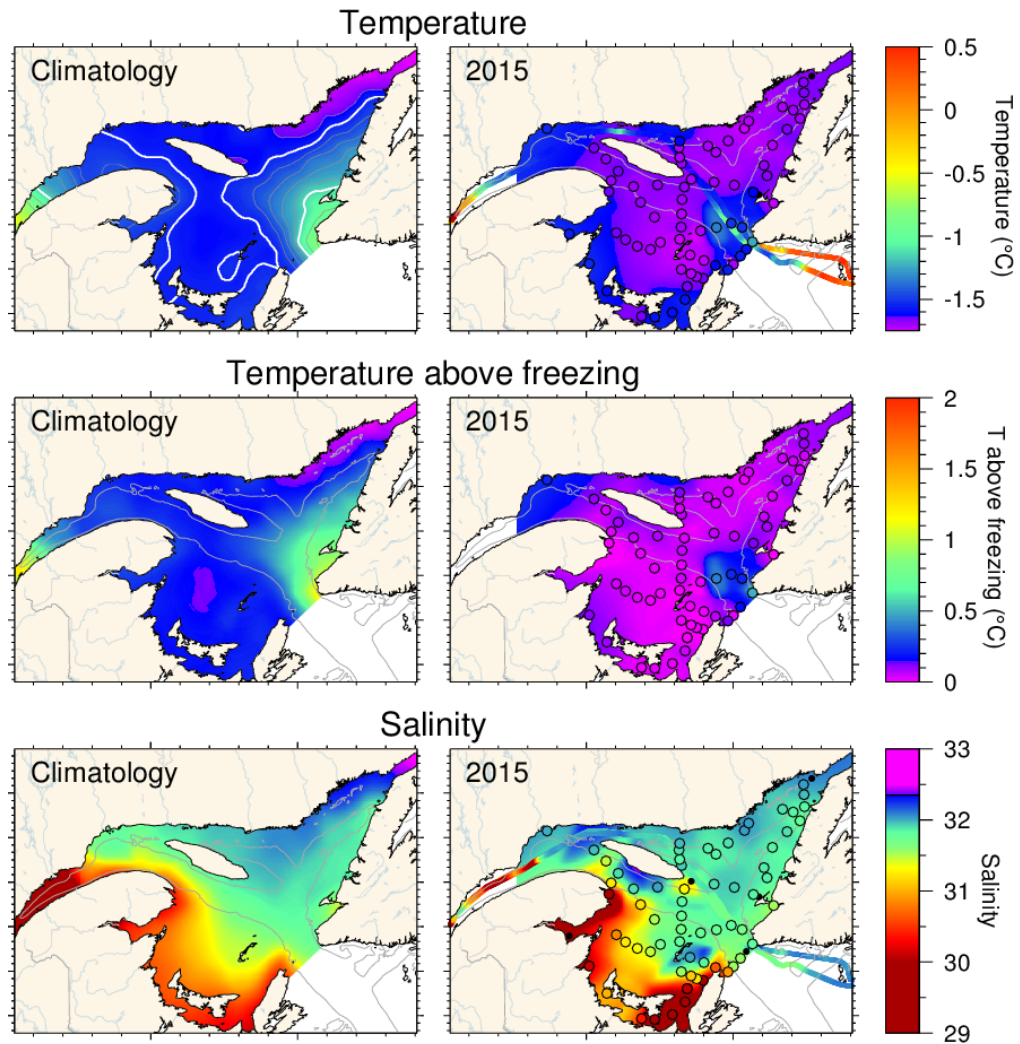


Figure 40. Winter surface layer characteristics from the March 2015 helicopter survey compared with climatological means: surface water temperature (upper panel), temperature difference between surface water temperature and the freezing point (middle panel), and salinity (lower panel). Symbols are coloured according to the value observed at the station, using the same colour palette as the interpolated image. A good match is seen between the interpolation and the station observations where the station colours blend into the background. Black symbols indicate missing or bad data. The climatologies are based on 1996-2015 for salinity but excludes 2010 as an outlier for temperature and temperature above freezing.

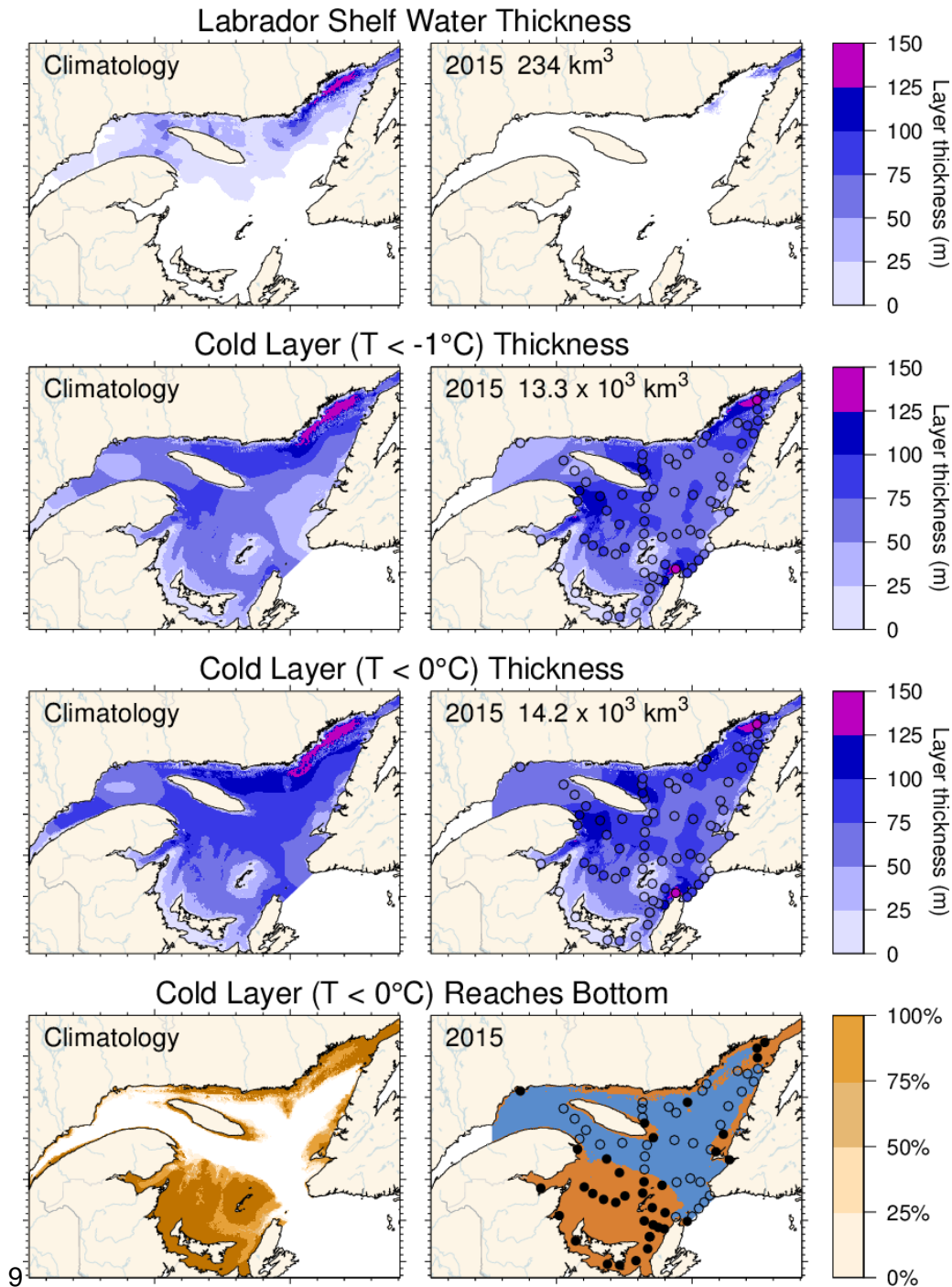


Figure 41. Winter surface layer characteristics from the March 2015 helicopter survey compared with climatological means: estimates of the thickness of the Labrador Shelf water intrusion (upper panels), cold layer ($T < -1^{\circ}\text{C}$, $T < 0^{\circ}\text{C}$) thickness (middle panels), and maps indicating where the cold layer ($T < 0^{\circ}\text{C}$) reaches the bottom (in brown; lower panels). Station symbols are coloured according to the observed values as in Figure 40. For the lower panels, the stations where the cold layer reached the bottom are indicated with filled circles while open circles represent stations where the layer did not reach the bottom. Integrated volumes are indicated for the first six panels (including an approximation for the Estuary but excluding the Strait of Belle Isle). The climatologies are based on 1997-2015 for the Labrador Shelf water intrusion, 1996-2015 for the cold layer ($T < 0^{\circ}\text{C}$) but excludes 2010 for $T < -1^{\circ}\text{C}$.

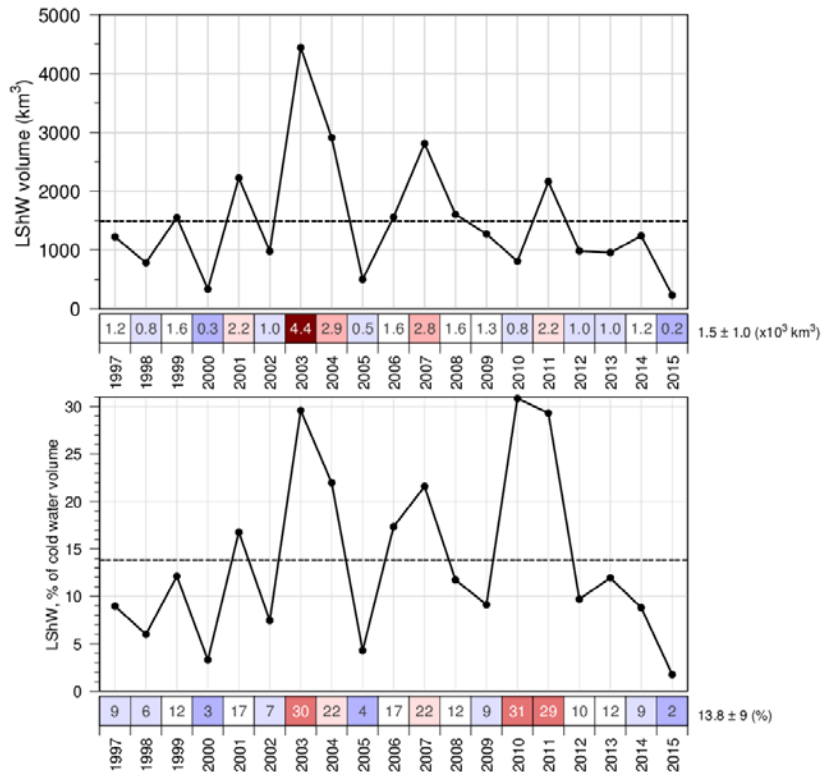


Figure 42. Estimated volume of cold and saline Labrador Shelf water that flowed into the Gulf over the winter through the Strait of Belle Isle. The bottom panel shows the volume as a percentage of total cold-water volume ($<-1^{\circ}\text{C}$). The numbers in the boxes are actual values colour-coded according to their anomaly.

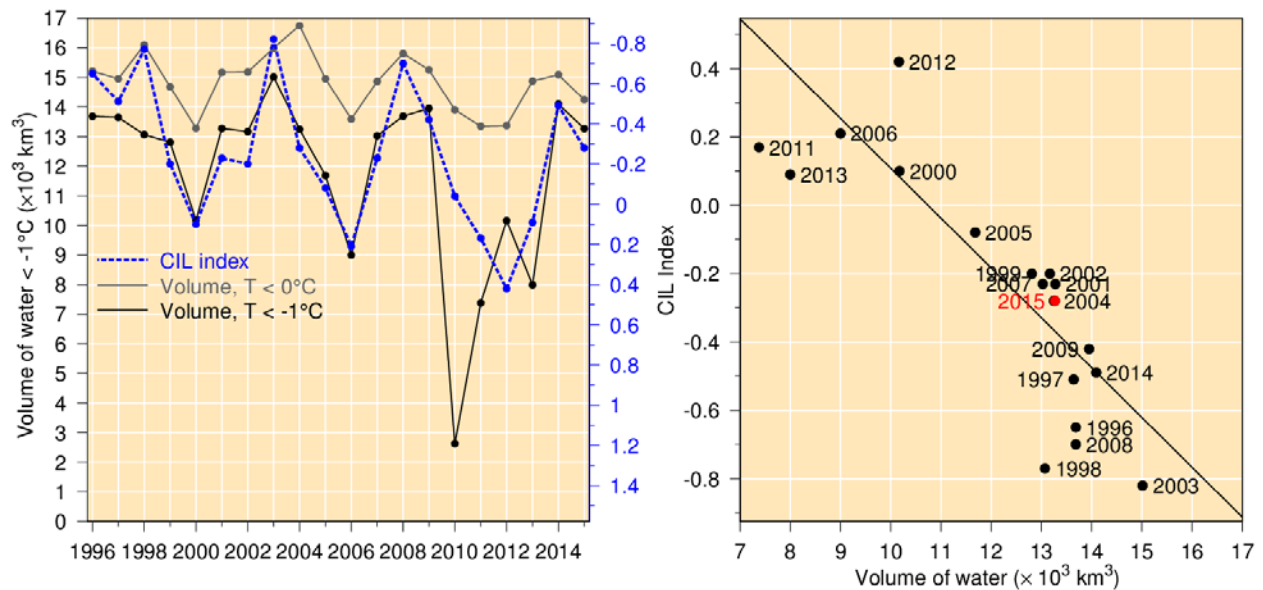


Figure 43. Left panel: winter surface cold ($T<-1^{\circ}\text{C}$ and $T<0^{\circ}\text{C}$) layer volume (excluding the Estuary and the Strait of Belle Isle) time series (black and grey lines) and summer CIL index (blue dashed line). Right panel: Relation between summer CIL index and winter cold-water volume with $T<-1^{\circ}\text{C}$ (regression for 1996-2014 data pairs, excluding 1998 [see Galbraith 2006] as well as the 2010 and 2011 mild winters). Note that the CIL scale in the left panel is reversed.

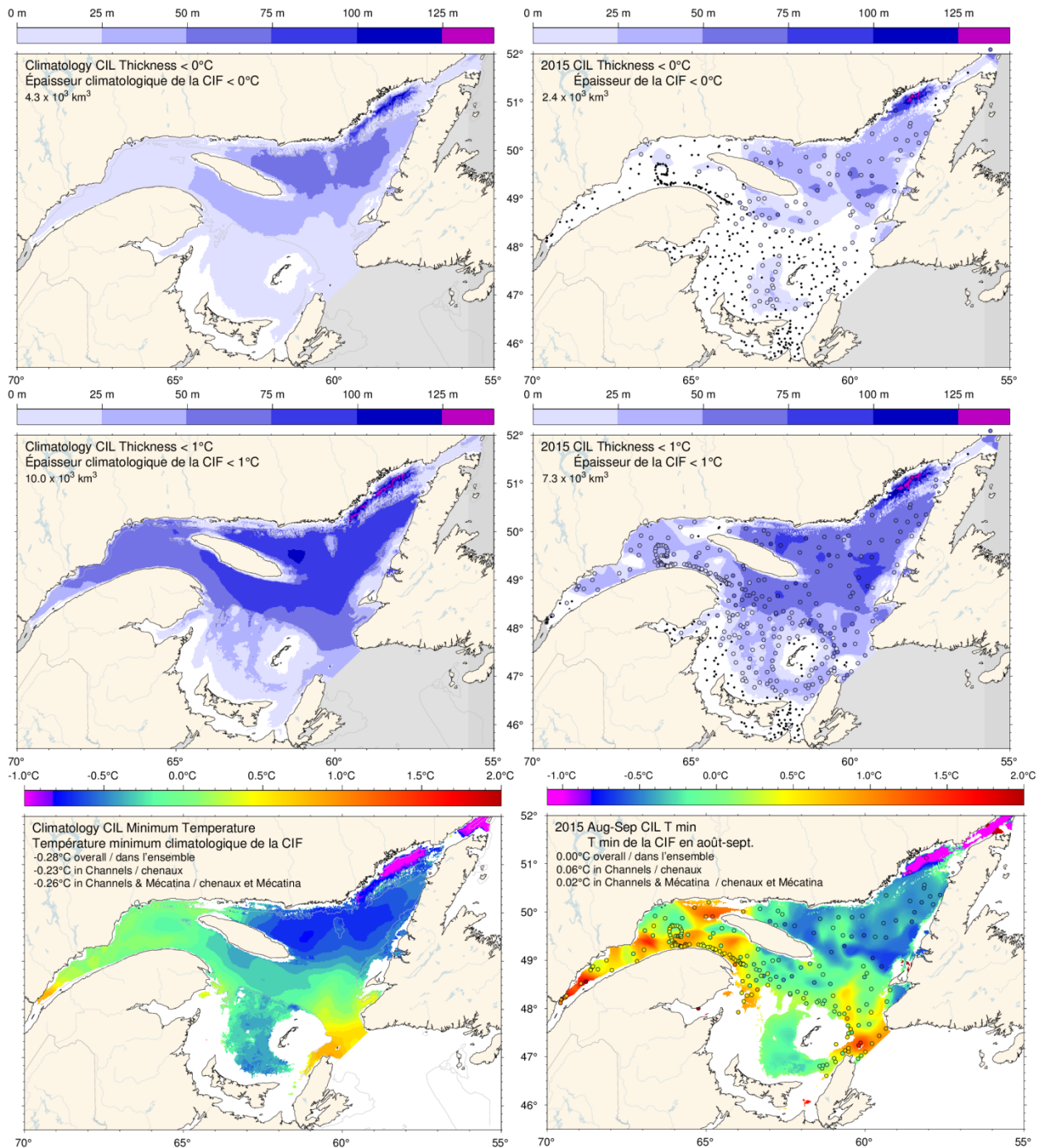


Figure 44. Cold intermediate layer thickness ($T < 0^{\circ}\text{C}$, top panels; $T < 1^{\circ}\text{C}$, middle panels) and minimum temperature (bottom panels) in August and September 2015 (right) and 1985-2010 climatology (left). Station symbols are colour-coded according to their CIL thickness and minimum temperature. Numbers in the upper and middle panels are integrated CIL volumes and in the lower panels are monthly average temperatures.

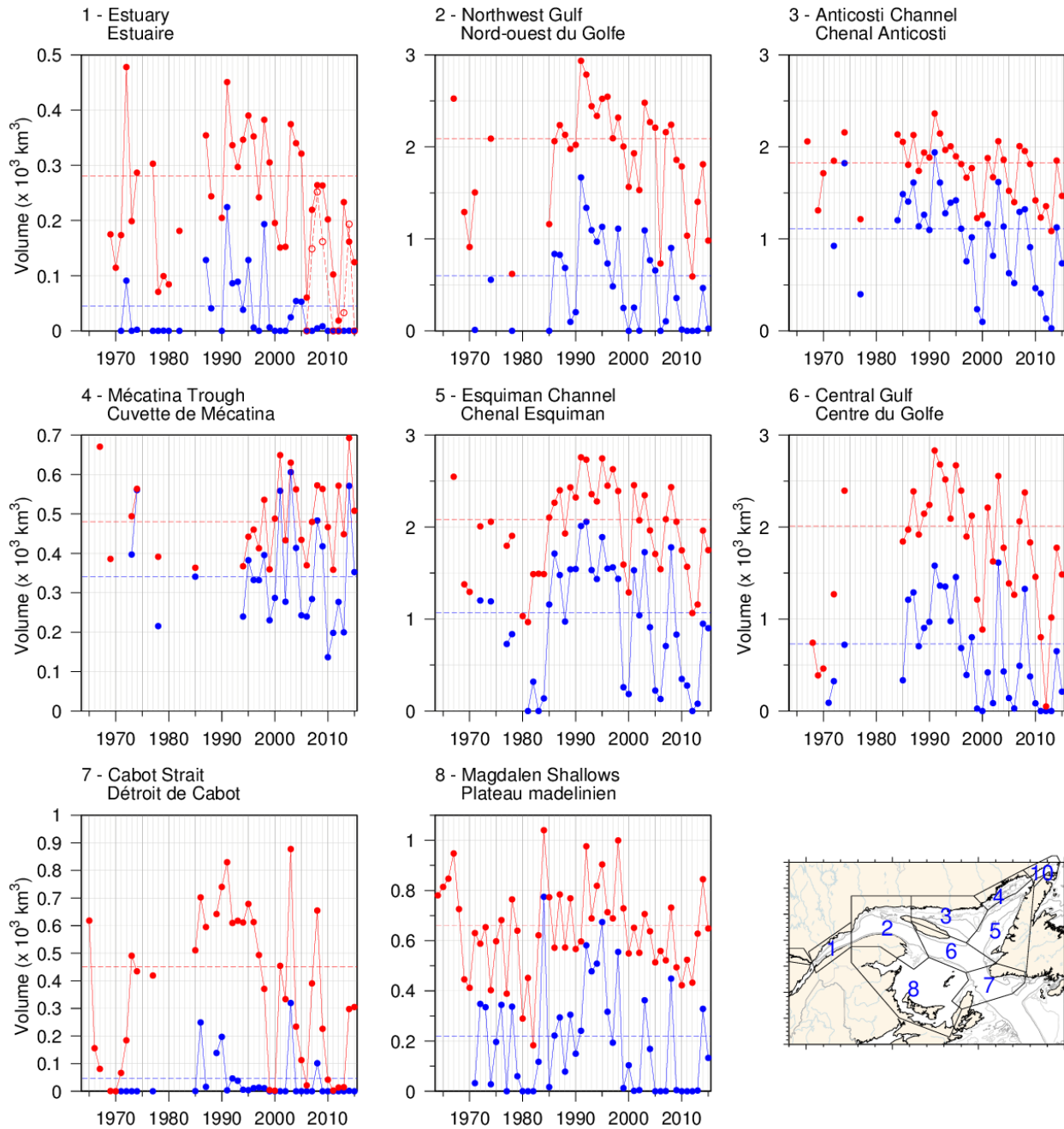


Figure 45. Volume of the CIL colder than 0°C (blue) and colder than 1°C (red) in August and September (primarily region 8 in September). The volume of the CIL colder than 1°C in November for available years since 2006 is also shown for the St. Lawrence Estuary (dashed line).

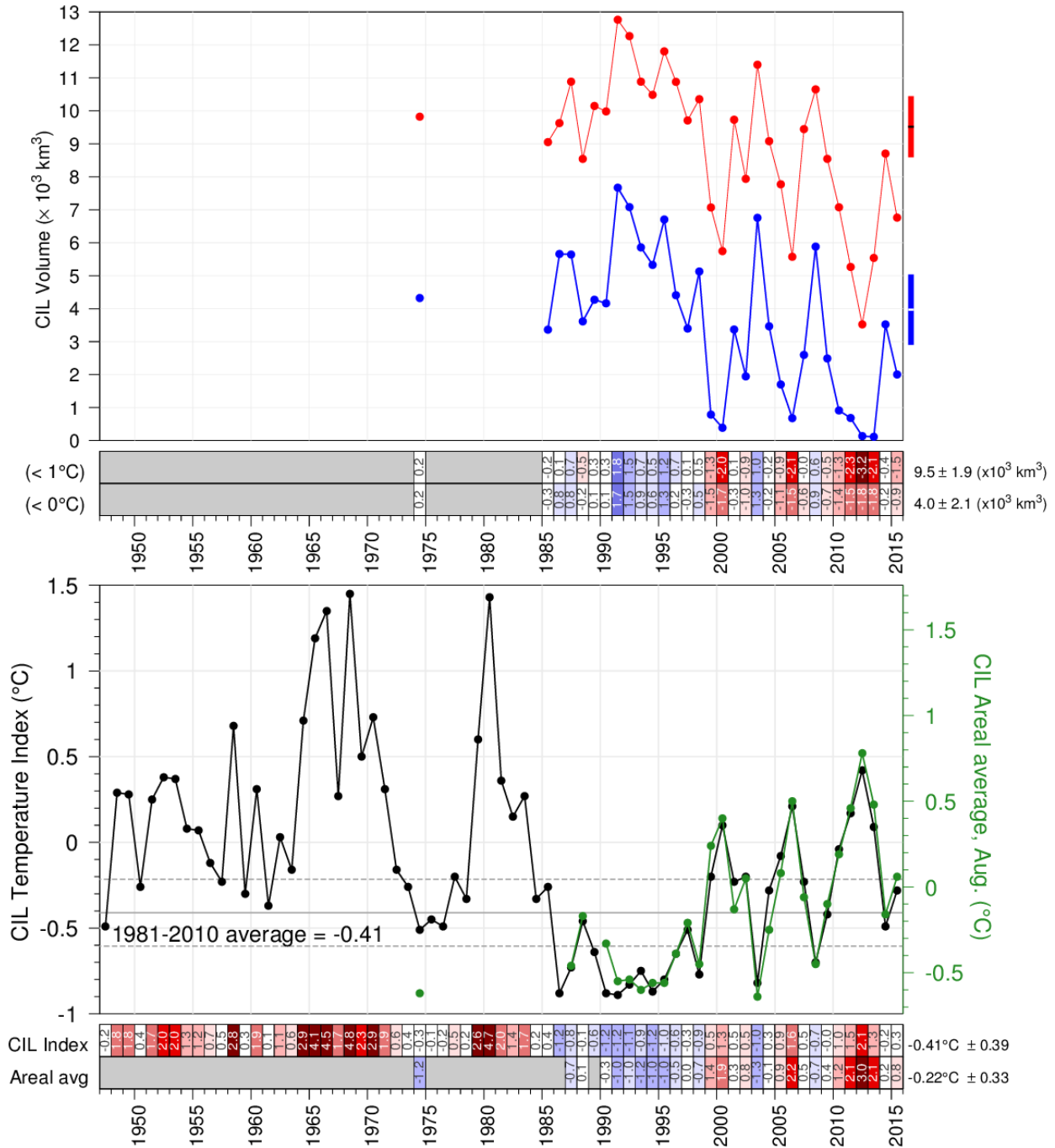


Figure 46. CIL volume (top panel) delimited by 0°C (in blue) and 1°C (in red), and minimum temperature index (bottom panel) in the Gulf of St. Lawrence. The volumes are integrals of each of the annual interpolated thickness grids such as those shown in the top panels of Figure 44 excluding Mécatina Trough and the Strait of Belle Isle. Rectangles on right side show mean ± 0.5 SD. In the lower panel, the black line is the updated Gilbert and Pettigrew (1997) index interpolated to 15 July (with dashed lines showing mean ± 0.5 SD) and the green line is the spatial average of each of the annual interpolated grid such as those shown in the two bottom panels of Figure 44, excluding Mécatina Trough, the Strait of Belle Isle and the Magdalen Shallows. The numbers in the boxes are normalized anomalies relative to 1980-2010 climatologies constructed using all available years.

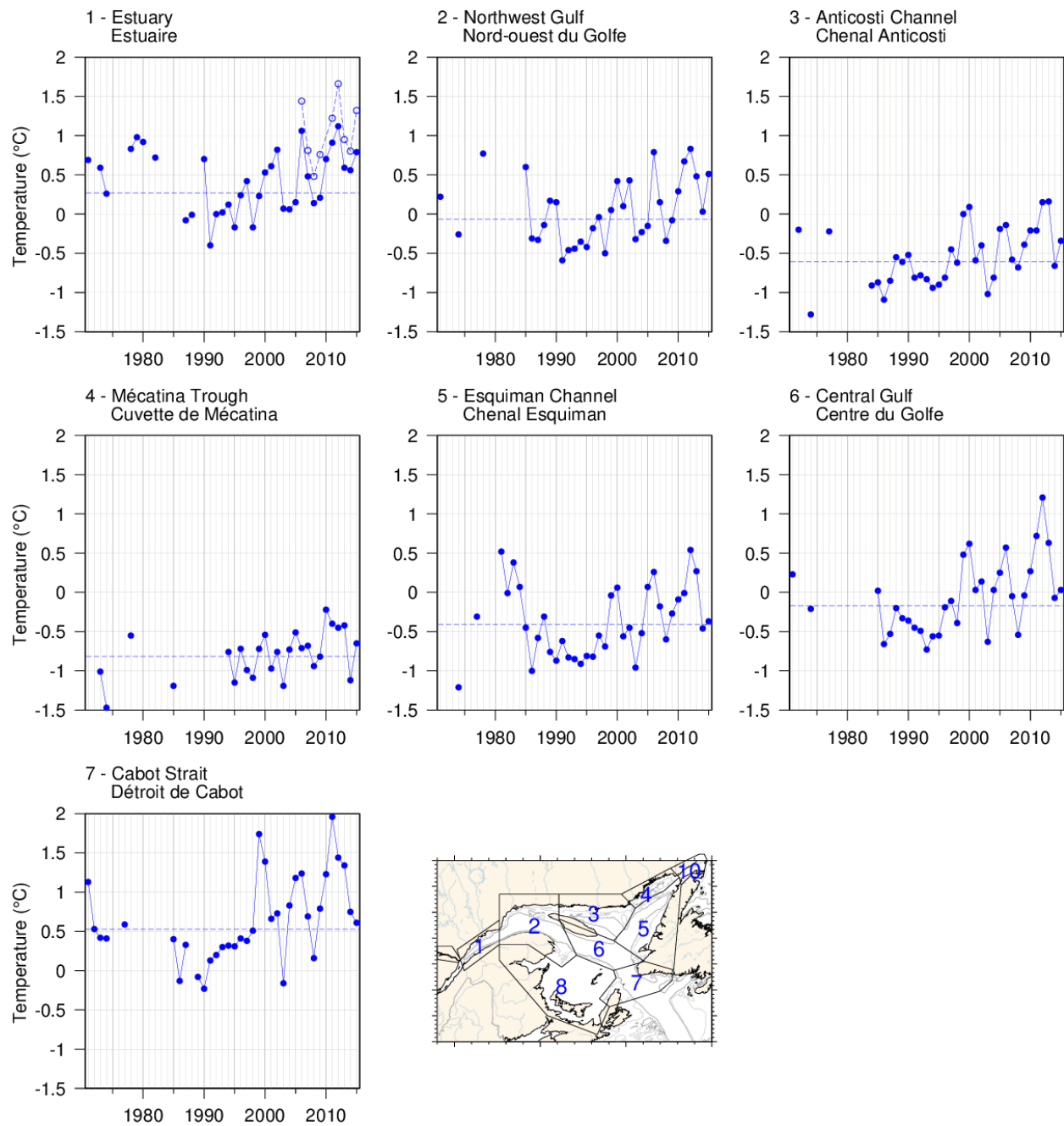


Figure 47. Temperature minimum of the CIL spatially averaged for the seven areas where the CIL minimum temperature can be clearly identified. The spatial average of the November CIL temperature minimum for available years since 2006 is also shown for the St. Lawrence Estuary (dashed line).

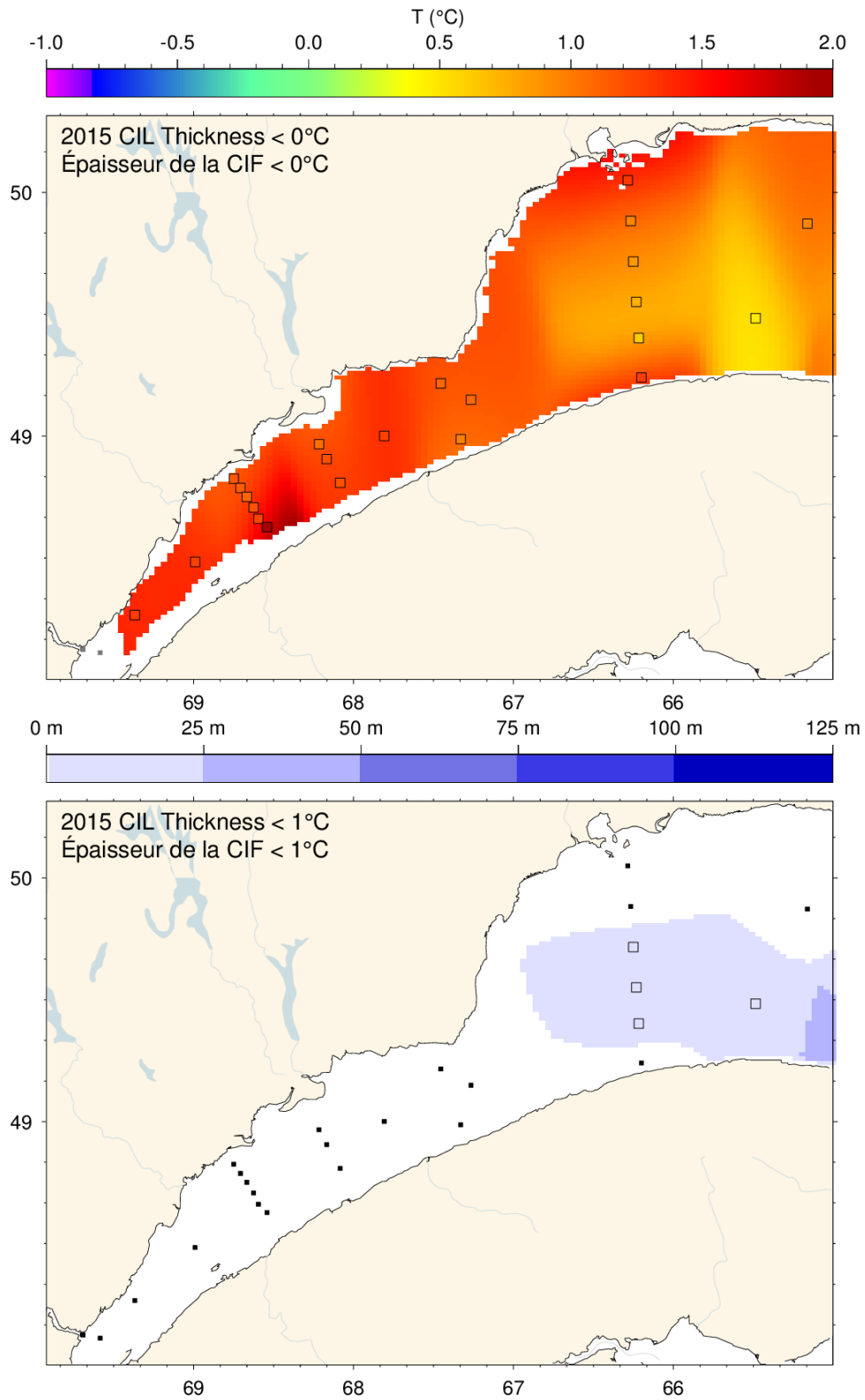


Figure 48. Cold intermediate layer minimum temperature and thickness ($T < 1^\circ\text{C}$) in November 2015 in the St. Lawrence Estuary.

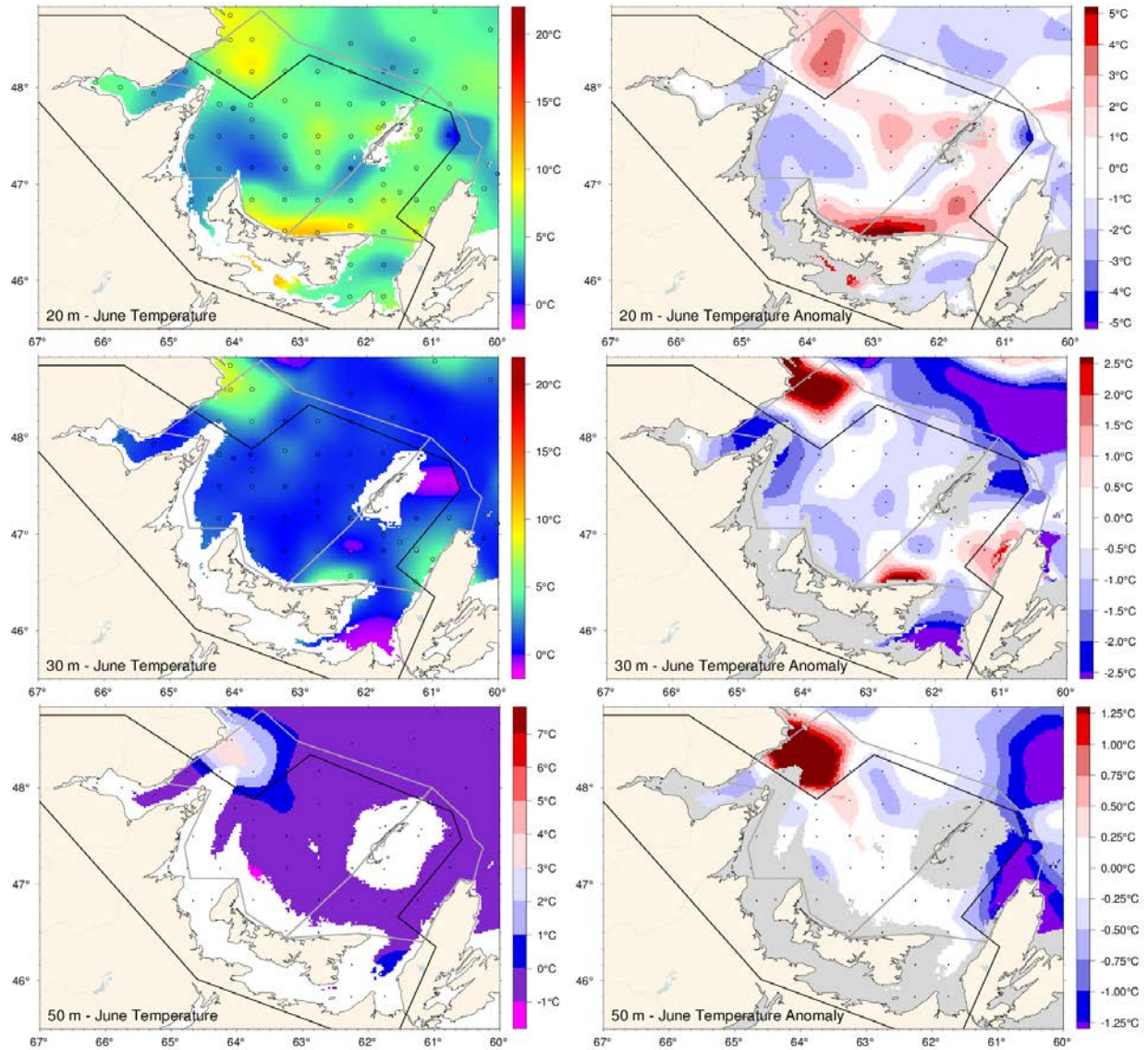


Figure 50. June depth-layer temperature and anomaly fields on the Magdalen Shallows at 10, 20 and 50 m. Anomalies are based on 1971-2010 climatologies for all available years (appearing on Figure 51) The black outline delimits Region 8 (Figure 2) and the gray outlines delimit western and eastern regions of the Magdalen Shallows (Figure 22).

	Western Shelf						Eastern Shelf																			
	SST June	10 m temp.	20 m temp.	30 m temp.	50 m temp.	75 m temp.	SST June	10 m temp.	20 m temp.	30 m temp.	50 m temp.	75 m temp.														
1960	-0.1	-0.3	0.9	3.0	8.4		1.0	1.2	0.9	4.8	10.5															
1965		-0.4	-0.0	1.9	4.4	7.2		0.4	0.1	1.4	3.5	6.3														
		-0.2	0.3	2.5	4.7	6.6		0.6	0.4	3.0	5.9	7.8														
		-0.1	0.2	1.8	3.6	7.7		1.2	0.9	2.1	3.7	7.3														
		0.1	0.2	1.9	3.3	5.2		-0.0	-0.2	0.5	1.8	5.4														
		-0.0	-0.3	1.7	5.6	8.7		1.1	1.1	2.7	5.0	7.9														
1970		0.8	0.8	2.5	4.6	8.1		1.3	1.3	3.6	5.3	8.4														
		0.6	-0.3	2.1	4.1	7.3		0.2	-0.3	1.6	3.5	7.3														
1975								-0.0	0.1	1.5	5.2	6.6														
		-0.2	-0.1	2.0	5.0	7.3		0.0	0.0	2.1	5.1	7.9														
		-0.5	-0.7	1.5	4.8	8.8		1.3	0.8	2.4	5.2	7.8														
		-0.1	0.8	2.6	4.1	7.1																				
1980		0.6	1.5	4.1	6.7	9.3		0.9	1.5	4.1	6.5	8.3														
		0.2	0.7	2.4	5.5	9.4		0.8	0.2	2.0	5.7	9.2														
		-0.7	-0.8	1.2	3.8	9.6		1.1	-0.2	1.3	4.8	10.2														
		-0.8	-0.5	2.6	6.1	7.9		0.9	0.3	3.3	6.1	7.0														
1985		0.7	-0.2	1.7	5.0	8.6	8.0	0.9	-0.1	1.4	4.4	8.1	7.1													
		-0.6	-0.4	3.4	6.8	8.6	8.6	-0.7	-0.7	3.8	7.6	8.5	8.3													
		-0.5	-1.0	1.1	4.4	10.2	10.6	-0.4	-0.9	0.3	3.7	8.3	9.8													
		-0.2	-0.4	2.1	4.2	7.9	8.0	0.8	-0.0	2.1	4.9	8.0	7.3													
							10.5					9.2														
							9.1					8.1														
							10.0					8.6														
		-0.3	-0.3	1.5	4.3	8.4	9.4	0.0	-0.9	0.4	2.9	7.0	8.1													
		-0.0	-1.1	1.6	5.8	7.4	8.8	0.5	-1.1	0.3	4.3	6.7	7.7													
		-0.5	-0.6	1.3	3.8	8.3	10.4	0.6	-0.7	1.7	4.7	7.7	9.8													
1995							11.1					10.0														
		-0.4	-0.6	1.6	3.9	9.7	11.2	0.0	-0.2	1.0	4.5	8.0	10.5													
		-0.8	0.0	2.7	4.3	7.4	9.0	-0.1	0.3	2.7	4.6	6.7	8.0													
							10.6					10.2														
		-0.2	0.2	2.0	4.9	9.9	11.6	0.8	0.9	3.4	7.0	10.5	11.1													
		-0.1	-0.0	3.0	5.6	9.1	9.8	1.1	0.5	3.4	6.0	8.8	9.3													
		-0.5	0.1	1.5	4.0	8.4	11.7	0.3	0.1	1.5	4.1	8.5	10.8													
		0.1	0.1	2.0	4.9	8.3	9.6	0.8	0.6	2.7	5.1	7.7	9.0													
		-0.6	-0.5	1.6	3.8	7.8	9.8	-0.2	-0.6	1.2	4.0	7.4	9.0													
		-0.5	0.0	3.1	5.5	8.0	8.8	0.5	0.3	3.2	5.4	7.4	8.2													
		0.0	0.2	1.6	3.2	8.5	9.6	1.1	0.9	2.0	4.3	7.1	8.9													
		0.7	0.2	1.1	3.7	11.5	11.9	1.1	0.8	0.8	3.5	11.5	11.5													
		0.1	0.1	2.0	5.0	8.6	9.8	0.6	0.2	1.0	3.0	7.9	9.5													
		-0.7	-0.7	0.7	3.5	7.9	10.1	0.1	-1.0	0.2	4.2	8.2	9.7													
		-0.1	-0.1	1.9	5.0	9.3	10.2	0.5	0.0	2.2	5.5	8.7	9.6													
2010		0.4	0.9	3.6	6.4	8.6	9.8	1.1	1.8	4.5	7.6	8.5	9.2													
		0.8	0.2	2.1	4.7	8.7	9.4	1.8	0.7	2.2	5.9	8.1	8.4													
		0.8	0.5	2.3	5.7	10.0	10.6	1.4	0.4	1.9	5.8	9.9	10.7													
		0.0	0.2	2.9	5.6	8.5	9.8	0.7	0.4	1.9	5.4	8.6	9.6													
		-0.4	-0.5	1.1	3.7	7.8	10.9	-0.3	-0.6	0.5	3.4	7.4	10.1													
2015		0.1	0.0	1.5	4.9	9.3	9.6	0.5	-0.6	1.6	5.7	8.1	8.1													
		9.92°C					±1.06																			
		8.73°C					±0.97																			
		4.72°C					±0.97																			
		1.97°C					±0.76																			
		-0.19°C					±0.50																			
		-0.24°C					±0.43																			

Figure 51. Depth-layer average temperature anomalies for western and eastern Magdalen Shallows for the June mackerel survey. The SST data are June averages from NOAA remote sensing repeated from Figure 23. The SST colour-coding is based on the 1985-2010 climatology and the numbers are mean temperatures in °C. The colour-coding of the 10 to 75 m lines are according to normalized anomalies based on the 1981-2010 climatologies, but the numbers are mean temperatures in °C.

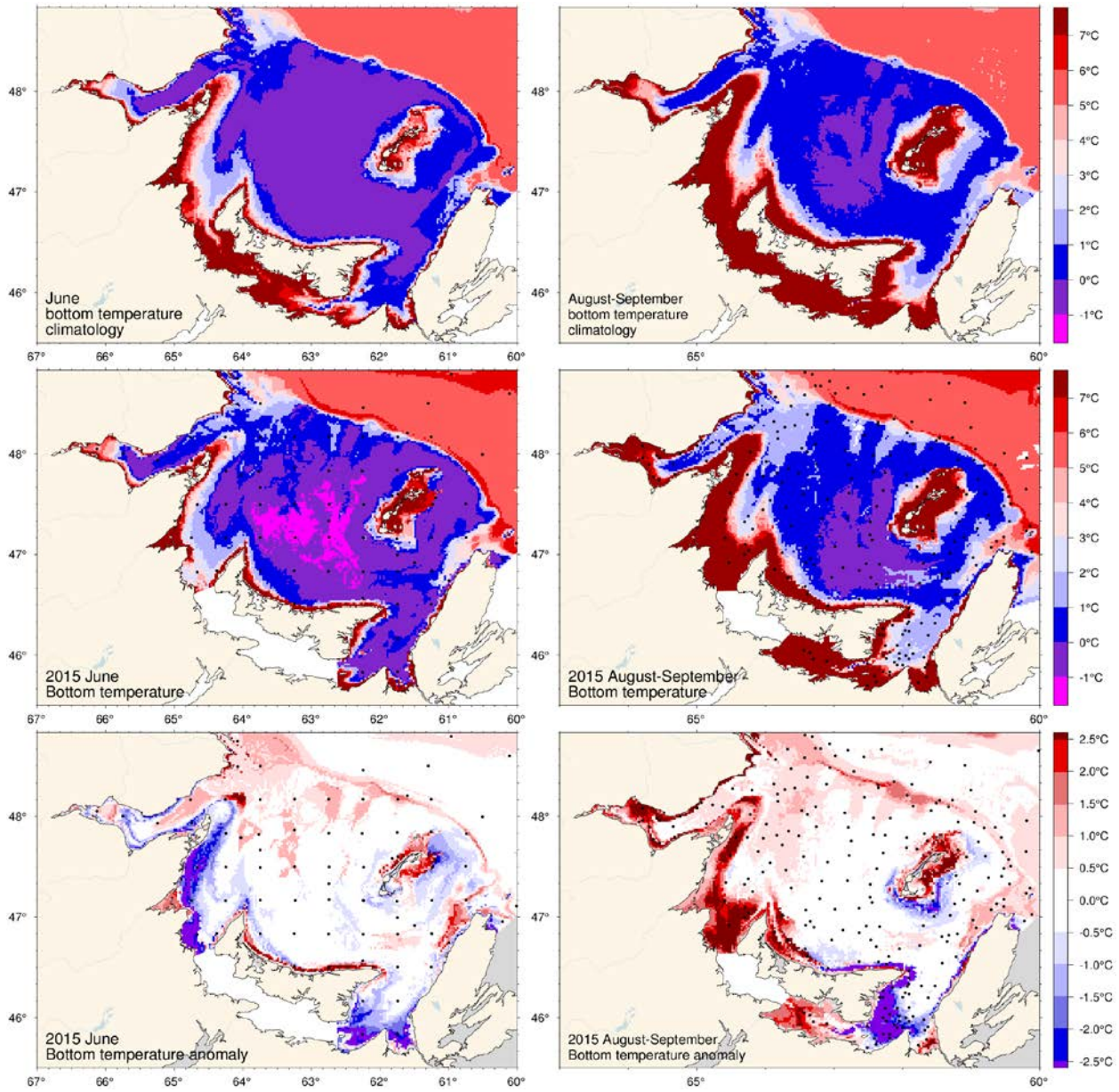


Figure 52. June (left) and August-September (right) bottom temperature climatology (top), 2015 observations (middle) and anomaly (bottom).

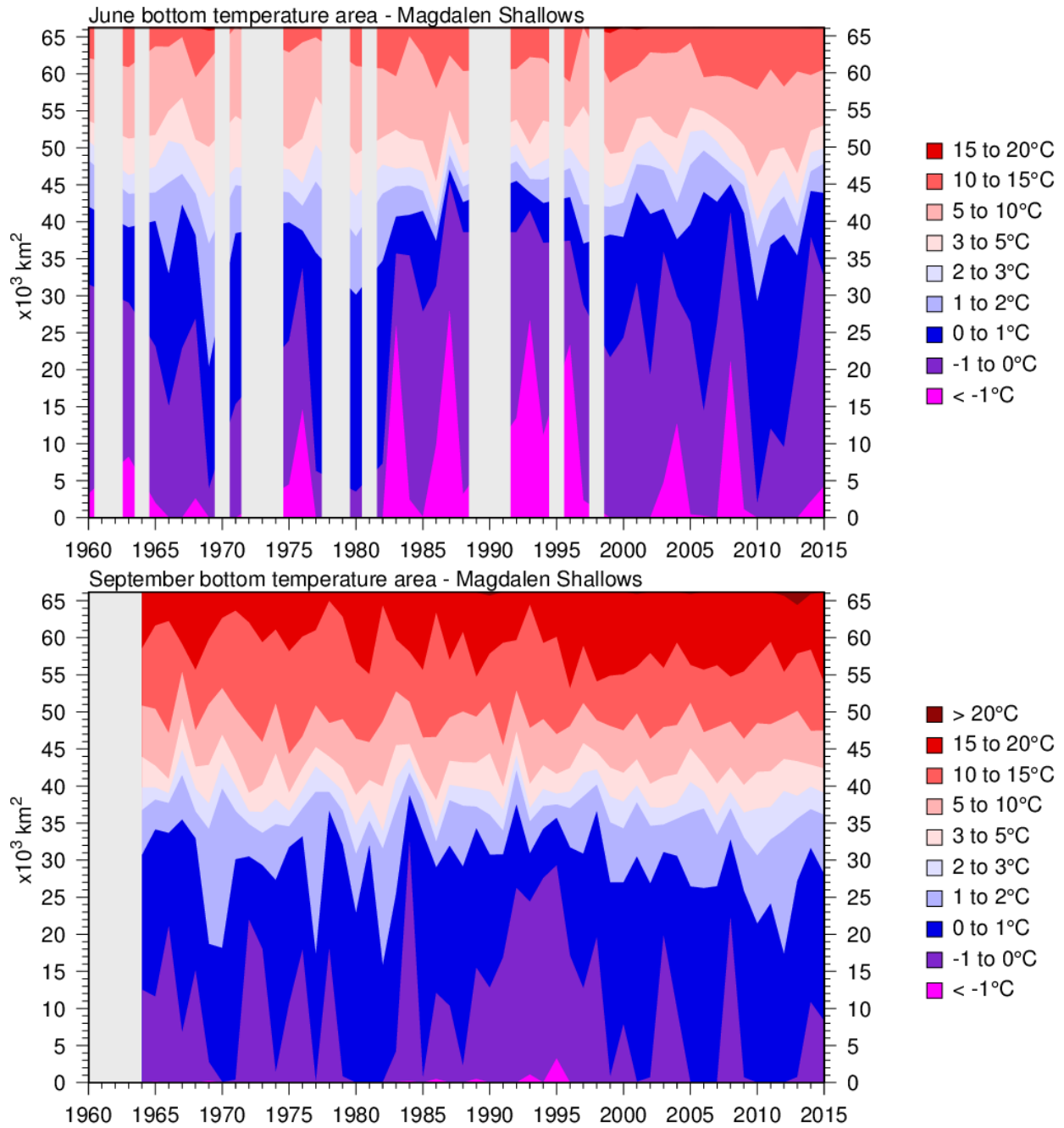


Figure 53. Time series of the bottom areas covered by different temperature bins in June (top) and August-September (bottom) for the Magdalen Shallows (region 8). Data are mostly from September for the bottom panel.

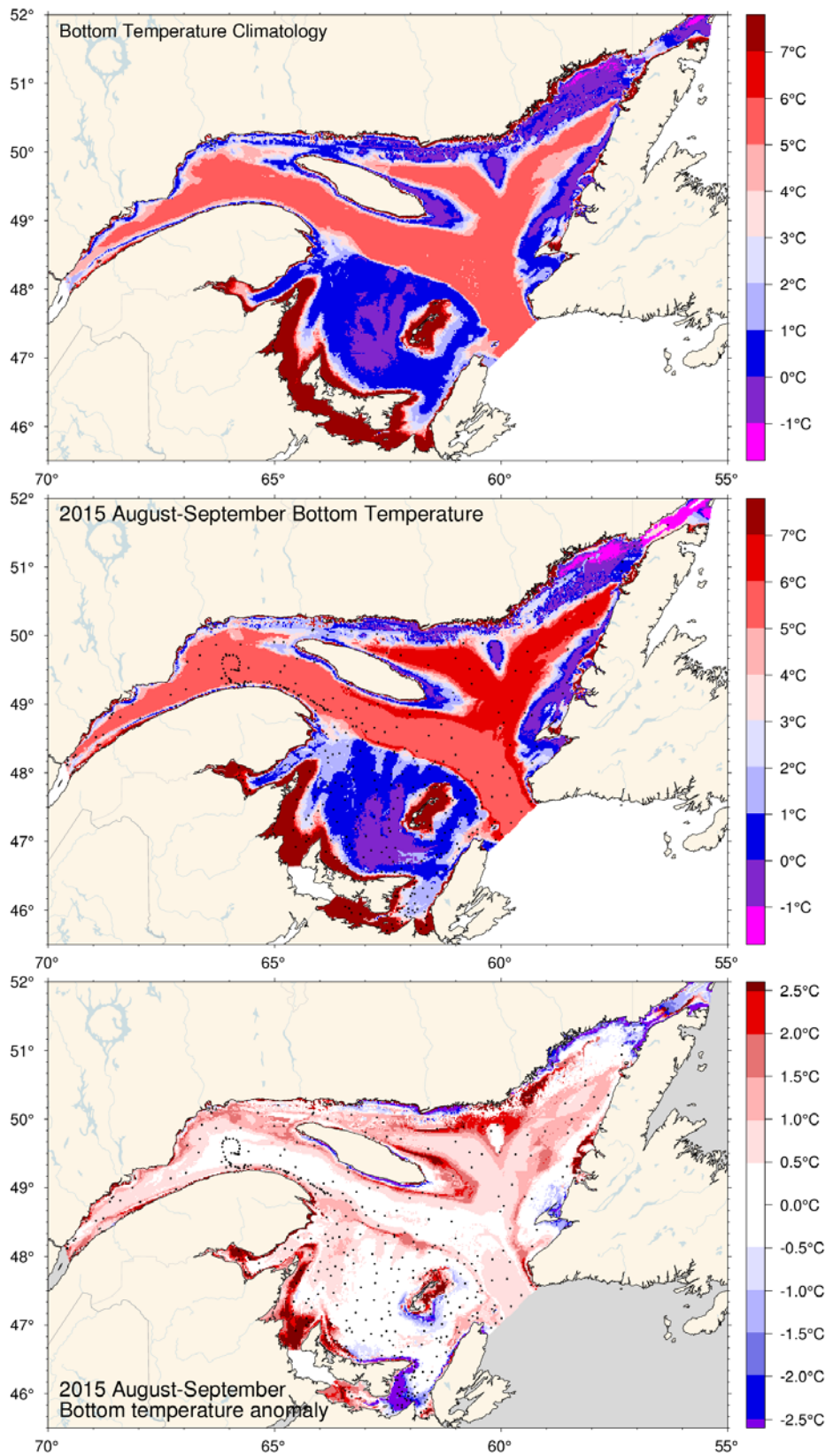


Figure 54. August-September bottom temperature climatology (top), 2015 observations (middle) and anomaly (bottom).

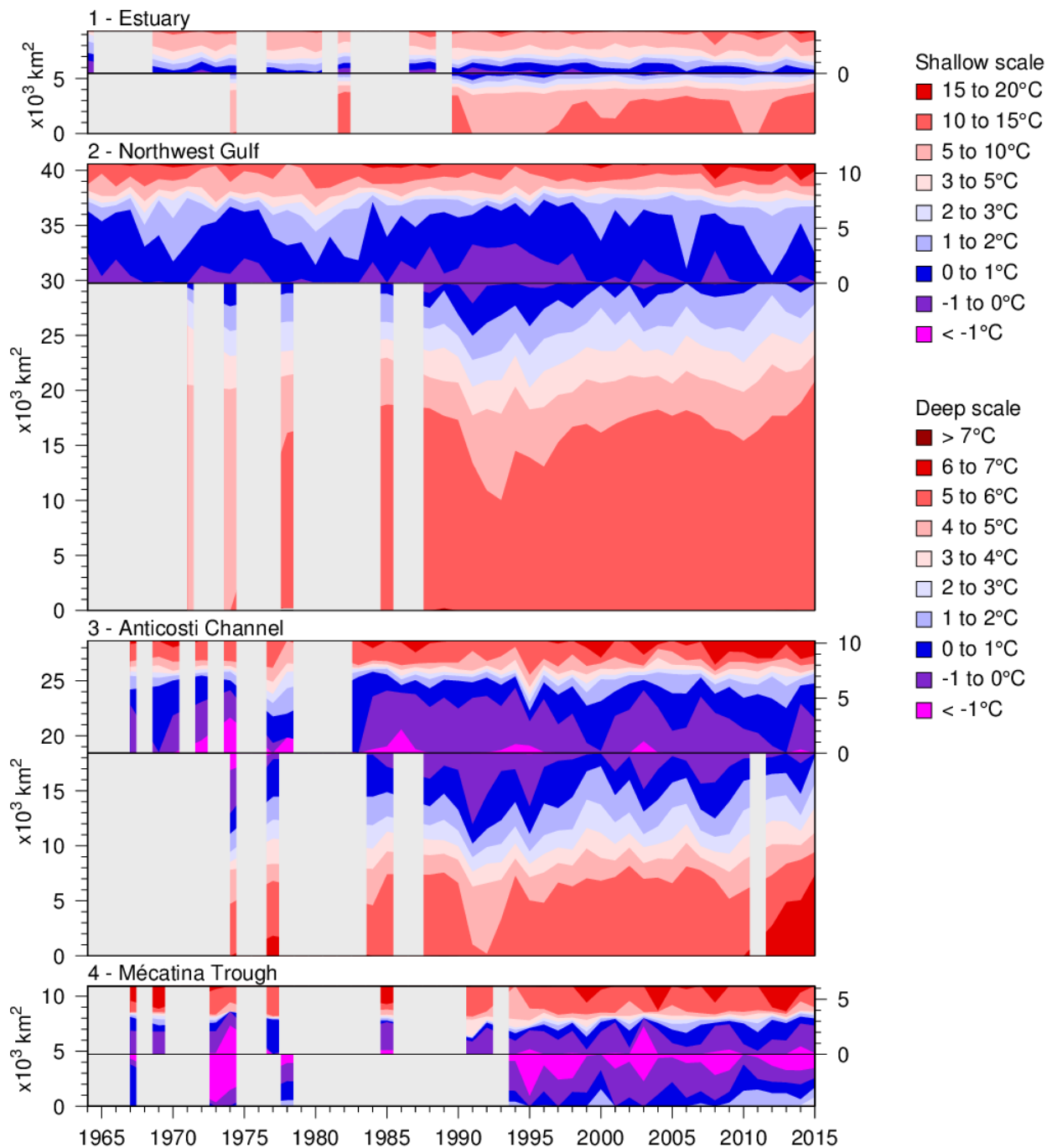


Figure 55. Time series of the bottom areas covered by different temperature bins in August and September for regions 1 to 4. The panels are separated by a black horizontal line into shallow (<100m) and deep (>100 m) areas to distinguish between warmer waters above and below the CIL. The shallow areas are shown on top using the area scale on the right-hand side and have warmer waters shown starting from the top end. The deep areas are shown below the horizontal line and have warmer waters starting at the bottom end. The CIL areas above and below 100 m meet near the horizontal line.

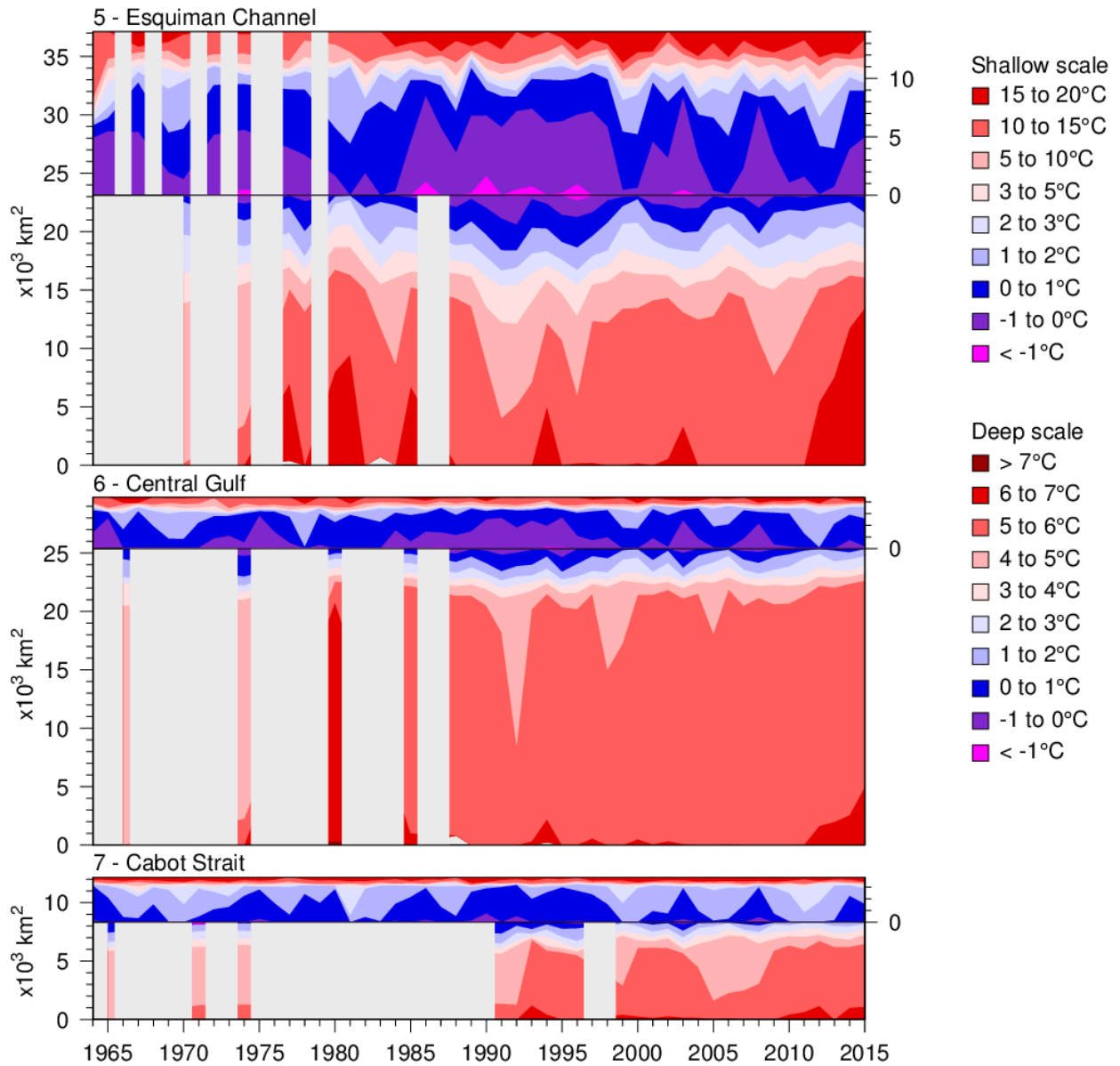


Figure 56. Time series of the bottom areas covered by different temperature bins in August and September for regions 5 to 7. The panels are separated into shallow (<100 m) and deep (>100 m) areas to distinguish between warmer waters above and below the CIL. See Figure 55 caption.

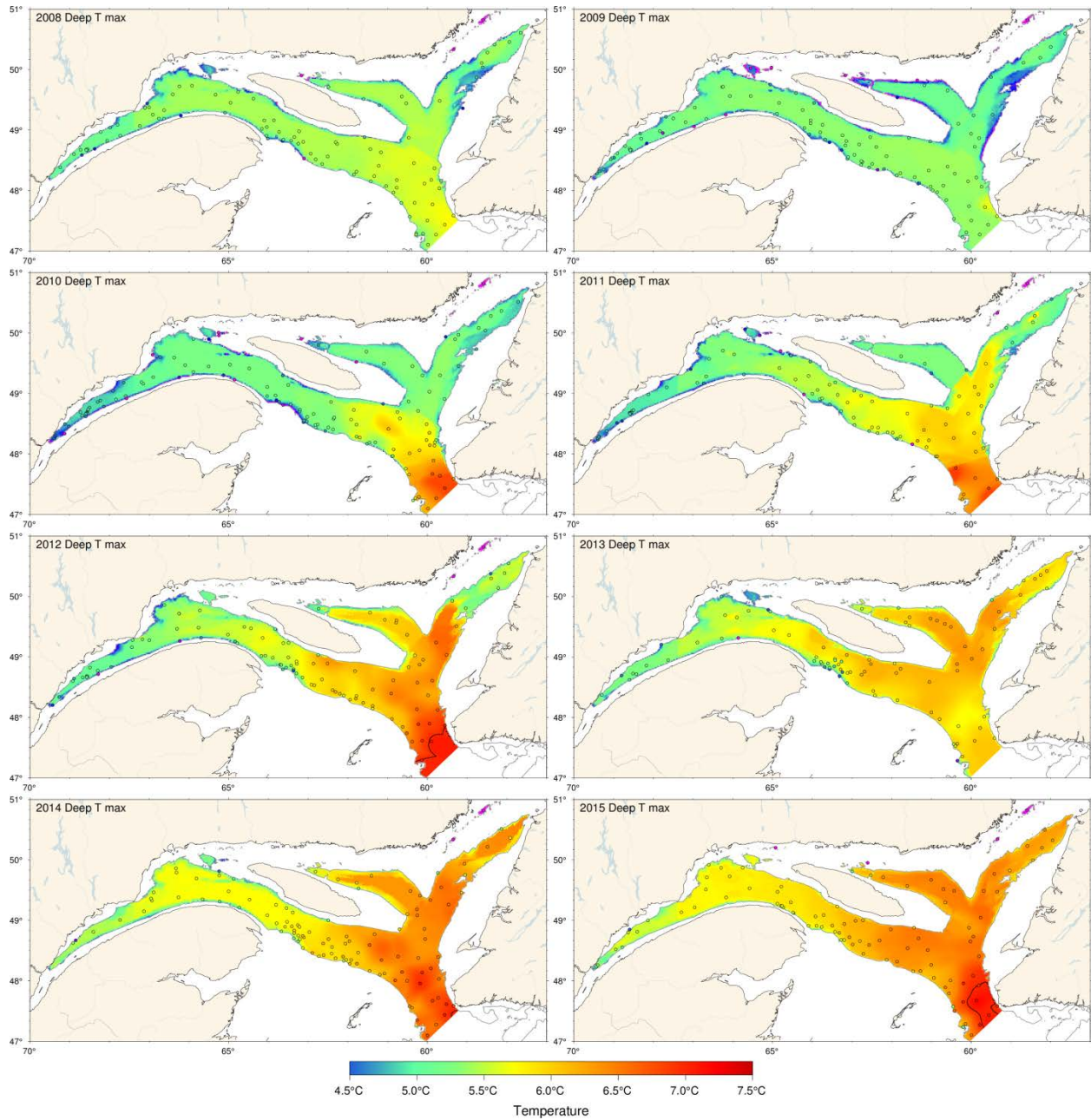


Figure 57. Map of the deep temperature maximum found typically between 200 and 300 m, 2008-2015. Maps are interpolated from August-September data available for each year.

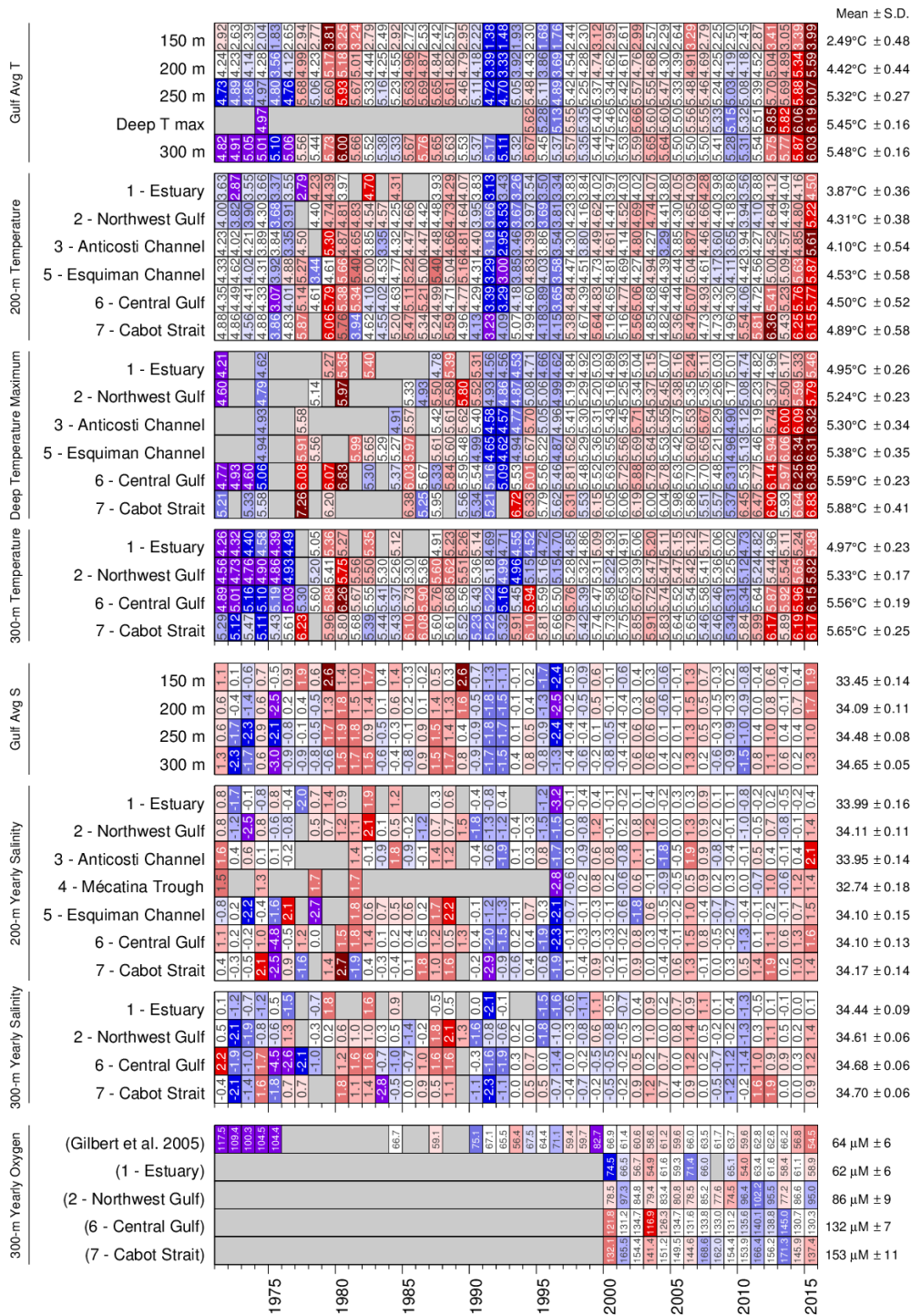


Figure 58. Deep layer temperature, salinity, and dissolved oxygen. Gulf averages for temperature and salinity are shown for 150, 200, 250, 300 m, as well as for the deep temperature maximum usually found between 200 and 300 m. Regional averages are shown for 200 and 300m, and deep temperature maximum. Dissolved oxygen is shown with an inverted colour scheme for the updated Gilbert et al. 2005 time series as well as recent regional averages at 300 m obtained using a Seabird SBE43 CTD sensor. The numbers on the right are the 1981–2010 climatological means and standard deviations. The numbers in the boxes are normalized anomalies, except for oxygen where physical values are shown for easier comparison between the Gilbert et al. 2005 time series and the CTD data.

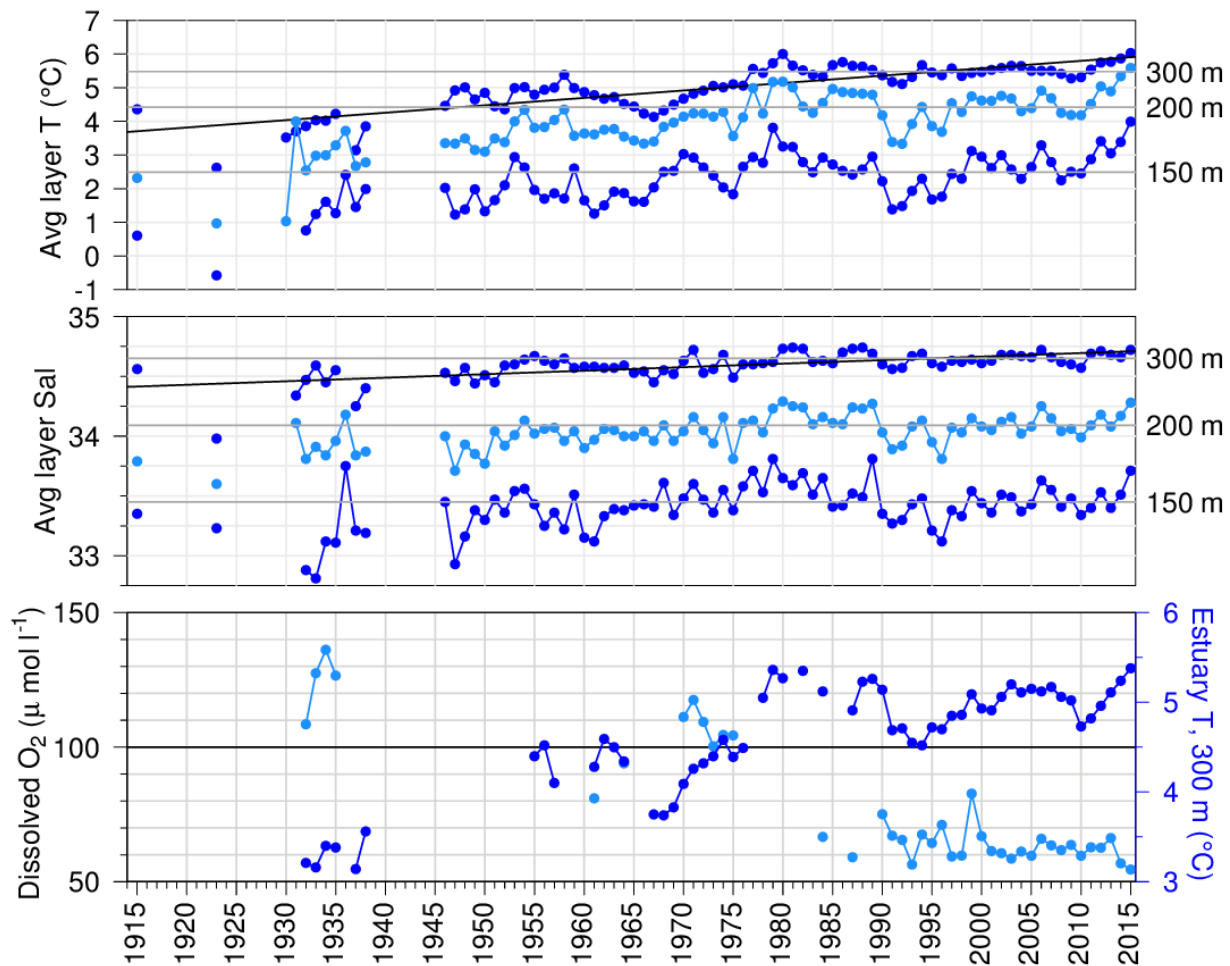


Figure 59. Layer-averaged temperature and salinity time series for the Gulf of St. Lawrence and dissolved oxygen between 295 m and the bottom in the deep central basin of the St. Lawrence Estuary. The temperature and salinity panels show the 150 m, 200 m, and 300 m annual averages and the horizontal lines are 1981–2010 means. Sloped lines show linear regressions for temperature and salinity at 300 m of respectively 2.2°C and 0.3 per century. The horizontal line in the oxygen panel corresponds roughly to 30% saturation and marks the threshold of hypoxic conditions. In addition to the dissolved oxygen time series (light blue), the lower panel also shows temperature (dark blue) at 300 m in the Estuary.

March/mars 2015

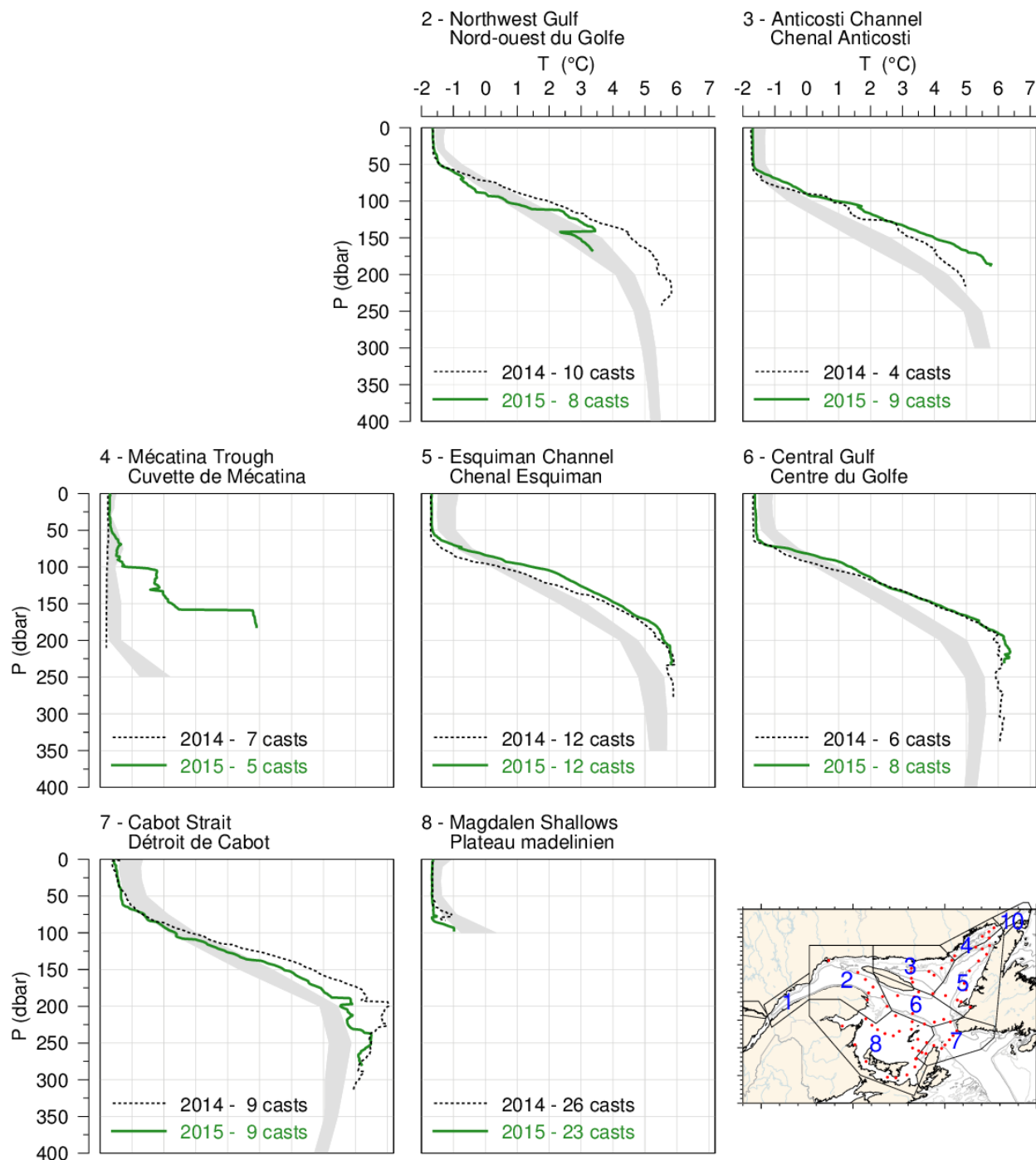


Figure 60. Mean temperature profiles observed in each region of the Gulf during the March helicopter survey. The shaded area represents the 1981–2010 (but mostly 1996–2010) climatological monthly mean ± 0.5 SD. Mean profiles for 2014 are also shown for comparison.

June/juin 2015

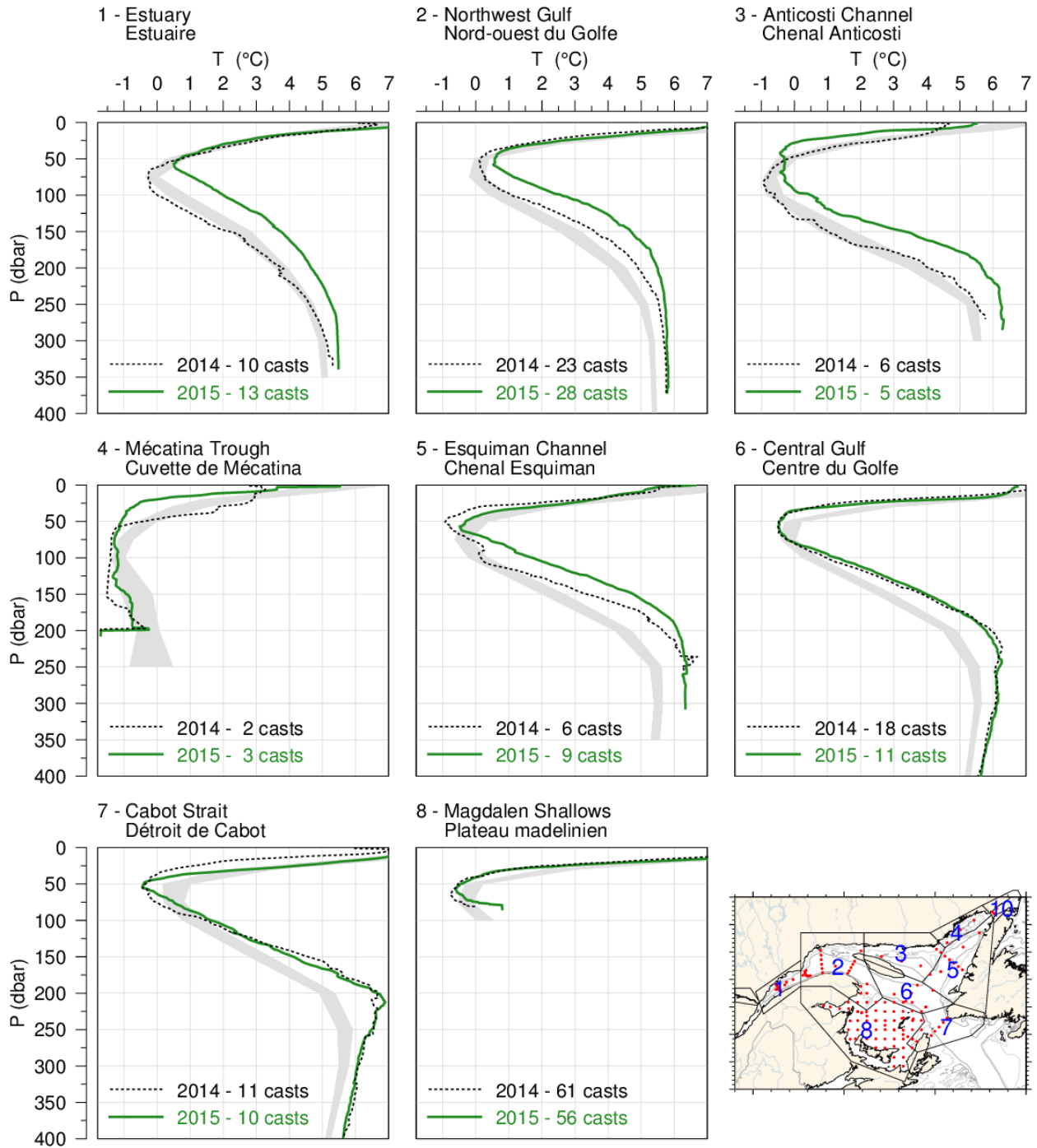


Figure 61. Mean temperature profiles observed in each region of the Gulf during June. The shaded area represents the 1981–2010 climatological monthly mean ± 0.5 SD. Mean profiles for 2014 are also shown for comparison.

August-September 2015

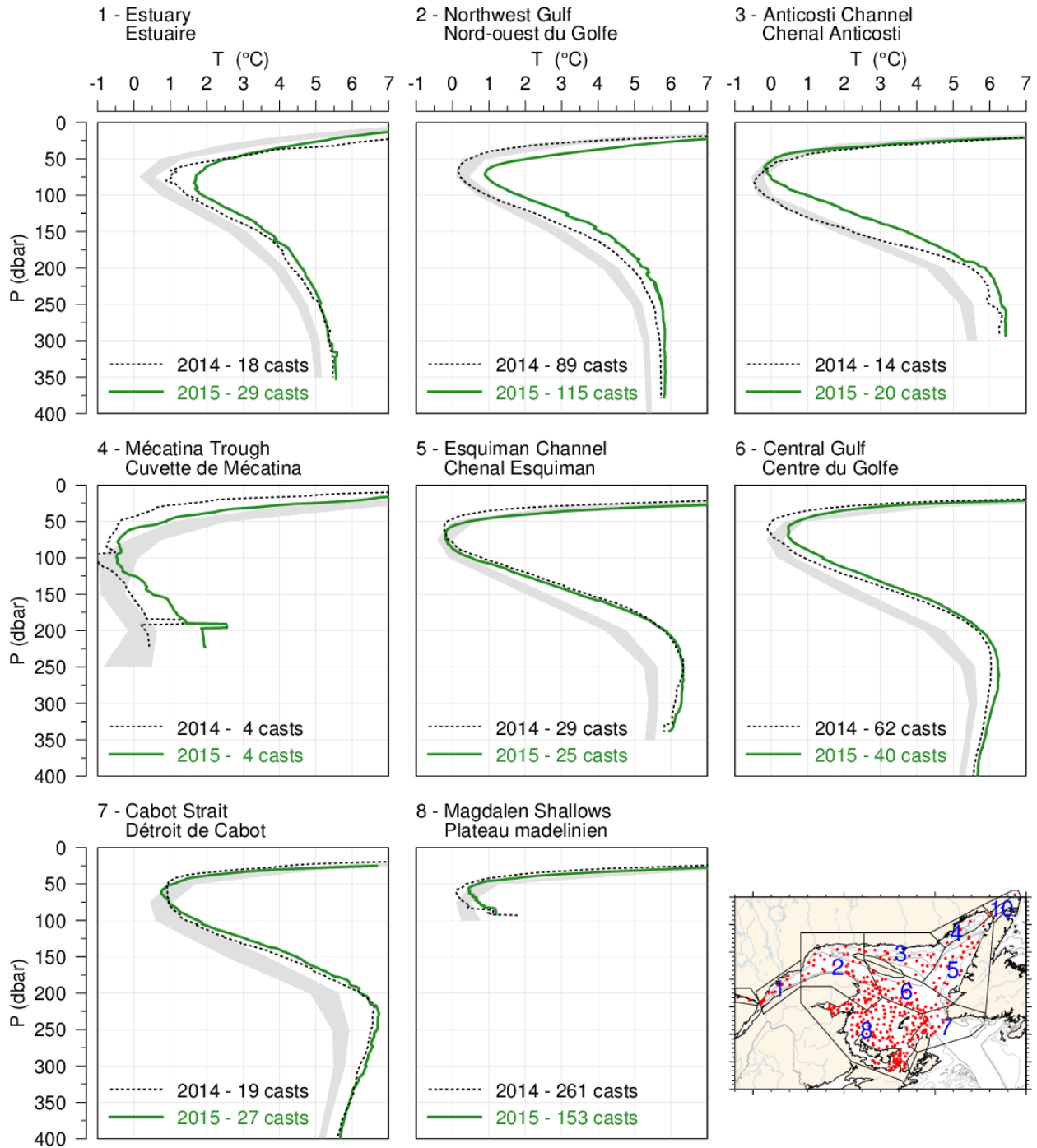


Figure 62. Mean temperature profiles observed in each region of the Gulf during August and September. The shaded area represents the 1981–2010 climatological monthly mean ± 0.5 SD for August for regions 1 through 7 and for September for region 8. Mean profiles for 2014 are also shown for comparison.

October/November 2015

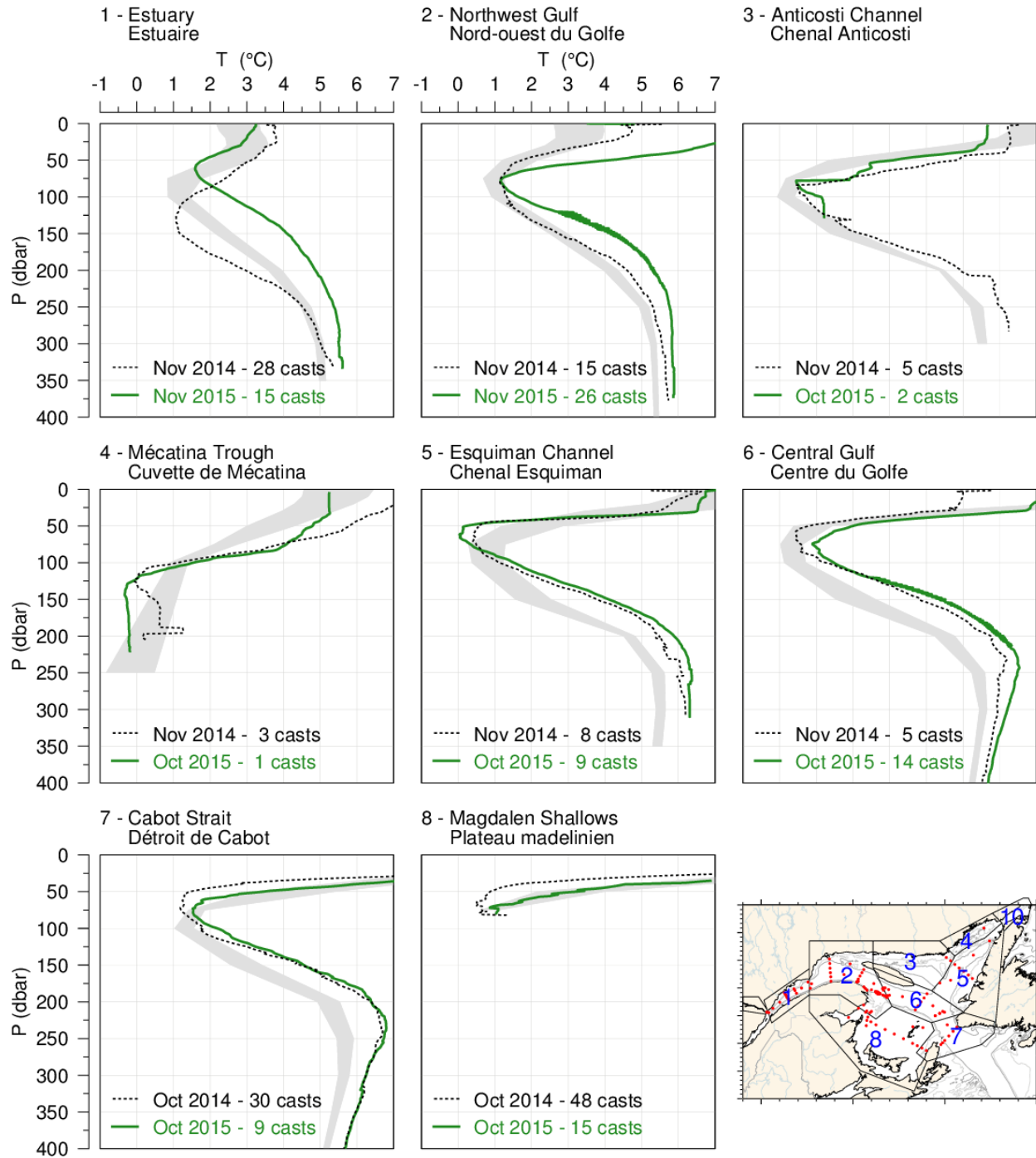


Figure 63. Mean temperature profiles observed in each region of the Gulf during the October AZMP survey. The shaded area represents the 1981–2010 climatological monthly mean ± 0.5 SD. Mean profiles for 2014 are also shown for comparison.

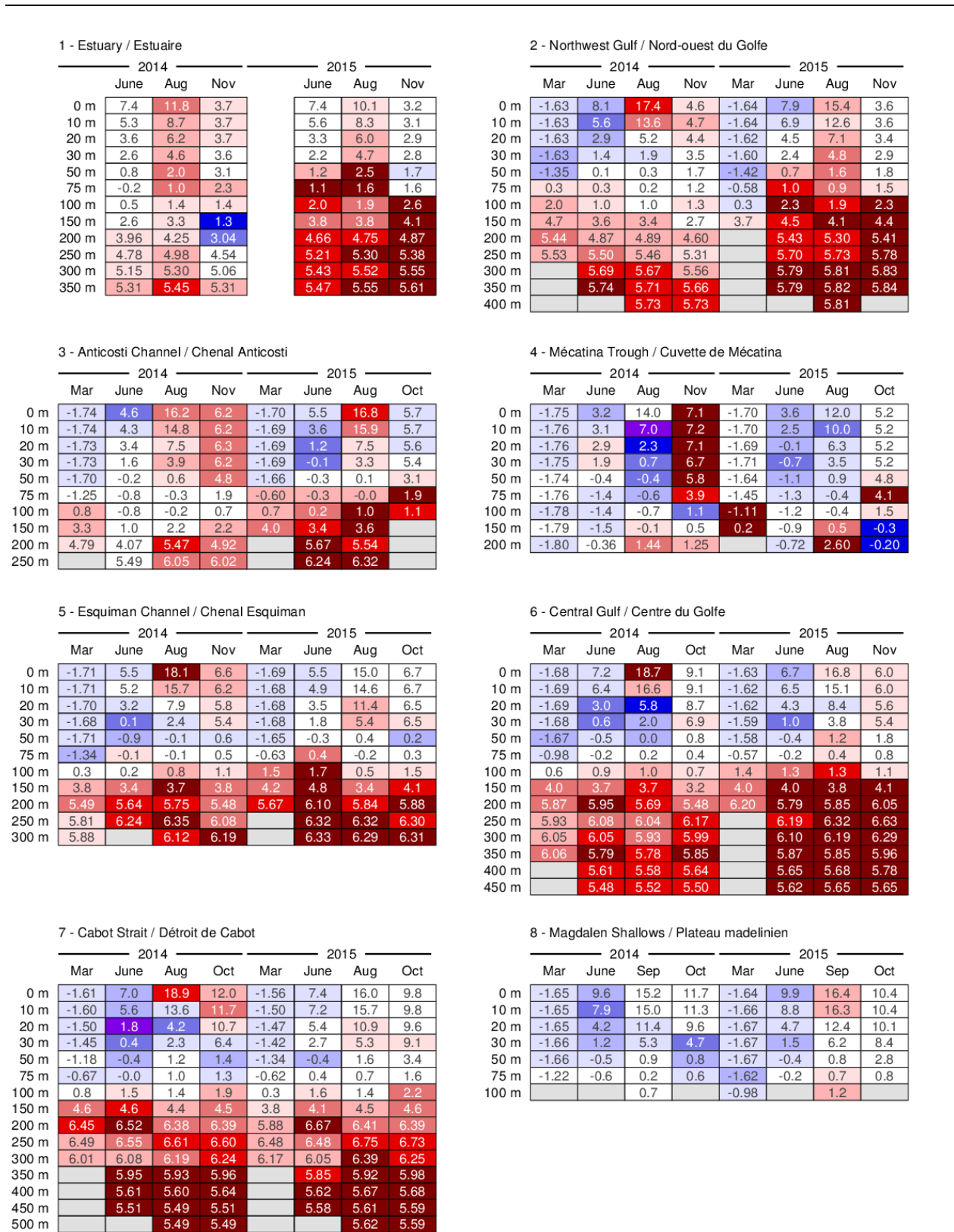


Figure 64. Depth-layer monthly average temperature summary for months during which the eight Gulf-wide oceanographic surveys took place in 2014 and 2015. The colour-coding is according to the temperature anomaly relative to the monthly 1981–2010 climatology of each region.

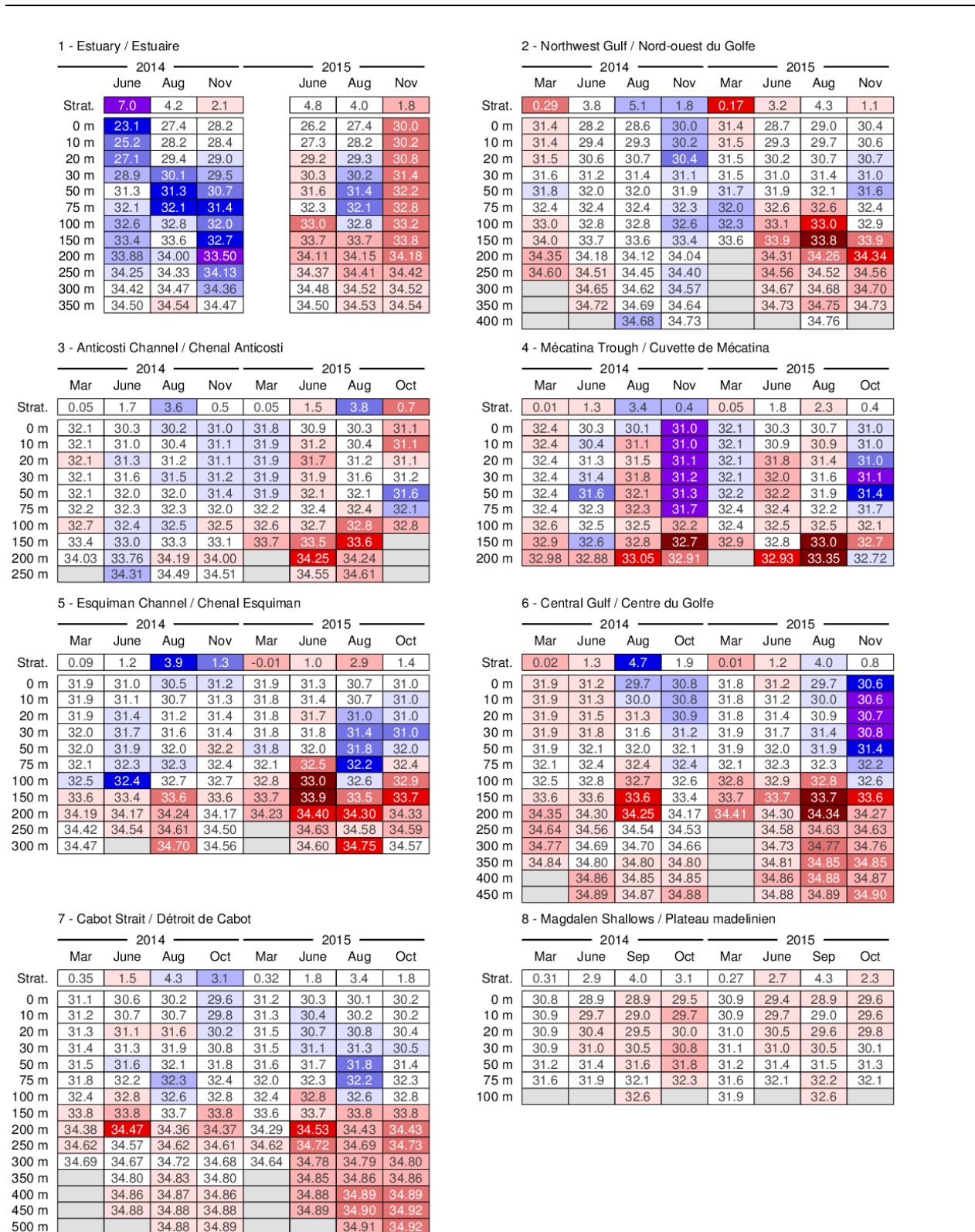


Figure 65. Depth-layer monthly average stratification and salinity summary for months during which the eight Gulf-wide oceanographic surveys took place in 2014 and 2015. Stratification is defined as the density difference between 50 m and the surface and its colour-coding is reversed (blue for positive anomaly).

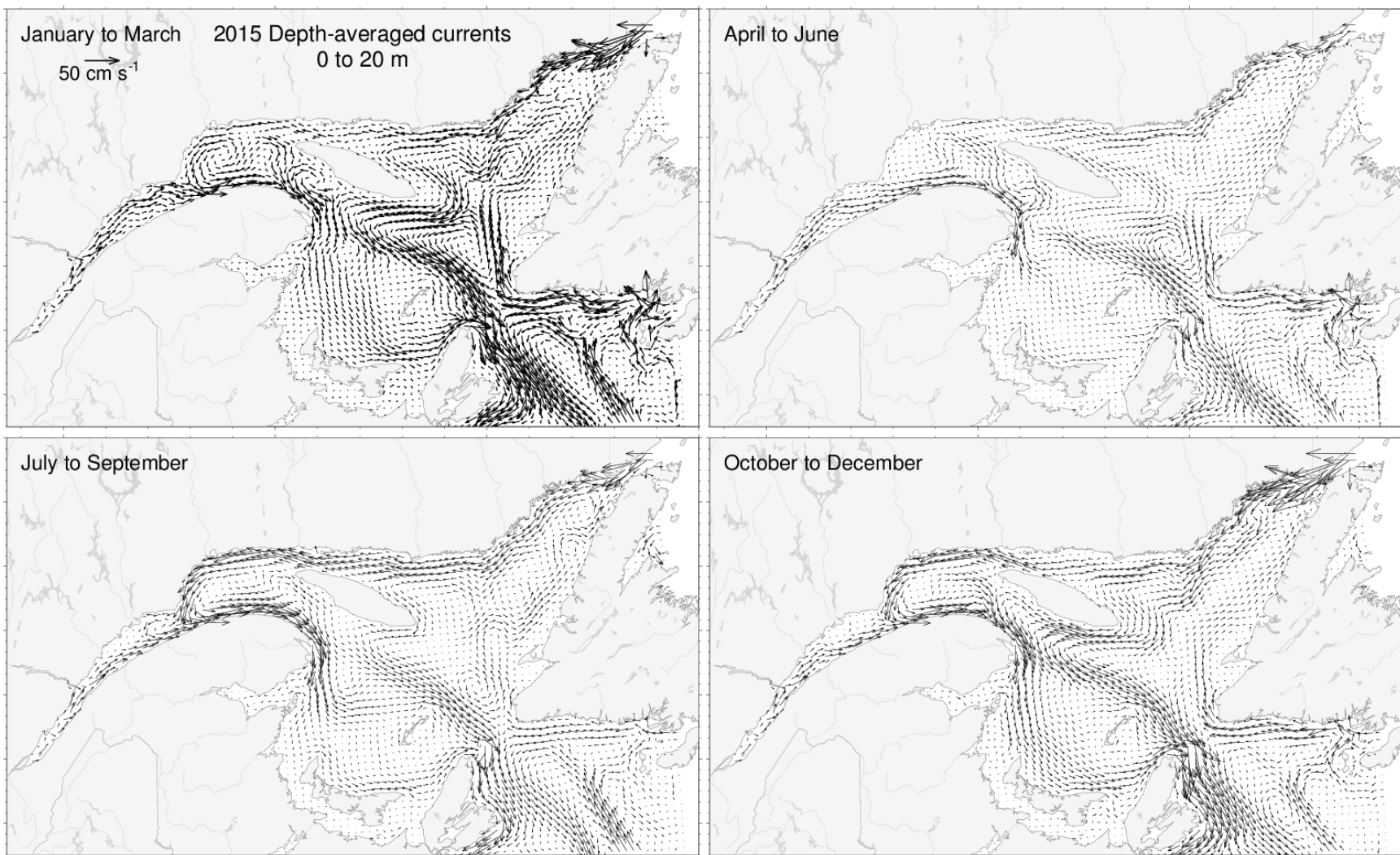


Figure 66. Depth-averaged currents from 0 to 20 m for each three-month period of 2015.

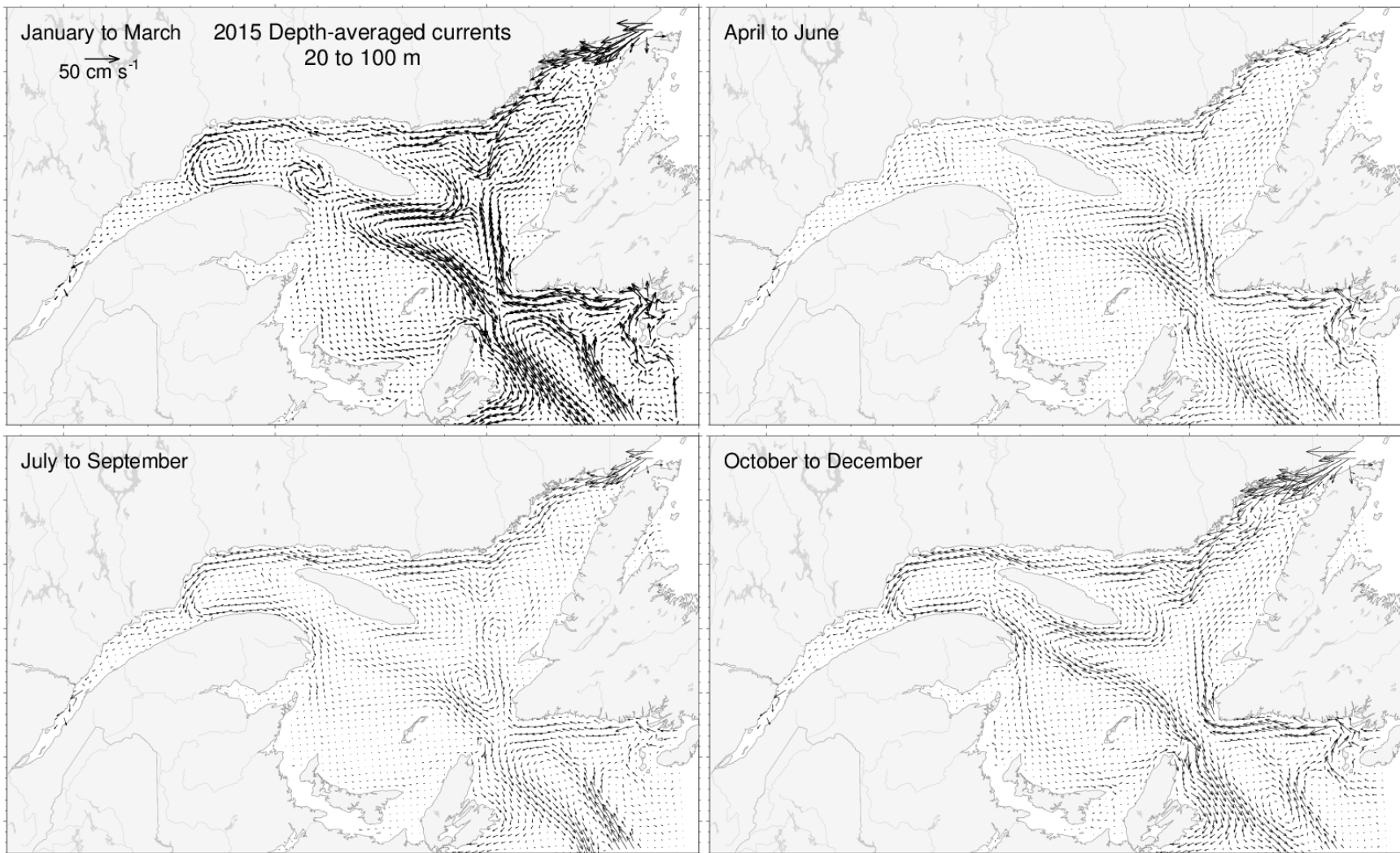


Figure 67. Depth-averaged currents from 20 to 100 m for each three-month period of 2015.

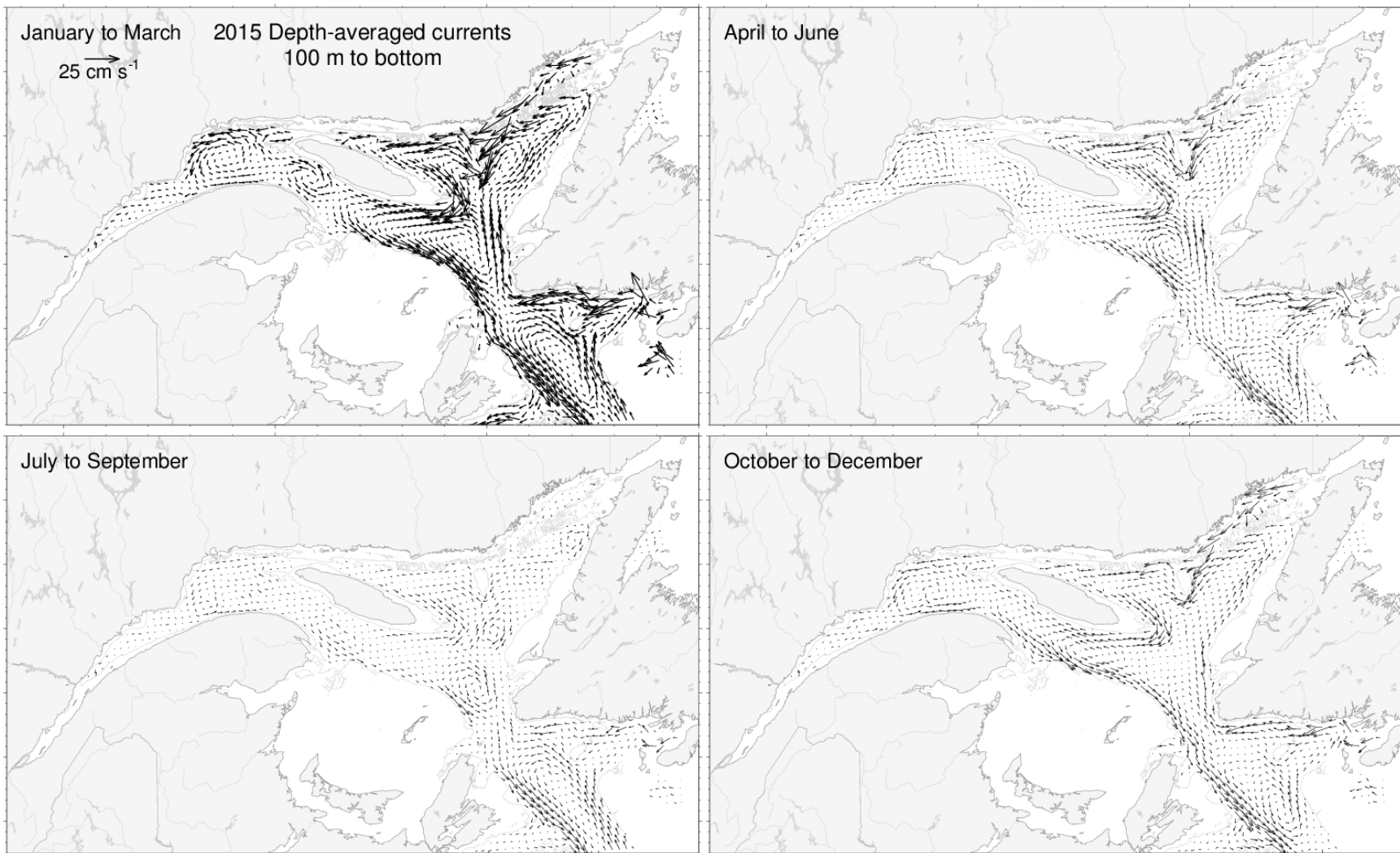
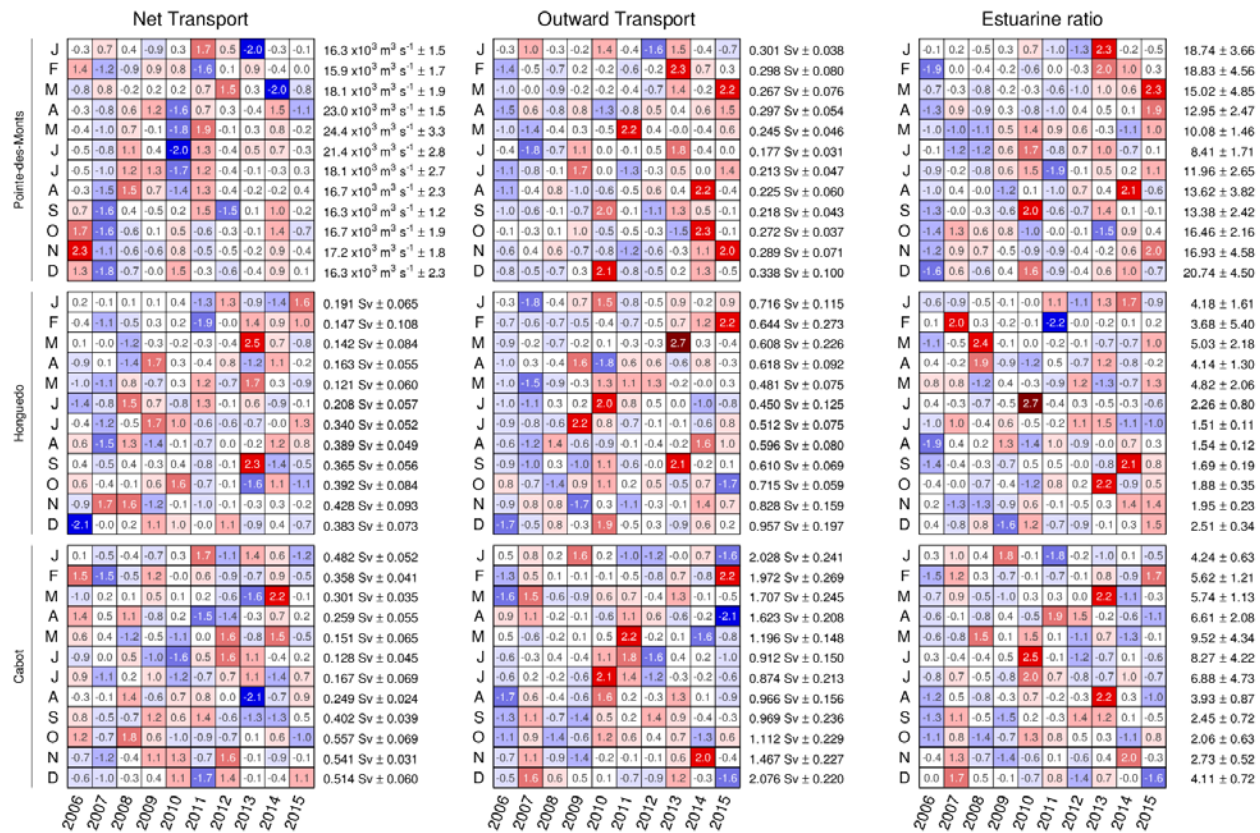


Figure 68. Depth-averaged currents from 100 m to the bottom for each three-month period of 2015.



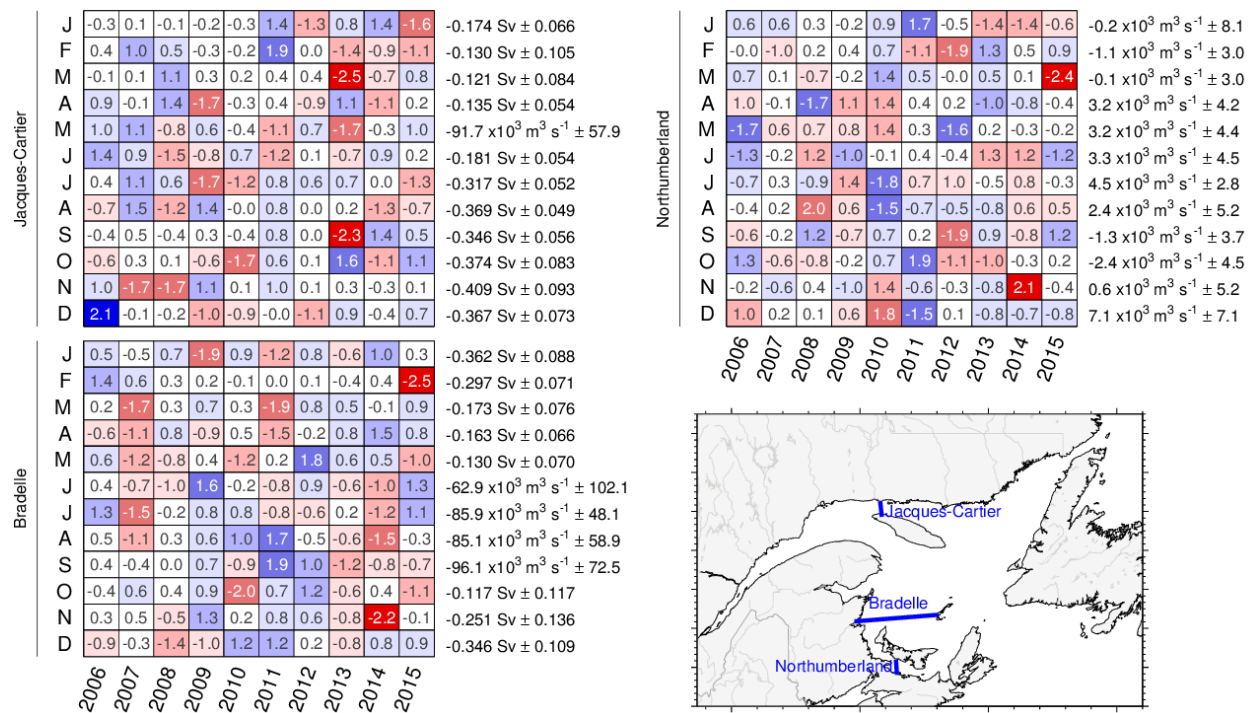


Figure 70. Monthly averaged modelled transports across sections of the Gulf of St. Lawrence since 2006. The numbers on the right are the 2006–2015 means and standard deviations, with positive values toward east and north. The numbers in the boxes are normalized anomalies. Colours indicate the magnitude of the anomaly (e.g., negative anomalies are still shown in red when the mean transport is negative across the section).

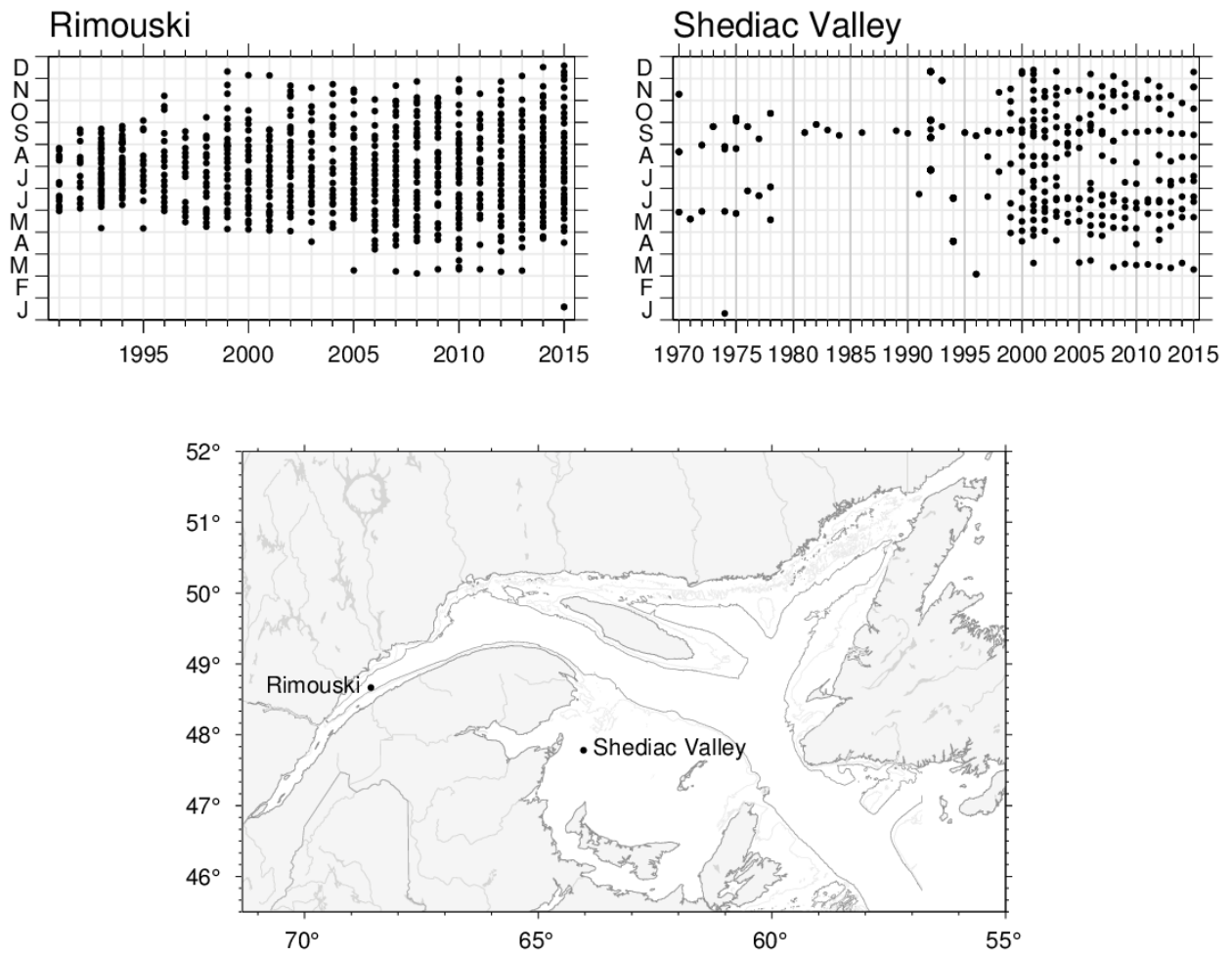


Figure 71. Sampling frequency and positions of the AZMP stations Rimouski and Shediac Valley.

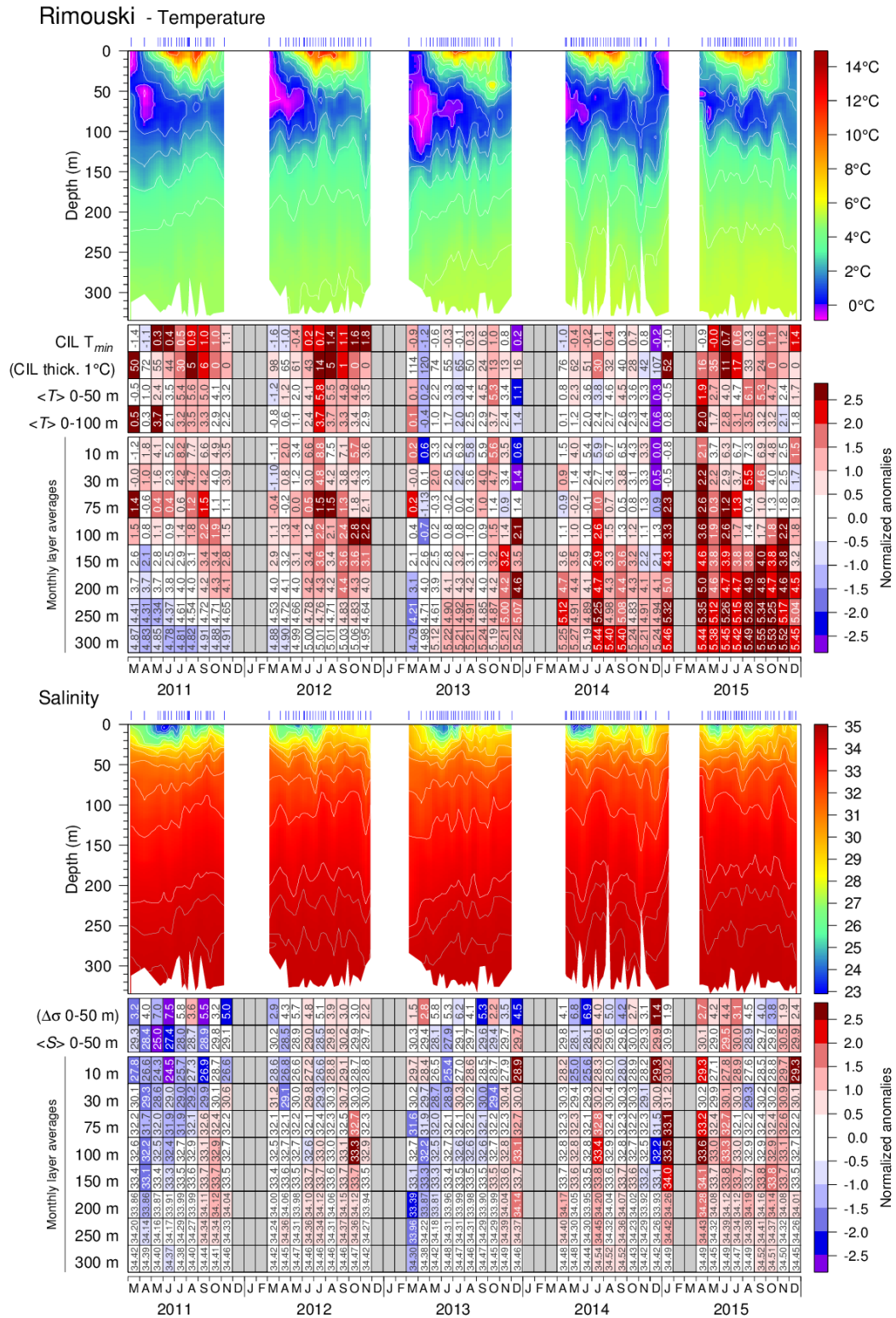


Figure 72. Isotherm (top) and isohaline (bottom) time series at the Rimouski station; tick marks above indicate sample dates. The scorecard tables are monthly layer averages colour-coded according to the anomaly relative to the 1991–2010 monthly climatology for the station (yearly climatology for 250 m and deeper). Thickness of the CIL and stratification have reversed colour codes where red indicates thinner CIL (warmer water) and less stratification (higher surface salinity).

	Rimouski												Shediac Valley																										
	T [0-50 m]			T [0-100 m]			T [290 m]			S [0-50 m]			$\Delta\sigma_t$ [0,50 m]			T [CIL min]			CIL thick. < 1°C			T [0-50 m]			T [0-84 m]			T [75 m]			S [0-50 m]			$\Delta\sigma_t$ [0,50 m]					
1991	86	-0.71	3.6	70	-0.62	4.7	29.6	29.6	29.6	3.6	4.7	28.9	26.9	30.0	-0.3	3.7	3.0	0.0	3.7	3.0	0.0	3.7	3.0	0.0	3.7	3.0	0.0	3.7	3.0	0.0	3.7	3.0	0.0	3.7	3.0	0.0			
1995	82	-0.58	5.0	82	-0.58	5.0	28.7	28.7	28.7	1.6	3.4	28.7	29.1	29.5	-0.5	29.1	29.5	-0.5	29.1	29.5	-0.5	29.1	29.5	-0.5	29.1	29.5	-0.5	29.1	29.5	-0.5	29.1	29.5	-0.5	29.1	29.5	-0.5	29.1	29.5	-0.5
2000	58	-0.29	4.8	58	-0.29	4.8	29.1	29.1	29.1	1.7	3.1	29.1	30.0	30.0	-0.4	30.0	30.0	-0.4	30.0	30.0	-0.4	30.0	30.0	-0.4	30.0	30.0	-0.4	30.0	30.0	-0.4	30.0	30.0	-0.4	30.0	30.0	-0.4	30.0	30.0	-0.4
2005	73	-0.66	4.0	73	-0.66	4.0	29.4	29.4	29.4	1.4	3.0	29.4	29.8	29.8	-0.2	29.8	29.8	-0.2	29.8	29.8	-0.2	29.8	29.8	-0.2	29.8	29.8	-0.2	29.8	29.8	-0.2	29.8	29.8	-0.2	29.8	29.8	-0.2	29.8	29.8	-0.2
2010	60	-0.21	5.5	60	-0.21	5.5	28.5	28.5	28.5	2.0	3.6	28.5	30.0	30.0	0.1	30.0	30.0	0.1	30.0	30.0	0.1	30.0	30.0	0.1	30.0	30.0	0.1	30.0	30.0	0.1	30.0	30.0	0.1	30.0	30.0	0.1	30.0	30.0	0.1
2015	49	-0.18	5.5	49	-0.18	5.5	28.8	28.8	28.8	1.8	3.2	28.8	30.4	30.4	-0.4	30.4	30.4	-0.4	30.4	30.4	-0.4	30.4	30.4	-0.4	30.4	30.4	-0.4	30.4	30.4	-0.4	30.4	30.4	-0.4	30.4	30.4	-0.4	30.4	30.4	-0.4
	60	-0.63	4.0	60	-0.63	4.0	29.0	29.0	29.0	1.9	3.6	29.0	3.5	29.9	0.2	3.5	29.9	0.2	3.5	29.9	0.2	3.5	29.9	0.2	3.5	29.9	0.2	3.5	29.9	0.2	3.5	29.9	0.2	3.5	29.9	0.2	3.5	29.9	0.2
	49	-0.21	3.3	49	-0.21	3.3	29.6	29.6	29.6	2.1	3.9	29.6	3.8	30.0	0.1	3.8	30.0	0.1	3.8	30.0	0.1	3.8	30.0	0.1	3.8	30.0	0.1	3.8	30.0	0.1	3.8	30.0	0.1	3.8	30.0	0.1	3.8	30.0	0.1
	50	0.08	4.5	50	0.08	4.5	29.5	29.5	29.5	2.8	3.3	29.5	3.4	30.0	0.0	3.4	30.0	0.0	3.4	30.0	0.0	3.4	30.0	0.0	3.4	30.0	0.0	3.4	30.0	0.0	3.4	30.0	0.0	3.4	30.0	0.0	3.4	30.0	0.0
	31	0.26	3.6	31	0.26	3.6	29.6	29.6	29.6	3.1	3.8	29.6	3.5	30.2	0.3	3.5	30.2	0.3	3.5	30.2	0.3	3.5	30.2	0.3	3.5	30.2	0.3	3.5	30.2	0.3	3.5	30.2	0.3	3.5	30.2	0.3	3.5	30.2	0.3
	36	0.35	4.1	36	0.35	4.1	29.9	29.9	29.9	3.0	3.8	29.9	3.6	30.6	-0.2	3.6	30.6	-0.2	3.6	30.6	-0.2	3.6	30.6	-0.2	3.6	30.6	-0.2	3.6	30.6	-0.2	3.6	30.6	-0.2	3.6	30.6	-0.2	3.6	30.6	-0.2
	69	-0.27	3.9	69	-0.27	3.9	29.9	29.9	29.9	2.3	3.3	29.9	3.8	29.7	-0.2	3.8	29.7	-0.2	3.8	29.7	-0.2	3.8	29.7	-0.2	3.8	29.7	-0.2	3.8	29.7	-0.2	3.8	29.7	-0.2	3.8	29.7	-0.2	3.8	29.7	-0.2
	59	-0.29	4.7	59	-0.29	4.7	29.1	29.1	29.1	1.4	3.2	29.1	3.8	29.8	-0.0	3.8	29.8	-0.0	3.8	29.8	-0.0	3.8	29.8	-0.0	3.8	29.8	-0.0	3.8	29.8	-0.0	3.8	29.8	-0.0	3.8	29.8	-0.0	3.8	29.8	-0.0
	53	-0.22	4.4	53	-0.22	4.4	28.9	28.9	28.9	2.4	3.6	28.9	3.9	30.0	0.6	3.9	30.0	0.6	3.9	30.0	0.6	3.9	30.0	0.6	3.9	30.0	0.6	3.9	30.0	0.6	3.9	30.0	0.6	3.9	30.0	0.6	3.9	30.0	0.6
	25	0.53	4.6	25	0.53	4.6	29.3	29.3	29.3	2.7	4.3	29.3	3.2	30.3	0.3	3.2	30.3	0.3	3.2	30.3	0.3	3.2	30.3	0.3	3.2	30.3	0.3	3.2	30.3	0.3	3.2	30.3	0.3	3.2	30.3	0.3	3.2	30.3	0.3
	41	0.13	4.6	41	0.13	4.6	29.7	29.7	29.7	2.3	3.9	29.7	5.2	29.4	-0.3	5.2	29.4	-0.3	5.2	29.4	-0.3	5.2	29.4	-0.3	5.2	29.4	-0.3	5.2	29.4	-0.3	5.2	29.4	-0.3	5.2	29.4	-0.3	5.2	29.4	-0.3
	54	-0.05	5.6	54	-0.05	5.6	28.8	28.8	28.8	2.3	4.2	28.8	3.9	30.0	0.6	3.9	30.0	0.6	3.9	30.0	0.6	3.9	30.0	0.6	3.9	30.0	0.6	3.9	30.0	0.6	3.9	30.0	0.6	3.9	30.0	0.6	3.9	30.0	0.6
	48	-0.07	4.6	48	-0.07	4.6	28.6	28.6	28.6	2.8	4.5	28.6	3.2	30.2	0.4	3.2	30.2	0.4	3.2	30.2	0.4	3.2	30.2	0.4	3.2	30.2	0.4	3.2	30.2	0.4	3.2	30.2	0.4	3.2	30.2	0.4	3.2	30.2	0.4
	39	0.26	4.1	39	0.26	4.1	29.2	29.2	29.2	2.6	4.2	29.2	3.8	29.4	0.5	3.8	29.4	0.5	3.8	29.4	0.5	3.8	29.4	0.5	3.8	29.4	0.5	3.8	29.4	0.5	3.8	29.4	0.5	3.8	29.4	0.5	3.8	29.4	0.5
	23	0.69	5.4	23	0.69	5.4	28.0	28.0	28.0	3.1	4.3	28.0	3.7	30.1	0.8	3.7	30.1	0.8	3.7	30.1	0.8	3.7	30.1	0.8	3.7	30.1	0.8	3.7	30.1	0.8	3.7	30.1	0.8	3.7	30.1	0.8	3.7	30.1	0.8
	21	0.77	4.2	21	0.77	4.2	29.4	29.4	29.4	2.9	4.5	29.4	3.9	29.6	0.4	3.9	29.6	0.4	3.9	29.6	0.4	3.9	29.6	0.4	3.9	29.6	0.4	3.9	29.6	0.4	3.9	29.6	0.4	3.9	29.6	0.4	3.9	29.6	0.4
	47	0.14	4.8	47	0.14	4.8	29.0	29.0	29.0	2.3	3.9	29.0	3.9	30.1	-0.0	3.9	30.1	-0.0	3.9	30.1	-0.0	3.9	30.1	-0.0	3.9	30.1	-0.0	3.9	30.1	-0.0	3.9	30.1	-0.0	3.9	30.1	-0.0	3.9	30.1	-0.0
	41	0.17	5.0	41	0.17	5.0	29.2	29.2	29.2	2.2	3.7	29.2	3.2	30.2	0.5	3.2	30.2	0.5	3.2	30.2	0.5	3.2	30.2	0.5	3.2	30.2	0.5	3.2	30.2	0.5	3.2	30.2	0.5	3.2	30.2	0.5	3.2	30.2	0.5
	20	0.54	4.0	20	0.54	4.0	29.5	29.5	29.5	2.9	4.6	29.5	3.2	30.2	0.5	3.2	30.2	0.5	3.2	30.2	0.5	3.2	30.2	0.5	3.2	30.2	0.5	3.2	30.2	0.5	3.2	30.2	0.5	3.2	30.2	0.5	3.2	30.2	0.5

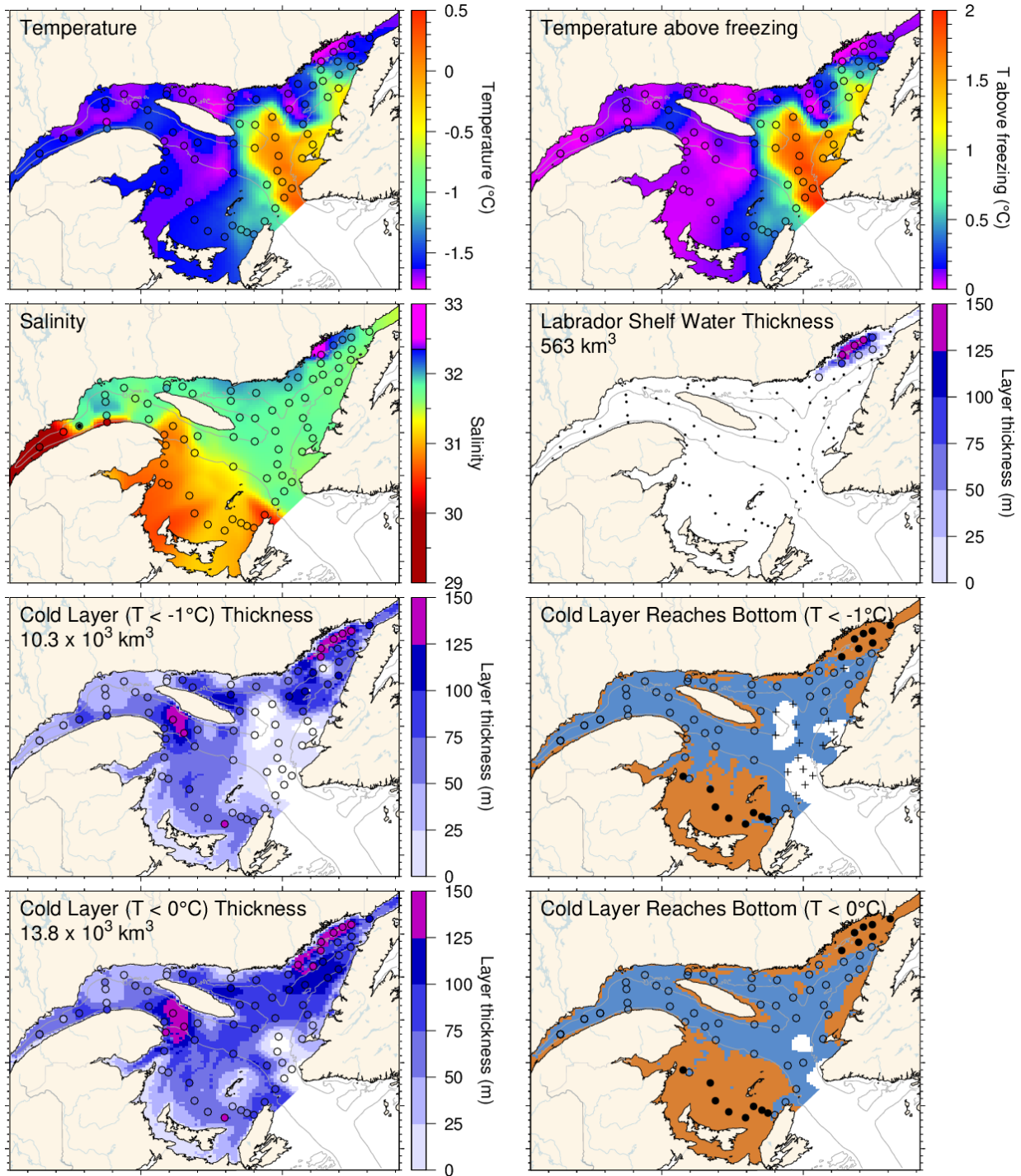


Figure 75. March 2016 surface cold layer characteristics: surface water temperature (upper left), temperature difference with the freezing point (upper right), salinity (second row left), estimate of the thickness of the Labrador Shelf water intrusion (second row right), and cold layer ($T < -1^{\circ}\text{C}$ and $< 0^{\circ}\text{C}$) thicknesses and where they reach bottom. The symbols are coloured according to the value observed at the station, using the same colour palette as the interpolated image. A good match is seen between the interpolation and the station observations where the station colours blend into the background.

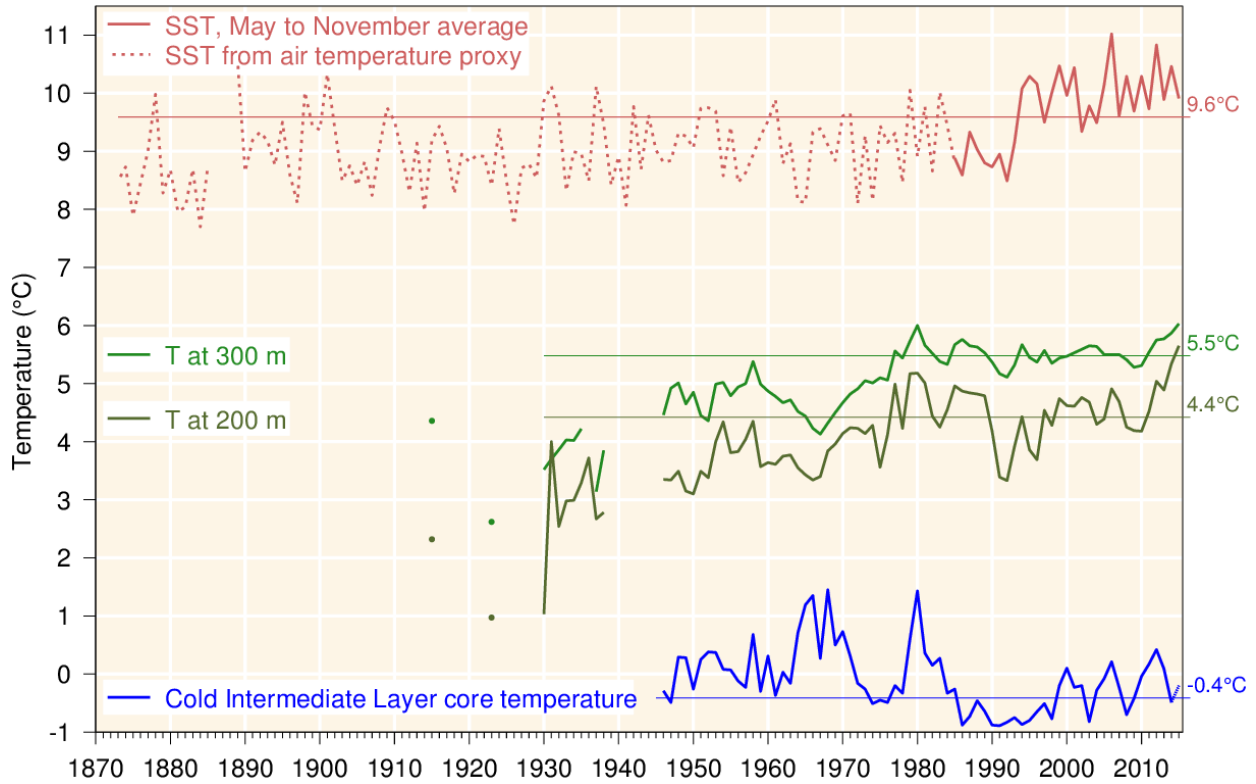


Figure 76. Water temperatures in the Gulf of St. Lawrence. May–November SST averaged over the Gulf excluding the Estuary (1985–2015, red line), completed by a proxy based on April–November air temperature (1873–1984, red dashed line; average of all AHCCD stations in Figure 4 but excluding Estuary stations at Baie Comeau and Mont-Joli). Layer-averaged temperature for the Gulf of St. Lawrence at 200 and 300 m (green lines). Cold intermediate layer minimum temperature index in the Gulf of St. Lawrence (blue line). SST air temperature proxy is similar to that of Galbraith et al. (2012). Climatological averages based on the 1981–2010 period are indicated by thin lines labeled on the right side. Figure adapted from (Benoît et al. 2012).

	1971	1975	1980	1985	1990	1995	2000	2005	2010	2015	Mean ± S.D.
Surface											
SST, GSL August average	-0.7	-0.1	0.3	0.1	-0.3	-4.8	-0.6	0.4	-2.3	1.5	15.61°C ± 0.75
SST, GSL May-Nov average	0.9	-0.6	-1.0	-0.5	1.0	5.1	-0.8	0.8	-2.2	-1.3	9.61°C ± 0.66
(SST, Spring timing)	1.6	0.0	-0.9	-0.3	1.0	-1.2	-0.2	-0.0	-0.7	-0.4	27.2 w ± 1.2
SST, fall timing	-2.5	-1.2	0.1	-0.5	-0.7	-3.8	-1.8	-0.0	-1.7	-0.3	37.9 w ± 1.2
Sum of standardized anomalies	-0.7	-1.0	0.0	1.9	-0.1	-4.8	-0.6	0.4	-2.3	1.5	
Intermediate											
(Ice, max volume)	1.0	-1.0	0.0	1.9	-0.1	-4.8	-0.6	0.4	-2.3	1.5	62.3 km ³ ± 25.5
GSL, summer CIL Index	0.8	0.6	-0.1	0.4	0.4	0.1	-0.7	-0.6	-0.3	-0.3	-0.41°C ± 0.39
(sGSL, Sep. T<1°C Btm Area)	0.5	1.4	0.4	-0.1	0.5	-1.3	-0.1	0.7	-0.2	0.4	30.0 ± 4.8 (x10 ³ km ²)
Bottom temp., Magdalen Shallows, Sep.	2.2	-0.5	-2.7	0.5	0.6	-2.7	-1.6	1.4	0.2	-0.1	5.10°C ± 0.49
Sum of standardized anomalies	1.0	-1.0	0.0	1.9	-0.1	-4.8	-0.6	0.4	-2.3	1.5	
Deep indicators											
150 m GSL avg temp.	5.8	-4.1	-2.2	-0.4	0.9	-5.3	3.6	1.6	-0.4	0.3	2.49°C ± 0.48
200 m GSL avg temp.	-5.2	-2.7	-1.7	-0.6	-0.2	-5.5	-2.9	-1.3	-0.3	-0.9	4.42°C ± 0.44
250 m GSL avg temp.	-7.6	-2.4	-1.9	-2.0	-1.4	-5.0	-2.6	-2.1	-0.7	0.3	5.32°C ± 0.27
300 m GSL avg temp.	4.1	0.5	1.3	1.3	0.9	-1.0	-0.2	-1.0	-0.4	0.6	5.48°C ± 0.16
Sum of standardized anomalies	5.8	-4.1	-2.2	-0.4	0.9	-5.3	3.6	1.6	-0.4	0.3	

Figure 77. Surface and deep indicators used in the composite climate index (Figure 78).

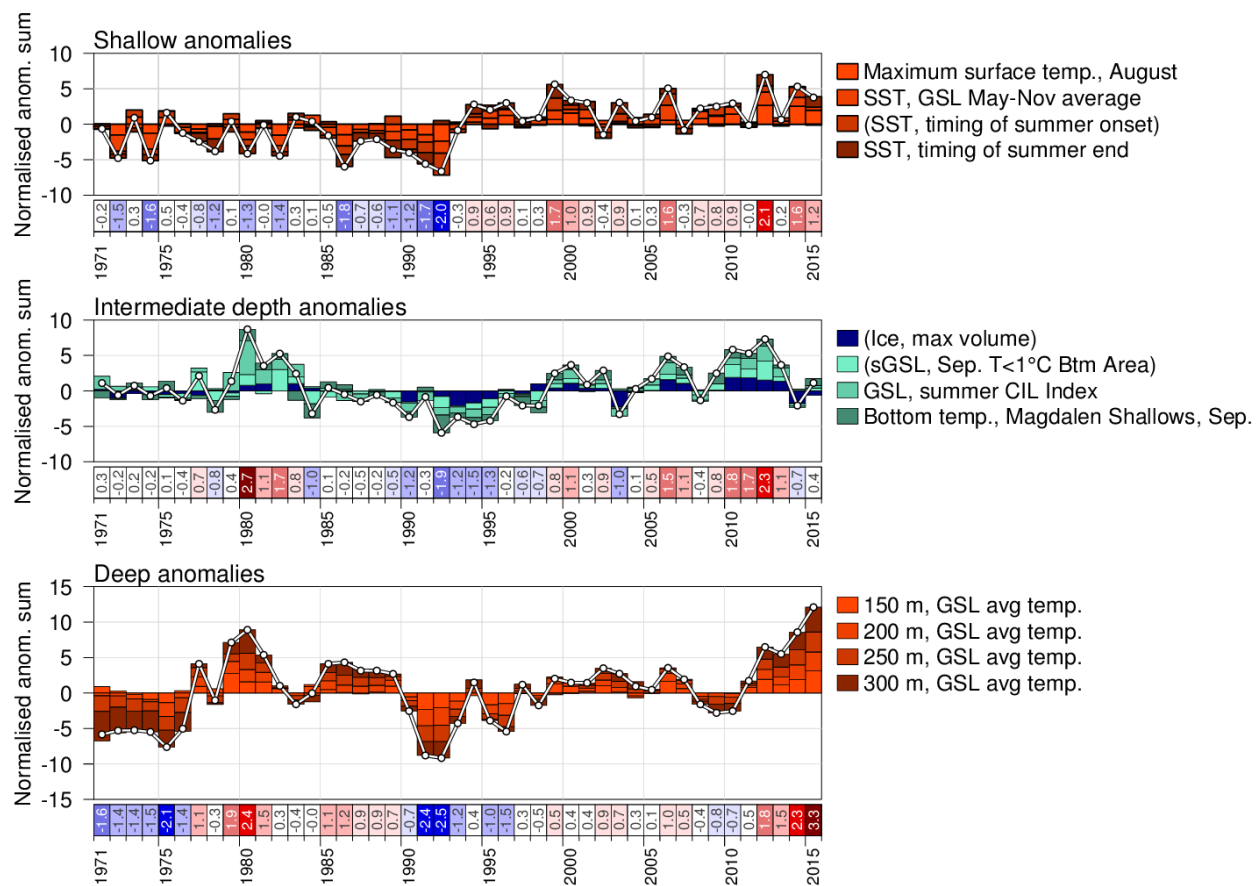


Figure 78. Composite climate indices (white lines and dots) derived by summing various normalized anomalies from different parts of the environment (colored boxes stacked above the abscissa are positive anomalies, and below are negative). Top panel sums anomalies representing the entire water column, middle panel sums shallow anomalies and bottom.